

**Republic of Iraq**  
**Ministry of Higher Education**  
**and Scientific Research**  
**Al-Nahrain University**  
**College of Science**



# **SIMULATION OF HUMAN EYE USING GENETIC ALGORITHM**

**A Thesis Submitted to the  
College of Science of Al-Nahrain University as a Partial Fulfillment  
of the Requirements for the Degree of Master of Science in  
Physics**

*By*

**Luay Abdul Saheb Rasool Al-Taei**

*Supervisor*

**Dr. Suha Mousa Al-Awsi**  
**Dr. Mohammed Saheb Al-Taei**

**Moharam**  
**December**

**1432 A. H.**  
**2010 A. D.**



*Dedicated  
to my family*

### *Supervisor's Certification*

We certify that this thesis was prepared under our supervision at Al –Nahrain University as a partial requirement for the Master of the Science in physics.

Signature :

Name : Dr. Suha Mousa Al-Awsi

Title : Instructor

Address : Department of Physics,  
College of Science,  
Nahrain University.

Date : / / 2010

Signature :

Name : Dr. Mohammed Saheb Al-Taei

Title : Instructor

Address : Department of Computer,  
College of Science,  
Nahrain University.

Date : / / 2010

In view of the available recommendation, I forward this thesis for debate by the examination committee.

Signature:

Name : Dr. Ahmad K. Ahmad

Title : Assist Professor

Adders : Department of Physics,  
College of Science,  
Nahrain University.

Date : / / 2010

## **Examining Committee Certification**

*We certify that we have read this thesis entitled " HUMAN EYE SYSTEM DESIGN AND SIMULATION " and as an examining committee, examined the student Luay Abdul Saheb Rasool Al-Taei on its contents, and that in our opinion it is adequate for the partial fulfillment of the requirements for the degree of Master of Science in physics.*

Signature:

Name: Dr. Ayad A. A. Al-Ani  
(Chairman, Professor)

Date: / / 2010

Signature:

Name: Dr. Mohamed Saleh Ahmeduna  
(Member, Assistant Professor)

Date: / / 2010

Signature:

Name: Dr. Bashar Jasim Hamad  
(Member, Instructor)

Date: / / 2010

Signature:

Name: Dr. Suha Mousa Al-Awsi  
(Supervisor, Instructor)

Date: / / 2010

Signature:

Name: Dr. Mohammed Saheb Al-Taei  
(Supervisor, Instructor)

Date: / / 2010

*A proof by university committee of graduate*

Signature:

Name: Dr. Laith A. A. Al-Ani  
(Dean of the College of Science, Assistant Professor)

Date: / / 2010

## **Acknowledgments**

**I would like to acknowledge my sincere thanks and appreciation to my supervisors Dr. Suha Mousa Al-Awsi and Dr. Mohammed Saheb Al-Taei for suggesting the research, assistance, encouragement, and valuable advice.**

**Thanks are due to the Head of Physics Department, and the staff of the Department for their kind attention especially Dr. Akram Alabod and the assistance Abraheem Abdul mahdi.**

**Sincere thanks to my wife Hadeel T. Khudhair, and to my family for their help and patience.**

**Luay**

# **Abstract**

The aim of this research is simulate an optical system for the human eye using Genetic algorithm. The considered optical characteristics of the optical system simulator include spot size (Z), spot diagram, and effective focal length (EFL). These characteristics are determined with the aid of some mathematical relations, which give the efficiency and accuracy of the adopted optical system design. The work has been performed in two stages:

In the first stage, Genetic Algorithm optimization (GA) is used to get the best design by optimizing the optical features of the eye elements. The optimal eye design was tested using Zemax software, the test includes estimation of the image quality, and optimal performance for the proposed optical eye system.

The second stage was implementing a specially developed software to simulate the behavior of the human eye. The simulator using visual basic 6 and works under Windows operating system, it is able to plot the eye design graphically, and can estimate the considered optical functions to determine the efficiency of the eye simulator.

The simulator showed good results for spot size, spot diagram and EFL, the present work has been gained some credibility when the considered optical functions achieved by the simulator are found compatible with those achieved by Zemax, since the comparison showed a behavioral matching between them, which ensure the correct path of the GA based eye design and the successful proposed eye design.

# **CONTENTS**

**Abstract**

**Contents**

**List of figures**

**List of tables**

## **Chapter One: *General Introduction***

1.1	Introduction	1
1.2	Human Eye Structure	2
1.2.1	Cornea	3
1.2.2	Iris and Pupil	4
1.2.3	Eye lens	5
1.2.4	Retina	6
1.2.5	Aqueous and Vitreous Humors	6
1.3	Published Models of Human Eye	6
1.4	Historical Review	11
1.5	Modern Work	12
1.6	Aim of Thesis	15
1.7	Thesis Outline	15

## **Chapter Two: *Optical-Material Properties of Human Eye***

2.1	Introduction	17
2.2	Skew Ray Tracing in Eye	17
2.3	Focusing in Eye	20
2.4	Eye Defects and Corrections	23
2.4.1	Myopia	23
2.4.2	Hyperopia	24
2.4.3	Correction Estimation	26
2.5	Factors Affecting Vision Quality	27
2.5.1	Pupil Variation	27
2.5.2	Physiological Characteristics	30
2.5.3	Field of View	31
2.5.4	Eye Movement	34
2.6	Image Quality Measurements	35
2.6.1	Resolution versus Point Spread Function (PSF)	35
2.6.2	Contrast and Modulation Transfer Function (MTF)	38
2.6.3	Spot Size and Spot Diagram	40
2.7	Material Properties of Human Eye	41
2.7.1	Refractive Index and Dispersion Coefficient	42

2.7.2	Transmittance and Density	44
-------	---------------------------	----

### **Chapter Three: *Modeling and Algorithms***

3.1	Introduction	48
3.2	Genetic Algorithm	48
3.3	Genetic Algorithm base Eye Design	50
3.3.1	Gene Restrictions	52
3.3.2	Eye Design Optimization	53
3.4	Skew Ray Tracing	56
3.5	Defect in Eye	58
3.6	Spot Size and Diagram Estimation	60
3.7	Illumination of Spot Image	62
3.8	The Effect of FOV on the Spot Radius	63
3.9	Object Distance Variation	66
3.10	Human Eye Simulation	69

### **Chapter Four: *Result Analysis and Simulation***

4.1	Introduction	71
4.2	Proposed Genetic Eye Design	71
4.3	Genetic Eye Evaluation	75
4.3.1	Performance Test	75
4.3.2	Imaging Test	76
4.4	Human Eye Simulation	78
4.5	Eye Defect Simulation	80
4.6	Spot Simulation	87
4.7	Simulated Spot versus Incidence Angles	89
4.8	Simulated Spot versus Object Distance	94

### **Chapter Five: *Conclusion and Future Work***

5.1	Conclusion	98
5.2	Future Work	99

<i>References</i>	100
-------------------	-----

Appendix A	107
Appendix B	108
Appendix C	109
Appendix D	110

## List of Figures

<b>Figure No.</b>	<b>Caption</b>	<b>Page No.</b>
1.1	A vertical cross section of the human eye	2
1.2	Schematic figure shows the human eye	3
1.3	List of the published human eye models	7
2.1	Geometry and notation for tracing skew ray between spherical surfaces	19
2.2	The thick lens	21
2.3	The effect of the refractive index variation	22
2.4	The variation of the lens curvature with age	23
2.5	Different focusing of normal and myopic eye	24
2.6	The correction of the myopic eye	24
2.7	Different focusing of normal and hyperopic eye	25
2.8	The correction of the hyperopic eye	26
2.9	The two imaginary parts of the correction lens	26
2.10	Papillary diameter as a function of field luminance (brightness)	28
2.11	Rayleigh resolution criterion	29
2.12	Variation in the width of the PSF with pupil diameter	30
2.13	The image of the two objects	31
2.14	The optical center	32
2.15	The effect of the nose in the field of view	32
2.16	Intensity distribution in the diffraction patterns	35
2.17	PSF of ideal system, emmetropic and ametropic eye	37
2.18	MTFs of ammetropic, and ametropic eyes	39
2.19	Spot distribution	40
2.20	The variation of index of refraction with wavelength	42
2.21	The dispersion of the white light between two surfaces (Violet, Blue, Green, Yellow, Orange, Red)	44
2.22	Total transmittance at the various anterior surfaces	45
3.1	Block diagram shows the general genetic algorithm	50
3.2	Eyelens	53
3.3	Fitting of refractive index of eyelens	54
3.4	The defects of the eye	58

<b>Figure No.</b>	<b>Caption</b>	<b>Page No.</b>
<b>3.5</b>	The elliptical shape of the eye	<b>65</b>
<b>3.6</b>	Geometrical analysis for the spot size ( $Z$ ) versus reflection angle ( $\theta$ )	<b>66</b>
<b>3.7</b>	Rays incident on the cornea	<b>67</b>
<b>3.8</b>	Angle of incidence versus object distance	<b>68</b>
<b>4.1</b>	The resulted optimal eye design achieved by GA approach	<b>73</b>
<b>4.2</b>	The improving states for the behavior of both (a) the EFL and (b) $Z$	<b>74</b>
<b>4.3</b>	The MTF behavior	<b>76</b>
<b>4.4</b>	Spot diagram achieved by Zemax at $0^\circ$ inclination	<b>77</b>
<b>4.5</b>	The interface of human eye simulator	<b>79</b>
<b>4.6</b>	The myopic eye of optimal design	<b>80</b>
<b>4.7</b>	The hyperopic eye of optimal design	<b>81</b>
<b>4.8-a</b>	simulated myopic eye	<b>83</b>
<b>4.8-b</b>	Correction of myopic eye	<b>84</b>
<b>4.9-a</b>	Simulated hyperopic eye	<b>85</b>
<b>4.9-b</b>	Correction of hyperopic eye	<b>86</b>
<b>4.10</b>	The simulator interface shows the spot diagram and spot size results	<b>88</b>
<b>4.11</b>	Different rays incident on the eye at different angles	<b>89</b>
<b>4.12</b>	The situation of oblique rays	<b>90</b>
<b>4.13</b>	The relation between the extension in the spot diagram with angle	<b>91</b>
<b>4.14</b>	The spot radius versus incident angle	<b>93</b>
<b>4.15</b>	The simulated spot diagram versus incident angle by simulation	<b>93</b>
<b>4.16</b>	The spot diagram versus incident angle given by Zemax	<b>94</b>
<b>4.17</b>	The object distance is logarithmically skewed	<b>95</b>
<b>4.18</b>	The spot diagram and size for different object distance	<b>96</b>
<b>4.19</b>	The variation in $R_1$ of the eyelens with respect to its value at reading distance ( $0.25m$ ) due to the object distance variation in the six considered cases	<b>96</b>
<b>4.20</b>	The variation in $R_2$ of the eyelens with respect to its value at reading distance ( $0.25m$ ) due to the object distance variation in the six considered cases	<b>97</b>

## List of Tables

<b>Table No.</b>	<b>Caption</b>	<b>Page No.</b>
<b>2-1</b>	The magnitude of the dispersion coefficient of the eye	<b>43</b>
<b>3-1</b>	shows the fixed (f) and variable (v) parameters of optical elements	<b>51</b>
<b>3-2</b>	Information table: suggested restriction parameters	<b>53</b>
<b>3-3</b>	Spot size values as a function of $\alpha$ and $\beta$	<b>61</b>
<b>3-4</b>	Angle of incidence $\delta$ correspondence to the object distance	<b>68</b>
<b>4-1</b>	The optical features of the optimal design resulted from GA	<b>72</b>
<b>4-2</b>	The optical features of myopic eye	<b>80</b>
<b>4-3</b>	The optical features of hyperopic eye	<b>81</b>
<b>4-4</b>	The spot and the effective focal length for three cases	<b>81</b>
<b>4-5</b>	Show the spot radius as a function of angle using Zemax	<b>92</b>

## List of Symbols

Symbol	Caption
$n$	Refractive index of the incident ray
$n'$	Refractive index of the refractive ray
$N$	Direction cosine of the incident ray
$L$	Direction cosine of the incident ray
$M$	Direction cosine of the incident ray
$\alpha$	The component of the unit normal
$\beta$	The component of the unit normal
$\gamma$	The component of the unit normal
$x_{-1}$	The coordinate of the coming ray
$y_{-1}$	The coordinate of the coming ray
$z_{-1}$	The coordinate of the coming ray
$x_0$	The ray intersection with (x-y) plan
$y_0$	The ray intersection with (x-y) plan
$D$	The length of segment
$s_0$	The object distance
$s_i$	The image distance
$f$	The focal length
$R_1$	Radius of curvature of the first surface
$R_2$	Radius of curvature of the second surface
$f_1$	The focal length of the first optical element
$f_2$	The focal length of the second optical element
$EFL$	The effective focal length
$d$	The distance between two lenses
$t$	The thickness of the lens
$P$	The power of the lens
$\lambda$	The wavelength
$D_0$	The diameter of the pupil aperture
$NA$	Numerical aperture
$C$	The contrast
$W$	The flux density
$\phi$	The phase
$Z$	The spot size
$c$	The velocity of light in vacuum
$v$	The velocity of light in medium
$N_0$	The dispersion coefficient
$A$	The dispersion coefficient

$B$	The dispersion coefficient
$R$	The reflection
$T$	The transmittance
$D$	The density
$r_p$	The position on the eyelens
$\sigma_x$	The variance of the values in the x-axis
$\sigma_y$	The variance of the values in the y-axis
$\mu_x$	The mean (expectation) value in the x-axis
$\mu_y$	The mean (expectation) value in the y-axis
$I_S$	The illumination of the spot
$I_0$	The illumination out the human body
$z_o$	The spot size at zero angle
$z_\theta$	The spot size at any angle
$f_{sphere}$	The effective focal length of the spherical shape
$f_{ellips}$	The effective focal length of the elliptical shape
$\Delta f$	The different between $f_{sphere}$ and $f_{ellips}$
$X_L$	The coordinate of the eyelens center
$Y_L$	The coordinate of the eyelens center
$X_E$	The coordinate of the position that the ray incident on the eye
$Y_E$	The coordinate of the position that the ray incident on the eye
$e$	The eccentricity of the eye
$\delta$	The angle of the ray incident

# *Chapter One*

## GENERAL INTRODUCTION

# **Chapter One**

## **General Introduction**

### **1.1 Introduction**

Our understanding of the optical system of the eye is evolving quite rapidly due to the combined effort of new experimental methodologies and advanced modeling. Optical design plays a central role since this branch of science and technology deals with finding the best combinations of optical elements to obtain a desired function, with optimal performance. Optical testing is also necessary for the verification and validation of designs. The study of the optical system of the eye has similarities, but also remarkable differences with optical design and testing [Nav 09]. The optical design of the eye is already given by nature (optimization through evolution), so its study can be seen as an inverse engineering problem: to unravel such design. Inverse problems are difficult in general and must be solved by successive approaches. Each approach consists of (1) some starting hypothesis based on previous knowledge; (2) a set of experimental data; and (3) a model relating those data and the hypothesis [Nav 09]. The testing stage (4) compares model predictions to experimentally assessed optical performance. To understand the optical design of the eye we need models of each component (cornea, lens) and from that we can construct a model of the complete optical system [Nav 09]. Many reasons exist to model the eye. Some of the more common reasons include; Clinical optometry, Ophthalmic diagnostics and refractive surgery, Design of intraocular, spectacle, contact lenses, Optical instrumentation, bio-optical engineering, Vision research, and Education [Bre 08].

## 1.2 Human Eye Structure

The shape of the human eye is spheric of about 22 mm diameter with a light sensing organ called retina lies on the inside back surface. The main body of the eye has to be a sphere so as to be able to rotate in its socket. It is not a perfect sphere in that there is a protuberance on its front that has a reduced radius of curvature compared to the remainder of the eye. A sphere of this index of refraction will not focus incoming plane waves onto its rear surface but to a point behind that surface [Ker 04]. The essential part of the eye, considered as an optical system, is shown in figure (1.1) and (1.2) [Sae 64]:

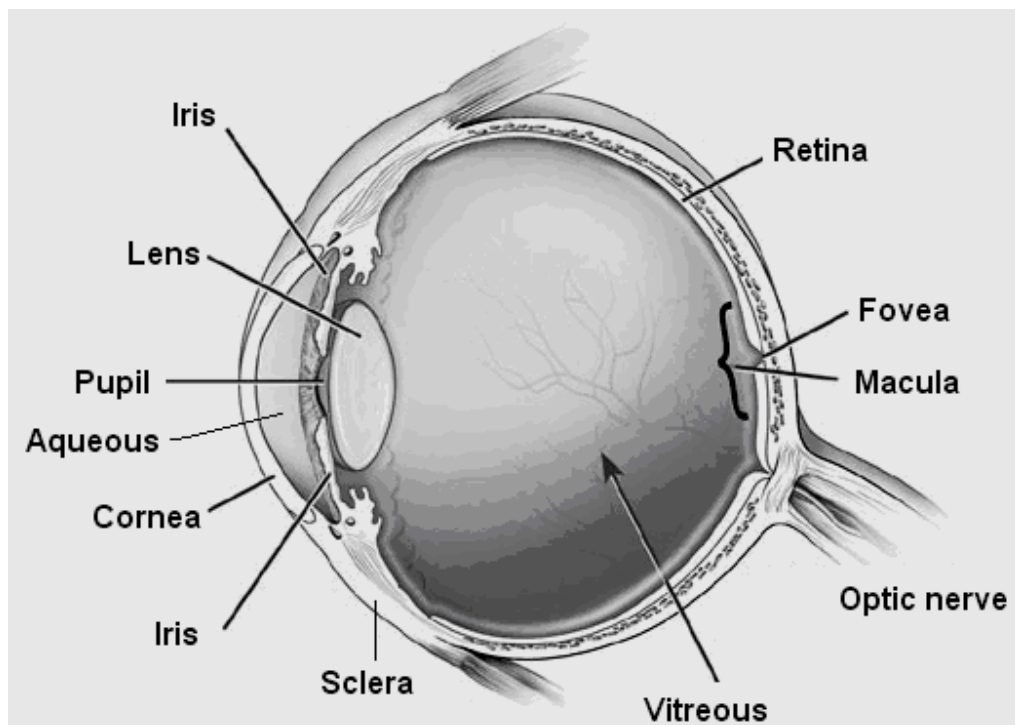


Figure (1.1): Vertical cross section of the human eye [Jen 81].

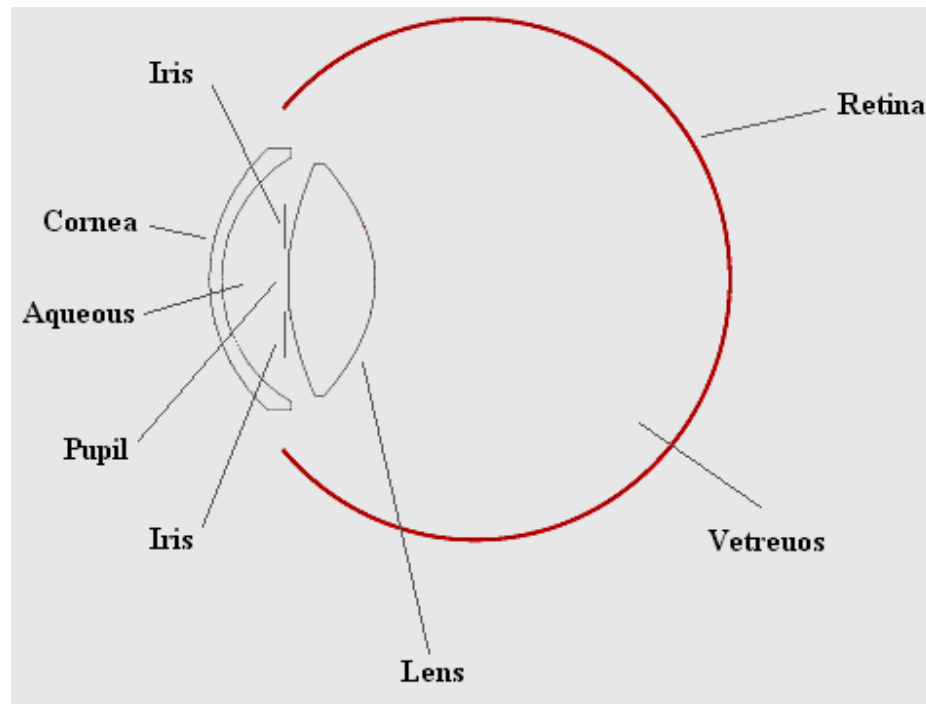


Figure (1.2): Schematic figure shows the human eye [Nav 09].

### 1.2.1 Cornea

Cornea is more sharply curved, tough, and transparent membrane [Sae 64]. The cornea is first surface of the eye. It is an extension of the sclera, which is the tough, white outer shell of the eye. The transparency of the cornea is facilitated by the regular arrangement of the layers of collagen fibers that comprise most of the corneal thickness. Periodic closures of the eyelid maintain a thin tear film on the cornea's external surface, which ensures a smooth refracting surface. The changes in the tear film give rise to scattering and small changes in optical aberrations. The cornea is about 0.5 to 0.6 *mm* thick at its center, it has a mean refractive index of about 1.376 and its first surface has a mean radius of curvature of about 6.5 to 7.7 *mm*. Combining this with a back surface whose a mean radius is about 6.8 *mm*

gives the cornea a total focal power of roughly  $43D$  (the focal power in *diopeters* “ $D$ ” is the inverse of the focal length in meters) [Roo 09, Ham 08].

Because the cornea accounts for most of the power of the eye, it is also a key contributor to aberrations of the eye. The high magnitude of aberrations that might have existed in the cornea is reduced by virtue of its conic, rather than spherical shape [Ped 88].

Upon entering the eye at the air-cornea interface, where the refractive index changes abruptly from (1 to 1.38) light undergoes a significant degree of bending. The corneal surface provides about 73% of the total refractive power of the eye [Ped 88].

### 1.2.2 Iris and Pupil

Before the pupil, the light must be passing through the Iris. The iris situated in the aqueous humor, it is a diaphragm that gives the eye its characteristic color and controls the amount of light that enters. The amount and location of pigment in the iris determine whether the eye looks blue, green, gray, or brown [Ped 88].

The entrance and exit pupils (images of the iris in the object and image space respectively) have a crucial role in image and vision quality. With high lightness (photopic) levels the pupil size is small, thus stopping peripheral rays, which are typically more aberrated. For low lightness levels, the number of photons is also low and the signal-to-noise ratio decreases due to quantum noise, then the pupil dilates to increase the number of received photons. In this way the pupil can balance optical blur and noise to obtain an optimal trade-off between these two major factors affecting the quality of vision [Nav 09].

The pupil adjusting the diameter from a minimum of about  $2\text{mm}$  on a bright day to a maximum of about  $8\text{mm}$  under very dark conditions [**Ped 88**]. The pupil serves two main optical functions. It limits the amount of light that reaches the retina, and it alters the numerical aperture of the eye's image system [**Don 03**].

The effect of aberrations in connection with pupil size was quantified firstly by Campbell; who determined that the pupil size that offered the best lateral resolution was typically between  $3$  and  $4\text{ mm}$  in diameter. Studies since that time have confirmed this finding [**Don 03**].

### 1.2.3 Eye Lens

The crystalline lens is a capsule containing a fibrous jelly hard at the center and progressively softer at the outer portions. The crystalline lens is held in place by ligaments which attach it to the ciliary muscle [**Sae 64**]. The human lens contributes with about  $1/3$  to the total power of the eye at zero *diopeters* of accommodation. The lens power changes strongly with accommodation from about  $21\text{-}22D$  for the unaccommodated state to above  $30D$  for the fully accommodated lens. Most of this strong change is explained by the change in curvature radii of the lens surfaces under the action of the ciliary muscles [**Nav 09**].

The most important optical constants of the lens of the normal human eye are the refractive index that varies between  $1.383$  at the periphery and  $1.406$  in the nucleus, the radius of curvature in unaccommodated state at anterior pole is  $10\text{mm}$  and at posterior pole is  $6\text{mm}$ , the thickness in unaccommodated state about  $3.6\text{mm}$  [**Bou 61**].

### 1.2.4 Retina

The retina is the inner layer of the eye. It contains the light receptors; *rods* and *cones*, thus it serves as the "film" of the eye. The retina also has many interneurons that process the signals arising in the rods and cones before passing them back to the brain. The rods and cones are *not at the surface* of the retina but lie underneath the layer of interneurons [Kim 09].

### 1.2.5 Aqueous and Vitreous Humors

The iris and lens divide the eye into two main chambers:

**A- The front chamber**, which is filled with a watery liquid called the *aqueous humor* [Kim 09]. The aqueous has an average refractive index of 1.336, almost equal to that of sea water 1.333. Because the refractive indices of the cornea and aqueous humor are nearly alike, little additional bending of rays occurs as light moves from the cornea into the front chamber [Ped 88].

**B- The rear chamber**, also it is filled with a jellylike material called the *vitreous humor* [Kim 09]. The vitreous humor, a transparent substance, whose refractive index 1.336 is also close to that of sea water. The vitreous humor, essentially structurless, contains small particles of cellular debris that are referred to as floaters [Ped 88].

## 1.3 Published Models of Human Eye

There are several schematic models for the human eye varies from very traditional models to modern ones. One of the most popular is that of Gullstrand which is inspired from Helmholtz's eye model. This model gains a Nobel prize in 1911. Although this model is reasonably accurate, there are several other models in the literature that have, each one, its own advantages

depending on the desired application [Car 03]. Figure (1.3) show the important schematic models in addition to their numerical specifications.

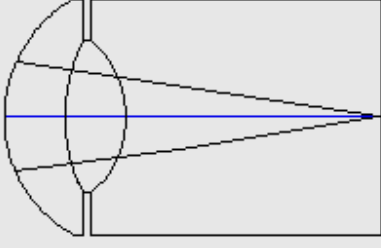
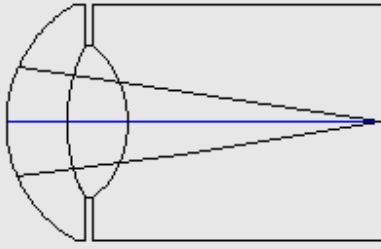
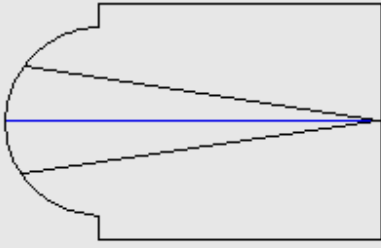
Model (1) [DeA 07]	Helmholtz-Laurace (1909)															
	<table border="1"> <thead> <tr> <th>Surface</th> <th>Radius(mm)</th> <th>Thickness(mm)</th> <th>Refraction index</th> </tr> </thead> <tbody> <tr> <td>1</td> <td>8</td> <td>3.6</td> <td>1.333</td> </tr> <tr> <td>2</td> <td>10</td> <td>3.6</td> <td>1.45</td> </tr> <tr> <td>3</td> <td>-6</td> <td>15.18</td> <td>1.333</td> </tr> </tbody> </table>	Surface	Radius(mm)	Thickness(mm)	Refraction index	1	8	3.6	1.333	2	10	3.6	1.45	3	-6	15.18
Surface	Radius(mm)	Thickness(mm)	Refraction index													
1	8	3.6	1.333													
2	10	3.6	1.45													
3	-6	15.18	1.333													
Model (2) [DeA 07]	Gullstrand (1911)															
	<table border="1"> <thead> <tr> <th>Surface</th> <th>Radius(mm)</th> <th>Thickness(mm)</th> <th>Refraction index</th> </tr> </thead> <tbody> <tr> <td>1</td> <td>7.8</td> <td>3.6</td> <td>1.336</td> </tr> <tr> <td>2</td> <td>10</td> <td>3.6</td> <td>1.413</td> </tr> <tr> <td>3</td> <td>-6</td> <td>16.97</td> <td>1.336</td> </tr> </tbody> </table>	Surface	Radius(mm)	Thickness(mm)	Refraction index	1	7.8	3.6	1.336	2	10	3.6	1.413	3	-6	16.97
Surface	Radius(mm)	Thickness(mm)	Refraction index													
1	7.8	3.6	1.336													
2	10	3.6	1.413													
3	-6	16.97	1.336													
Model (3) [DeA 07]	Emsley (1946)															
	<table border="1"> <thead> <tr> <th>Surface</th> <th>Radius(mm)</th> <th>Thickness(mm)</th> <th>Refraction index</th> </tr> </thead> <tbody> <tr> <td>1</td> <td>5.55</td> <td>22.22</td> <td>1.3333</td> </tr> </tbody> </table>	Surface	Radius(mm)	Thickness(mm)	Refraction index	1	5.55	22.22	1.3333							
Surface	Radius(mm)	Thickness(mm)	Refraction index													
1	5.55	22.22	1.3333													

Figure (1.3): List of the published human eye models.

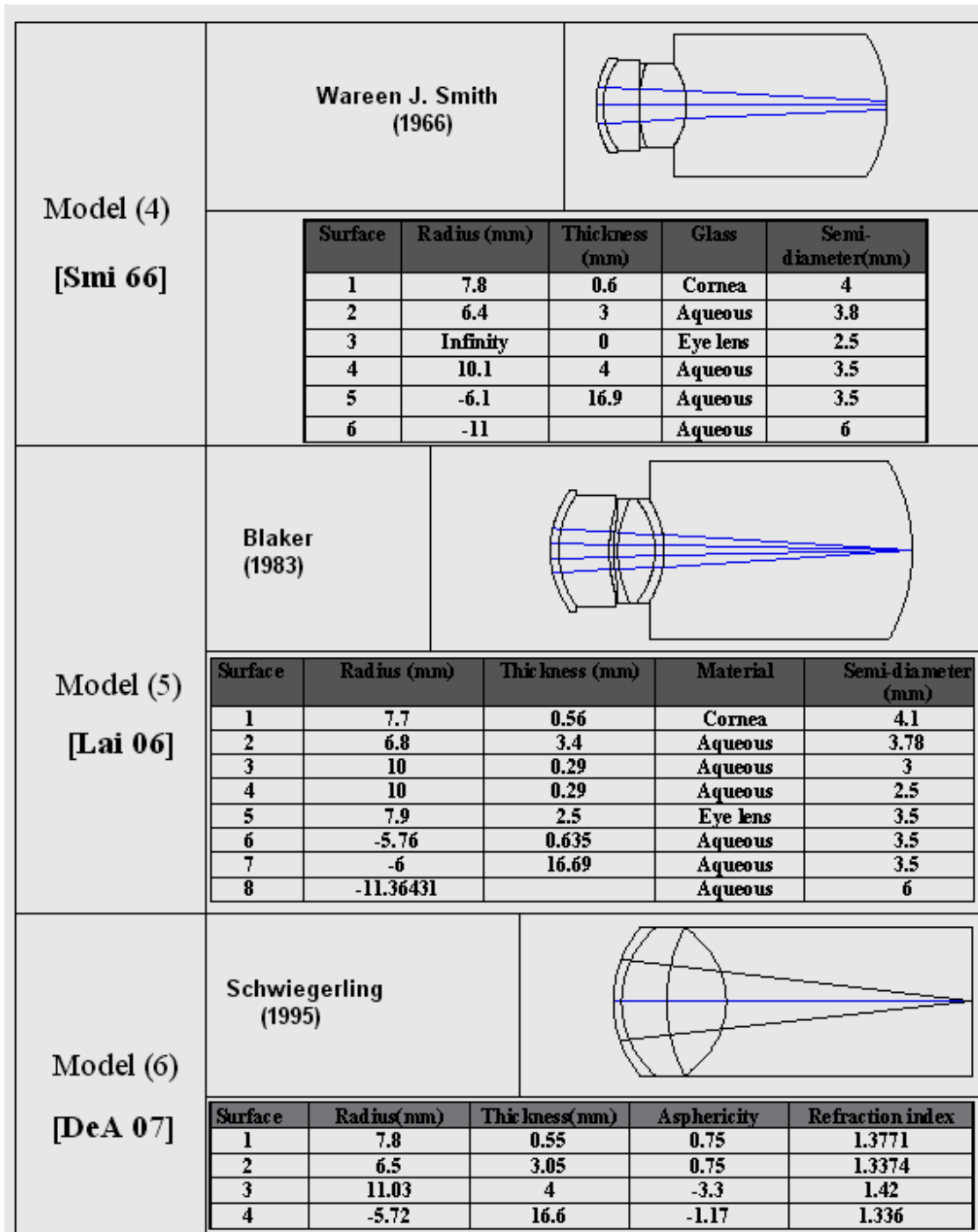


Figure (1.3): Continued.

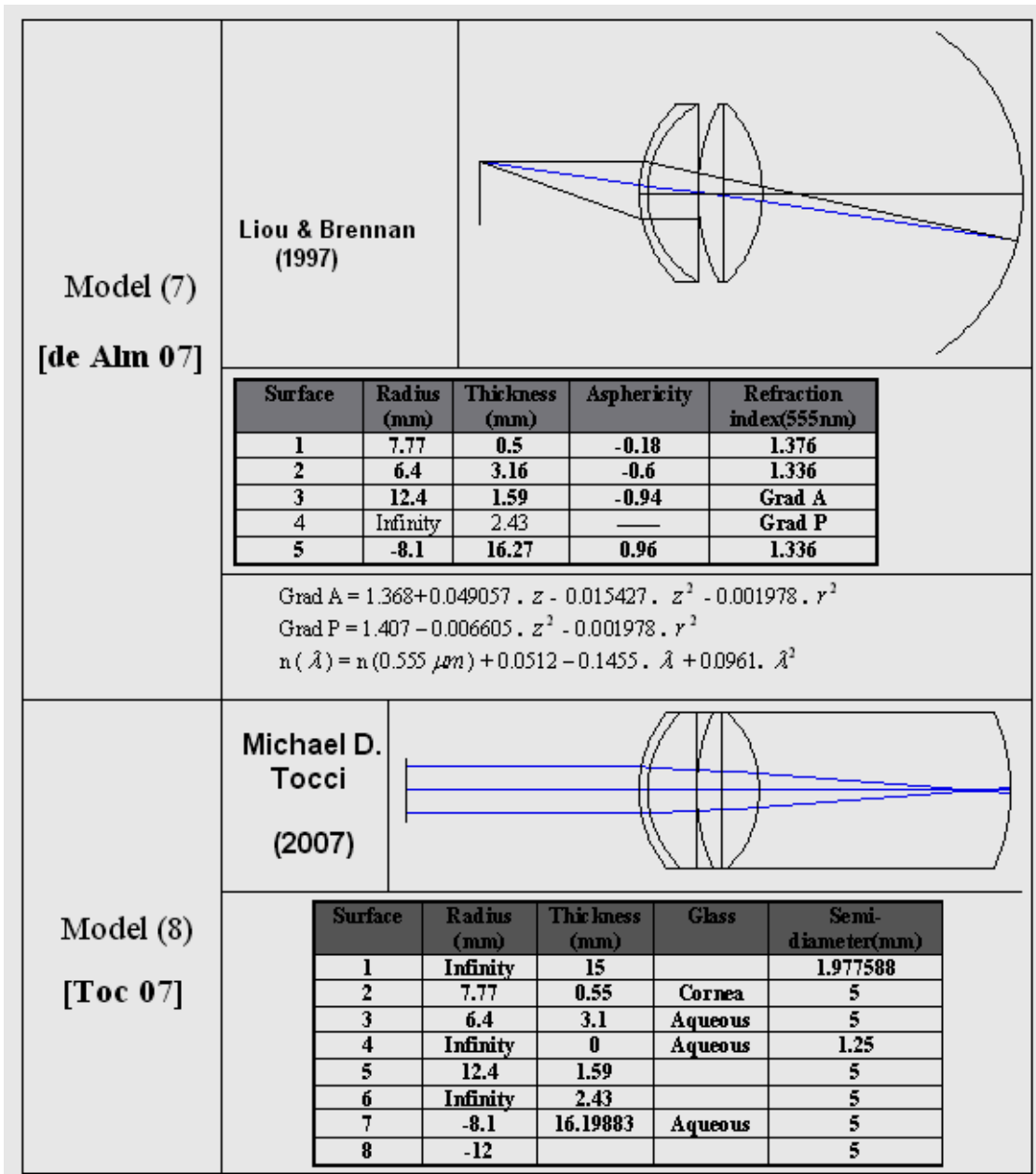


Figure (1.3): Continued.

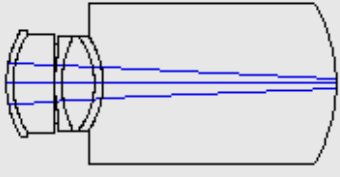
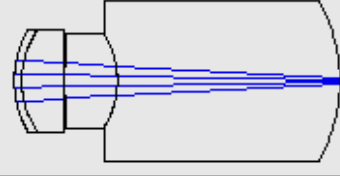
Model (9) [Dob 08]	Alexander Dobinin & et al (2008)				
	<b>Surface</b>	<b>Radius (mm)</b>	<b>Thickness (mm)</b>	<b>Glass</b>	<b>Semi-diameter (mm)</b>
	1	7.7	0.5	Cornea	4
	2	6.8	3.1	Aqueous	3.7
	3	Infinity	0	Eye lens	3
	4	10	-0.54	Aqueous	2.5
	5	7.91	2.419	Aqueous	3.5
	6	-5.76	0.635	Aqueous	3.5
	7	-6	17.4	Aqueous	3.5
	8	-11.8			6
Model (10) [Sak 08]	Julia A. Sakamoto & et al (2008)				
	<b>Surface</b>	<b>Radius (mm)</b>	<b>Thickness (mm)</b>	<b>Glass</b>	<b>Semi-diameter(mm)</b>
	1	7.46	.554	Cornea	3.8
	2	6.72	3.17	Aqueous	3.8
	3	Infinity	0	Aqueous	2.5
	4	10.35	3.97	Eye lens	1.313163
	5	-6.28	16.61	Aqueous	3.5
	6	-12		Aqueous	6

Figure (1.3): Continued.

It is noticeable that the eye design number 5 found in figure (1.4) gains more interest than others, since it contains all optical surfaces found in the biological eye, although, this model designates refractive indices to eye components that not necessarily correspond to true measured values. In addition, Blacker model treats the cornea as double surface, which guarantees a perfect image formation at the retina. Also, Blackers data was modified to include dispersion data for the cornea, lens and aqueous to be similar to water.

## 1.4 Historical Review

First, Gauss in 1841 established the basic laws that govern image formation properties, many theoretical models have been proposed later [Von 00].

In the late 19<sup>th</sup> century, Helmholtz undertook a very thorough study on this subject, and published the now famous collection “Helmholtz Treatise on Physiological Optics”. This model was later modified by Laurance and became known as the “Helmholtz-Laurance model”, which contains all optical surfaces found in the biological eye. Although this model designates refractive indices to eye components that not necessarily correspond to true measure values, its overall properties have a close resemblance to those of the human eye [Tun 89].

The Swedish Ophthalmologist Allvar Gullstrand conducted important research in the field of physiology, and in 1911 received the Nobel prize for his work regarding the eye as an optical design. While Gullstrand’s simplified schematic eye treats the cornea as a single refracting surface, just as the previous model from Helmholtz-Laurence, in Gullstrand’s non-simplified model the cornea is considered to have two surfaces, which guarantees a perfect image formation at the retina. Although it simplifies the cornea, the vitreous and the aqueous humor, this model is especially suitable for the computation of intraocular lens (IOL) power, as it also contains the anterior and posterior surface of the crystalline lens [Sch 92].

In 1953, Emsley schematic eye was introduced. It is the simplest eye model since it contains just a single refractive surface. Due to its simplicity, it is widely used in undergraduate courses in optometry, ophthalmology and vision science [San 93].

In 1971, Lotmar was modified the Gullstrands data to include dispersion data for the lens, cornea, and aqueous to be similar to water. Also, the anterior cornea surface was modified to be aspheric. In 1983, Blaker presented more convenient model based on Lotmar model [**Lai 06**].

In 1995, Greivenkamp and colleagues proposed an eye model containing four refracting non-spherical surfaces that considered retinal contrast sensitivity and refraction-limited properties [**Ped 98**].

## **1.5 Modern Work**

During the last years of 90's decade, an incredible amount of techniques and instrumentation for visual quality measurements were implemented. After this time and up to modern days, the literatures tend to orient in more advanced domain. In the following, a detailed explanation about some important studies in the field of interest:

In 1997 Liou and Brennan have proposed an interesting model, which is the closest to anatomical, biometric and optical data as compared to the physiological eye. Their objective was to develop a model that could be used to predict visual performance under normal and altered conditions of the eye, using empirical values of ocular parameters [**Alp 78**].

Pablo Artal et al in 2006 show that the compensation is larger in the less optically centered eyes that mostly correspond to hyperopic eyes. This suggests a type of mechanism in the eye's design that is the most likely responsible for this compensation. Spherical aberration of the cornea is partially compensated by that of the lens in most eyes. Lateral coma is also compensated mainly in hyperopic eyes. They found that the distribution of aberrations between the cornea and lens appears to allow the optical

properties of the eye to be relatively insensitive to variations arising from eye growth or exact centration and alignment of the eye's optics relative to the fovea. These results may suggest the presence of an auto-compensation mechanism that renders the eye's optics robust despite large variation in the ocular shape and geometry [**Art 06**].

Michael D. Tocci attained a Ph.D. in 2007 after he created model of a human eye in ZEMAX using the Liou and Brennan (1997) eye model. This is a fairly up-to-date and comprehensive model of the eye. It accounts for many realistic factors that other models do not, such as an offset pupil, a curved retina surface, an inward-pointing eyeball, and a crystalline lens with two different gradient refractive index profiles (one for the front half and a second profile for the rear half). After successfully generating this eye model in ZEMAX, technicians used it to design a free-form progressive eyeglass lens [**Toc 07**].

Sakamoto et al in 2008 developed a method for estimated patient-specific ocular parameters, including surface curvatures, conic constants, tilts, decentrations, thicknesses, refractive indices, and index gradients. The data consist of the raw detector outputs from one or more Shack-Hartmann wave front sensors, and the parameters in the eye model are estimated by maximizing the likelihood [**Sak 08**].

Donnelly W. obtained Ph.D. in 2008 when he developed a commercially available eye modeling system, the advanced human eye model (AHM). Two mainstream optical software engines, ZEMAX (ZEMAX Development Corp.) and ASAP (Advanced Systems and Analysis Program) were used to construct a similar software eye model and compared. The method of using the AHM is described and various eye modeling scenarios are created. These scenarios consist of retinal imaging of

targets and sources; (optimization capability; spectacles, contact lens, and intraocular lens insertion and correction; Zernike surface deformation on the cornea; cataract simulation and scattering; a gradient index lens; a binocular mode; a retinal implant; system import/export; and ray path exploration) **[Don 08]**.

Navarro R. in 2009 analyzed and compared the eye models to experimental findings to assess properties and eventually unveil optical design principles involved in the structure and function of the optical system of the eye. Models and data often show good match but also some paradoxes are found. The optical design seems to correspond to a wide angle lens. Compared to conventional optical systems, the eye presents a poor optical quality on axis, but a relatively good quality off-axis, thus yielding higher homogeneity for a wide visual field. This seems the result of an intriguing combination of the symmetry design principle with a total lack of rotational symmetry, decentrations and misalignments of the optical surfaces **[Nav 09]**.

Einighammer J. et al in 2009 constructed a model from an eye's geometry, including axial length and topographic measurements of the anterior corneal surface. All optical components of a pseudophakic eye are modeled with computer scientific methods. A spline-based interpolation method efficiently includes data from corneal topographic measurements. The geometrical optical properties, such as the wave front aberration, are simulated with real ray-tracing using Snell's law. Optical components can be calculated using computer scientific optimization procedures. The geometry of customized aspheric intraocular lenses (IOLs) was calculated for 32 eyes and the resulting wave front aberration was investigated **[Ein 09]**.

## **1.6 Aim of Thesis**

The aim of this research is to built a theoretically studying and analyzing the optical constituting structure of the human eye. Then, proposing an optical system for the human eye has the same size, optical elements, material properties and performance. The proposed eye was tested by the simulation technique, which requires formation a digital image in the simulated retina. This offers the chance to measure the performance efficiency in comparison with real life eye. Also, eye defects; myopia and hyperopia and their correction are simulated.

## **1.7 Thesis Outline**

The thesis consists of five chapters; chapter one is a general introduction about the general topic of the work. Whereas the other four chapters deal with studying the optical system of human eye, its design and implementation. The following is a brief description for these chapters:

### **Chapter Two, entitled "*Optical-Material Properties of Human Eye*"**

This chapter presents the theoretical concepts of the optics related to human eye. In addition, there is details explanation about the optical properties for the material constituting the eye.

### **Chapter Three, entitled "*Algorithm and Implementation*"**

This chapter describes the use of the mathematical relationship employed to achieve the proposed eye design. Also, the algorithm of eye design and simulation are mentioned in details.

**Chapter Four, entitled "Results Analysis and Simulation"**

The results of the design, performance, efficiency, and simulation are demonstrated in this chapter. Moreover, the analysis and graph behavior discussion are presented.

**Chapter Five, entitled "Conclusion and Future Work"**

In this chapter, some conclusions are driven from the work and proposed the work for the future.

## *Chapter Two*

# OPTICAL-MATERIAL PROPERTIES OF HUMAN EYE

## **Chapter Two**

# **Optical-Material Properties of Human Eye**

## **2.1 Introduction**

This chapter reviews the theoretical concepts related to the human eye configuration and performance. The optical features and material characteristics of eye elements are shown in details, since they determined the performance of the eye. The study of the performance associated with tracing the rays income from the object to be seen. Such that, skew ray tracing is consider in different cases of incident angle variation. The collection of the rays on the retina will constituting a spot image. The quality of such image is affected by some factors such as; pupil radius variation, physiological characteristic, field of view, and even eye movement. Most of the factors affecting the imaging process are considered in details. Also, the most important measures of image quality are taken in account to be used in testing the resulted image.

## **2.2 Skew Ray Tracing in Eye**

Ray tracing is the numerical method used for determining the effective behavior of lenses on the ray. Ray tracing provides the geometrical path of light through the lens, and defines the aberration content of the image. Optical path values are obtained from the ray trace and use for computation of the physical image. All of the required information about clear apertures, tolerances and image quality is obtained from computations based upon ray tracing [Sha 97]. Skew ray tracing includes all possible rays in the optical system; paraxial rays, meridional rays and skew rays. To define the ray path between two surfaces of lens, first the intersection of the given ray with the tangent

plane is found as shown in Figure (2.1). The z-axis is the optical axis, and to employ Snell's law of the refraction in terms of geometrical forms, it has been reformulated as [Wil 72]:

$$\left. \begin{aligned} n'L' - nL &= k\alpha \\ n'M' - nM &= k\beta \\ n'N' - nN &= k\gamma \end{aligned} \right\} \quad (2.1)$$

Where

$$k = n' \cos I' - n \cos I \quad (2.2)$$

Where  $L$ ,  $M$ , and  $N$  are the direction cosines of the incident rays.  $\alpha$ ,  $\beta$ , and  $\gamma$  are the components of the unit normal at the incident. The non-primed parameters belong to the previous medium. This method involves two sets of equation; the first for the transfer between spherical surface and the second for the refraction [Wil 72].

The equations for transferring skew rays between spherical surfaces are [Wil 72]:

$$\left. \begin{aligned} x_0 &= x_{-1} + \frac{L}{N}(d - z_{-1}) \\ y_0 &= y_{-1} + \frac{M}{N}(d - z_{-1}) \end{aligned} \right\} \quad (2.3)$$

Where,  $(x_{-1}, y_{-1})$  are the coordinates of the coming ray, and  $(x_0, y_0)$  are the coordinates of the ray intersection with the (x-y) plan. The ray intersects the spherical surface in the coordinates are given by [Wil 72]:

$$\left. \begin{aligned} x &= x_0 + LD \\ y &= y_0 + MD \\ z &= ND \end{aligned} \right\} \quad (2.4)$$

Where  $D$  is the length of segment from the (x-y) plane to the surface; which is expressed as [Wil 72]:

$$D = \frac{F}{G + \sqrt{G^2 - cF}} \quad (2.5)$$

Where  $F$  and  $G$  are coefficients given by [Wil 72]:

$$F = c(x_0^2 + y_0^2) \quad (2.6)$$

$$G = N - c(Lx_0 + My_0) \quad (2.7)$$

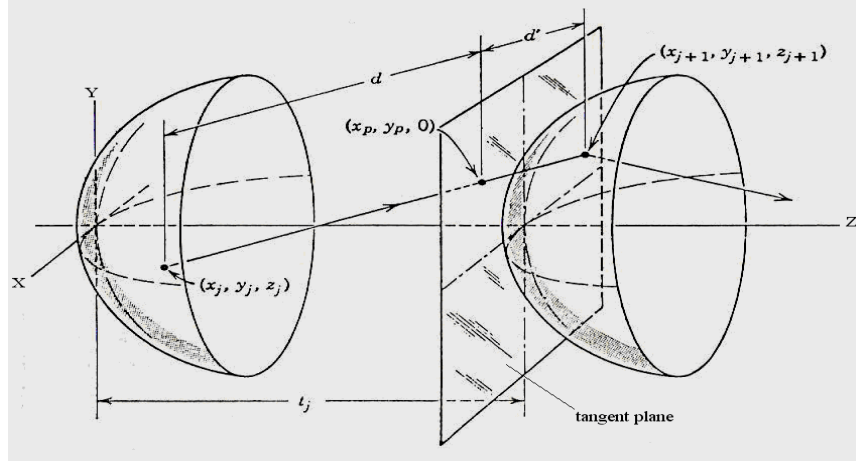


Figure (2.1): Geometry and notation for tracing skew ray between spherical surfaces [Wil 72].

To obtain equation through spherical surface it is needed to know the components of the unit normal  $(\alpha, \beta, \gamma)$  at the point of incidence. These components can be obtained from [Wil 72]:

$$(\alpha, \beta, \gamma) = \frac{-\left\{ \frac{\partial Z}{\partial x}, \frac{\partial Z}{\partial y}, \frac{\partial Z}{\partial z} \right\}}{\sqrt{\left\{ \frac{\partial Z}{\partial x} \right\}^2 + \left\{ \frac{\partial Z}{\partial y} \right\}^2 + \left\{ \frac{\partial Z}{\partial z} \right\}^2}} \quad (2.8)$$

Using (2.8) in equation (2.1), the new values of the directional cosines (after refraction) can be expressed as [Wil 72]:

$$\left. \begin{aligned} n'L' &= nL - Kx \\ n'M' &= nM - Ky \\ n'N' &= nN - Kz + n' \cos I' - n \cos I \end{aligned} \right\} \quad (2.9)$$

Where

$$K = c(n' \cos I' - n \cos I) \quad (2.10)$$

$$\cos I = \sqrt{G^2 - cF} \quad (2.11)$$

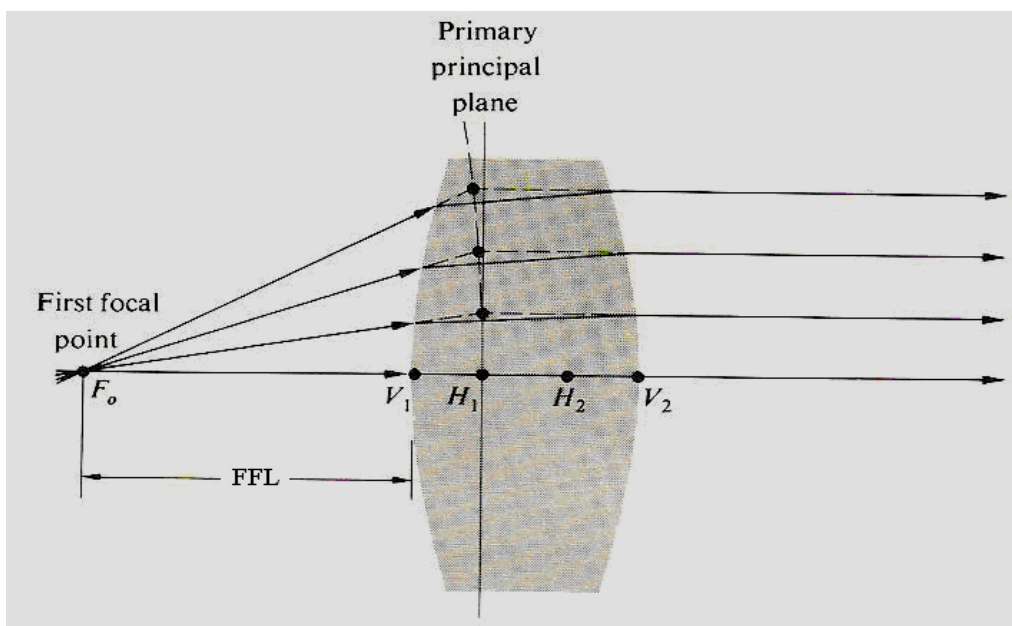
$$n' \cos I' = \sqrt{(n')^2 - n^2(1 - \cos^2 I)} \quad (2.12)$$

Equation (2.9 – 2.12) completes the refraction process. Substituting the direction cosines of equation (2.9) in equation (2.13), the transform process from one surface to another is done. After each refraction process the direction cosines should be checked in order to assert the tracing validity. This can be done by [Wel 74]:

$$(L')^2 + (M')^2 + (N')^2 = 1 \quad (2.13)$$

### 2.3 Focusing in Eye

In thick lens (as simple optical system), the first and second focal points, (object and image foci)  $F_o$  and  $F_i$ , can conveniently be measured from the two vertices. The front and back focal lengths (FFL and BFL) refers to that the incident and emerged rays will meet at points, the focus of which forms a curved surface that may or may not reside within the lens, such surface is termed principal plane. Points where the principal plane intersect the optical axis are known as the principal points ( $H_1$  and  $H_2$ ) as shown in figure (2.2). They provide a set of useful references from which to measure several of the system parameters [Zaj 74].



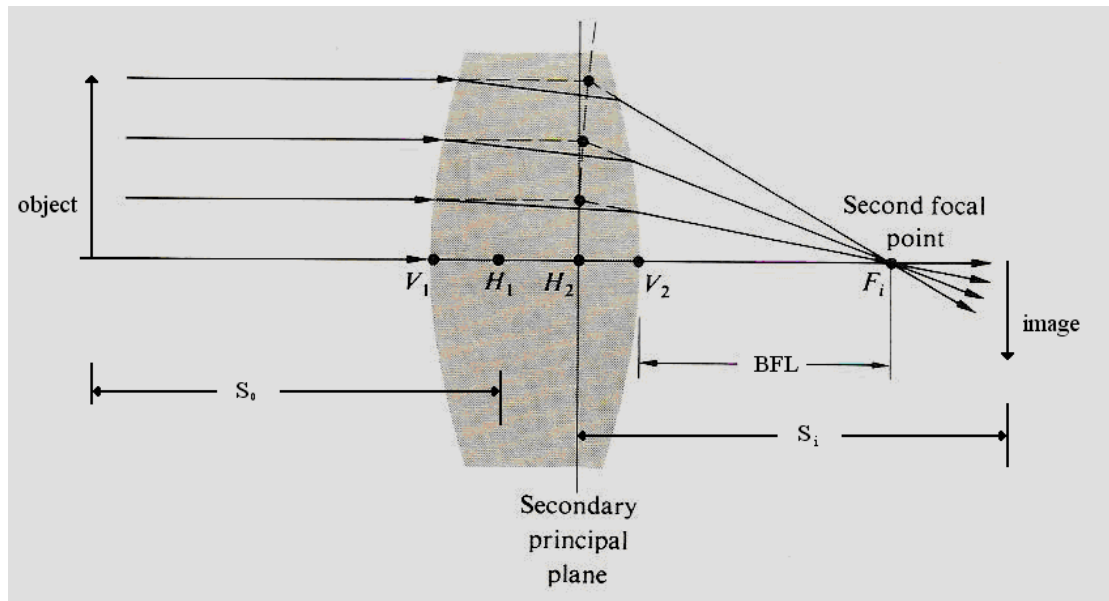


Figure (2.2): The thick lens [Zaj 74].

The conjugate points relates the object and image distances ( $s_0$  and  $s_i$ ) are driven in Gaussian form as [Zaj 74]:

$$\frac{1}{s_0} + \frac{1}{s_i} = \frac{1}{f} \quad (2.14)$$

Where  $s_0$  and  $s_i$  are measured from the first and second principal planes. The focal length  $f$  of a thick lens is reckoned with respect to the principal planes as [Zaj 74]:

$$\frac{1}{f} = (n-1) \left[ \frac{1}{R_1} - \frac{1}{R_2} + \frac{(n_1-1)t}{n_1 R_1 R_2} \right]. \quad (2.15)$$

Where  $t$  is the thickness,  $R_1$  is the radius of curvature for the first surface and  $R_2$  is the radius of curvature for the second surface. For a thin lens  $t = 0$ , and for mirror  $R_2$  not exist.

In general, the effective focal length (EFL) of an optical system consist of lenses and mirrors given by [Hud 69]:

$$\frac{1}{EFL} = \frac{1}{f_1} + \frac{1}{f_2} - \frac{d}{f_1 f_2} \quad (2.16)$$

Where  $f_1$  and  $f_2$  are the focal length of the first and second optical element, and  $d$  is the distance between them.

The previous mentioned discussion is exactly identifying the optical elements of the eye. It should be mentioned that the defocusing occurs either due to aberration existence or due to defects (a mostly physiological reason) affect the eye such a myopia or hyperopia.

The focusing in the human eye is dynamic, where the eyelens is capable to reduce or enlarge its radii of curvature when see at target object. This mechanism of the eyelens make exact focusing whether the viewed object is close or distant. As a result, the focus on the retina of the rays coming from close object is same as that of distant object, this is due to the radius of curvature of the eye lens determined for distant object imaging is greater than that of close object.

In addition, the decrease in the index of refraction through the distance from the center to the rim of the eye lens causes to make all the rays in the paraxial and meridional modes are focused in same point as shown in figure (2.3). Therefore, there is no spherical aberration happened, but may a residual spherical aberration exist as effective less traces [Hud 69].

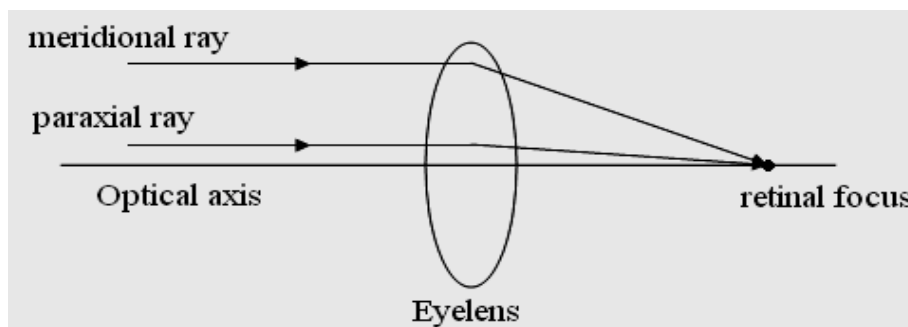


Figure (2.3): The effect of the refractive index variation [Hud 69].

While the muscles are relaxed, the lens assumes its flattest shape, providing the least refraction of incident light rays. In this state, the eye is

focused on distant objects. When the muscles are tensed, the shape of the lens becomes increasingly curved, providing increased refraction of light. In this "strained" state, the eye is focused on nearby objects. The lens is itself a complex, onion like layered mass of tissue held intact by an elastic membrane, due to the rather intricate laminar structure of fibrous tissue [Ped 88].

## 2.4 Eye Defects and Correction

Common defects of vision are due to incorrect relation between the various parts of the eye considered as an optical system. A normal eye forms on the retina an image of an object at infinity when the eye is relaxed, such eye is called emmetropic. If the far point of an eye is not at infinity, the eye is ametropic. The two simplest forms of ametropia are myopia and hyperopia [Sae 64]. In addition, the lens changes with accommodation and continuously grows with age. Therefore, to inter subject variability, the lens presents huge variations with time, both fast (or short-term, accommodation) and slow (or long-term, aging) as shown in figure (2.4).

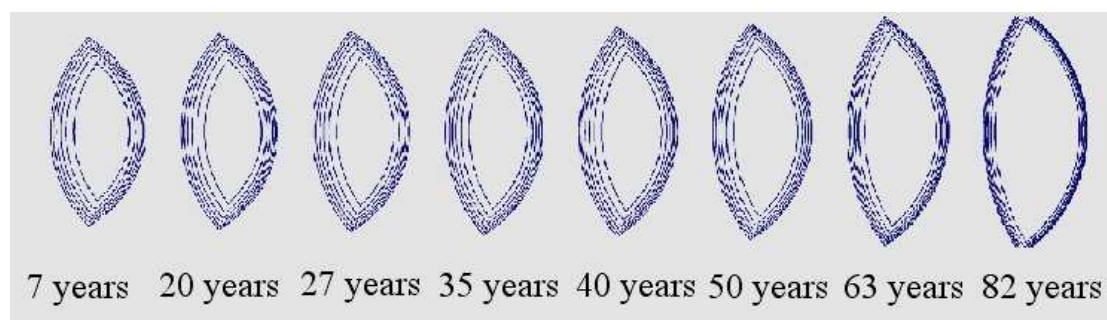


Figure (2.4): The variation of the lens curvature with age [Nav 09].

### 2.4.1 Myopia

In the myopic eye, the eyeball is too long in comparison with the radius of curvature of the cornea, and rays from an object at infinity are

focused in front of the retina. The most distant object (far point) for which an image will be formed on the retina is then nearer than infinity. On the other hand, the near point of the myopic eye, if the accommodation is normal, is even closer to the eye than is that of a person with normal vision as shown in figure (2.5) [Sae 64].

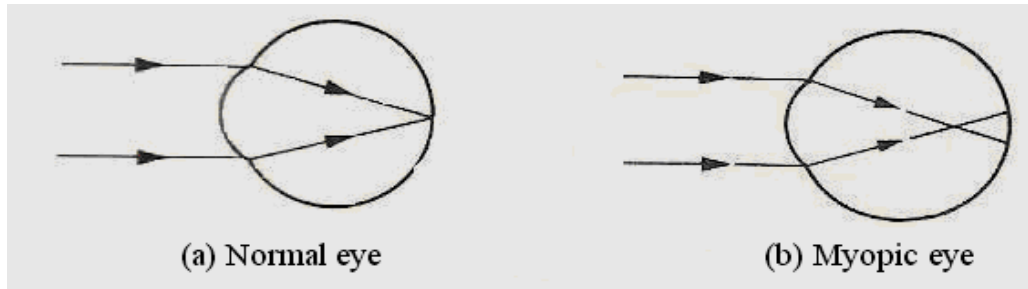


Figure (2.5): Different focusing of normal and myopic eye [Sae 64].

In order to correct myopic eye, a negative lens must be used which will form an image of such objects, not farther from the eye than the far point as shown in figure (2.6) [Sae 64].

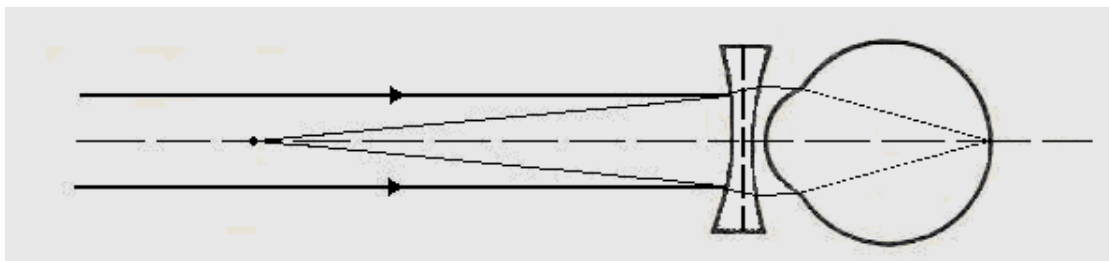


Figure (2.6): The correction of the myopic eye [Sae 64].

### 2.4.2 Hyperopia

In the hyperopic eye, the eyeball is too short, and the image of an infinity distant object would be formed behind the retina. By accommodation, these parallel rays may be made to converge on the retina but, evidently, if the range of accommodation is normal, the near point will be more distant than that of an emmetropic eye. These defects

may be stated in a somewhat different way. The myopic eye produces too much convergence in a parallel bundle of rays for an image to be formed on the retina; the hyperopic eye, not enough as shown in figure (2.7) [Sae 64].

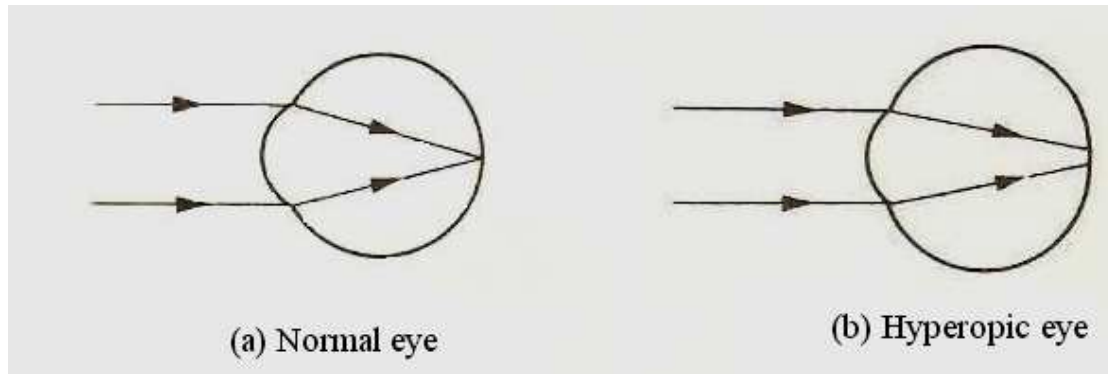


Figure (2.7): Different focusing of normal and hyperopic eye [Sae 64].

In order to correct the hyperopic eye, (this distance is usually assumed to be  $25\text{ cm}$  or  $10\text{ inches}$ ), a positive lens of  $25\text{ cm}$  focal length (or  $10\text{ inches}$ ; normal distance) is placed in the front of the eye that it forms an image of the object, at the near point. Thus the function of the lens is not to make the object appear larger, since the object and its image subtend equal angles at the lens, but in effect to move the object farther away from the eye to a point where a sharp retinal image can be formed, as shown in figure (2.8) [Sae 64].

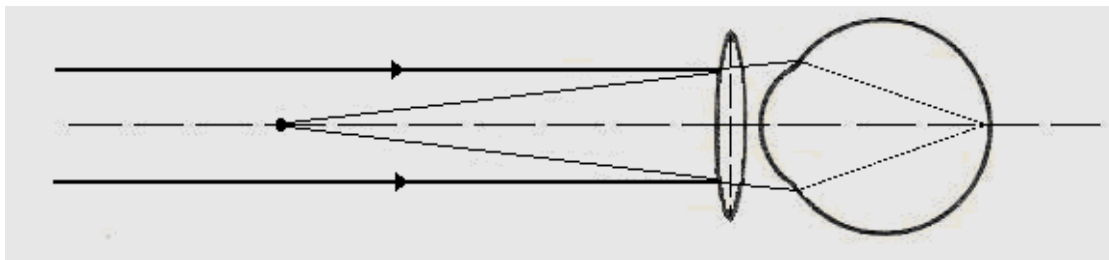


Figure (2.8): The correction of the hyperopic eye [Sae 64].

### 2.4.3 Correction Estimation

Because of the distance between the correction lens and the eye is very small in comparison with the object distance, both the correction lens and the eye are regarded contact, such that the focal length for two thin lenses in contact is given as:

$$\frac{1}{f} = \frac{1}{f_1} + \frac{1}{f_2} \quad (2.17)$$

This means that the combined power ( $P$ ) is the sum of the individual powers:

$$P = P_1 + P_2 \quad (2.18)$$

To compute the power ( $P_2$ ) of the correction lens, one can imagine that the double convex (or double concave) correction lens as being composed of two planer-convex (or planer concave) lenses in intimate contact back to back, as showing in figure (2.9):

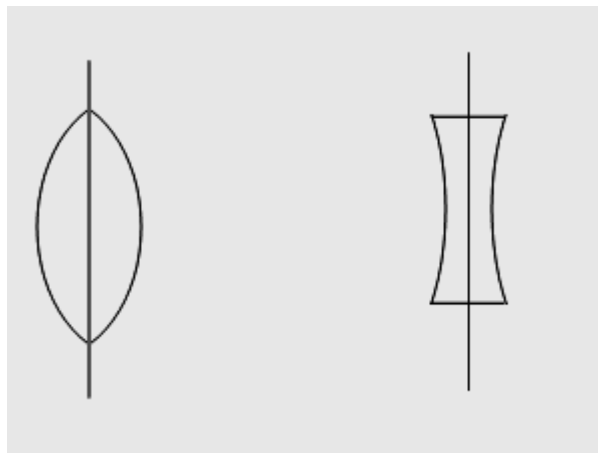


Figure (2.9): The two imaginary parts of the correction lens.

The power of each planer convex (or planer concave) lens is achieved from equation (2.15), thus for the first planer convex (or planer concave) lens ( $R_2 = \infty$ ).

$$P_{21} = \frac{(n-1)}{R_1} \quad (2.19)$$

While for the second ( $R_1 = \infty$ )

$$P_{22} = \frac{n-1}{R_2} \quad (2.20)$$

As a result, the power of the correction lens is the sum of both its parts, i.e.

$$P_2 = P_{21} + P_{22} \quad (2.21)$$

## 2.5 Factors Affecting Vision Quality

There are many factors affecting on the image quality, some of them are introduced in the following [Ham 08]:

### 2.5.1 Pupil Variation

The pupil is the important element that is affecting the vision quality because it controls the magnitude of the illumination entering the eye, this is due to the variation in the point spread function (PSF), more details are explained in the following:

#### A- Pupil Diameter versus Illumination

Illumination is the major reason to vary the pupil diameter when light enters the eye through the pupil, the brain regulates the amount of light that enters the eye by constricting or dilating the pupil of the eye. When the pupil becomes small in bright light situations, it allows less light into the eye to protect the sensitive eye nerves and also to improve the vision. In darker situations the brain order the pupil to be dilated, this allows more light to enter the eye, thus allowing better vision in lower light settings [Ste 09].

Figure (2.10) illustrates the manner in which the size of a normal pupil varies with the field brightness. One can note that the range of pupillary diameter is only about four *fold* over a range of brightness from  $10^{-2}$  to  $10^3$  *candles/m<sup>2</sup>* which is 100,000 *fold*. In account of the

relatively enormous variation in light entering the eye, the compensation by the change in size of the pupil is not enough to make best vision. Therefore, the receptive mechanism of the retina being able to adapt itself to large differences in quantity of light [Sae 64].

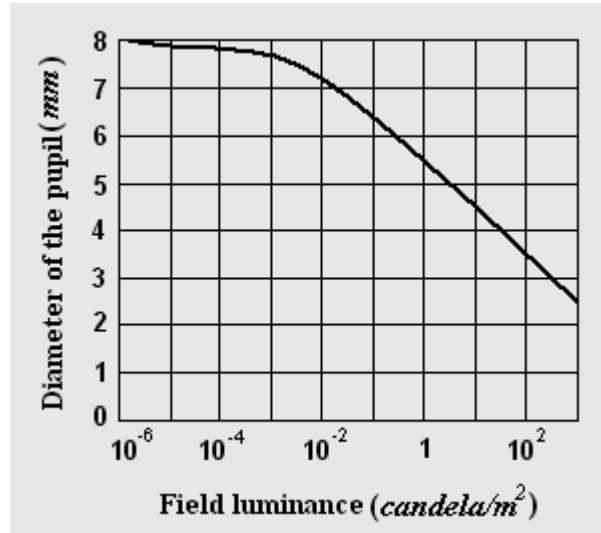


Figure (2.10): Pupillary diameter as a function of field luminance (brightness) [Sae 64].

### B- Point Spread Function versus Pupil Diameter

Due to the variation of the pupil as a response of illumination, the point spread function (PSF) is frequently affected. Rayleigh resolution criterion states that for a diffraction limited system, two point sources can just be resolved if the peak of the image of one lies on the first minimum of the other as illustrated in Figure (2.11). This distance is effectively equal to the width of the diffraction-limited intensity point spread function (PSF) that given by [Ham 08]

$$PSF_{width} = \frac{1.22\lambda f}{nD_o} \quad (2.22)$$

Where  $\lambda$  is the wavelength,  $f$  is the focal length,  $n$  is the refractive index and  $D_o$  is the pupil diameter. Hence, for a fixed wavelength, the larger the pupil the smaller the width of the PSF and the higher the resolution.

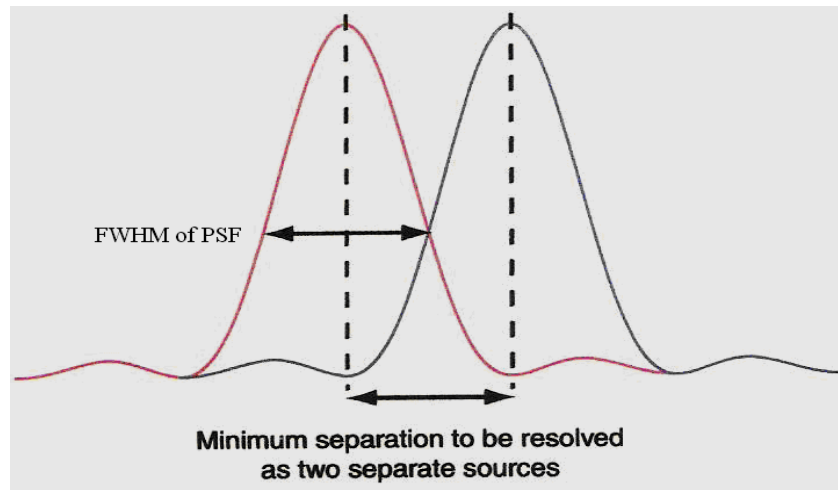


Figure (2.11): Rayleigh resolution criterion [Ham 08].

Figure (2.12) shows how the width of the PSF varies with pupil diameter  $D$ , taking  $\lambda$  as  $550\text{ nm}$ ,  $f$  as  $22.2\text{ mm}$  and  $n$  as  $1.33$ . The cone photoreceptors (which provide a color vision) are separated by around  $2\text{ mm}$  at the fovea this interpret why the vision in fovea is gray not colored. In general, for a diffraction limited the eye, the pupil needs to be greater than  $5.5\text{ mm}$  in diameter to make resolved image. Studies have shown that the eye approaches the diffraction limit for a pupil diameter of around  $3\text{ mm}$ , else greater than  $3\text{ mm}$  the image quality is limited by aberrations [Ham 08].

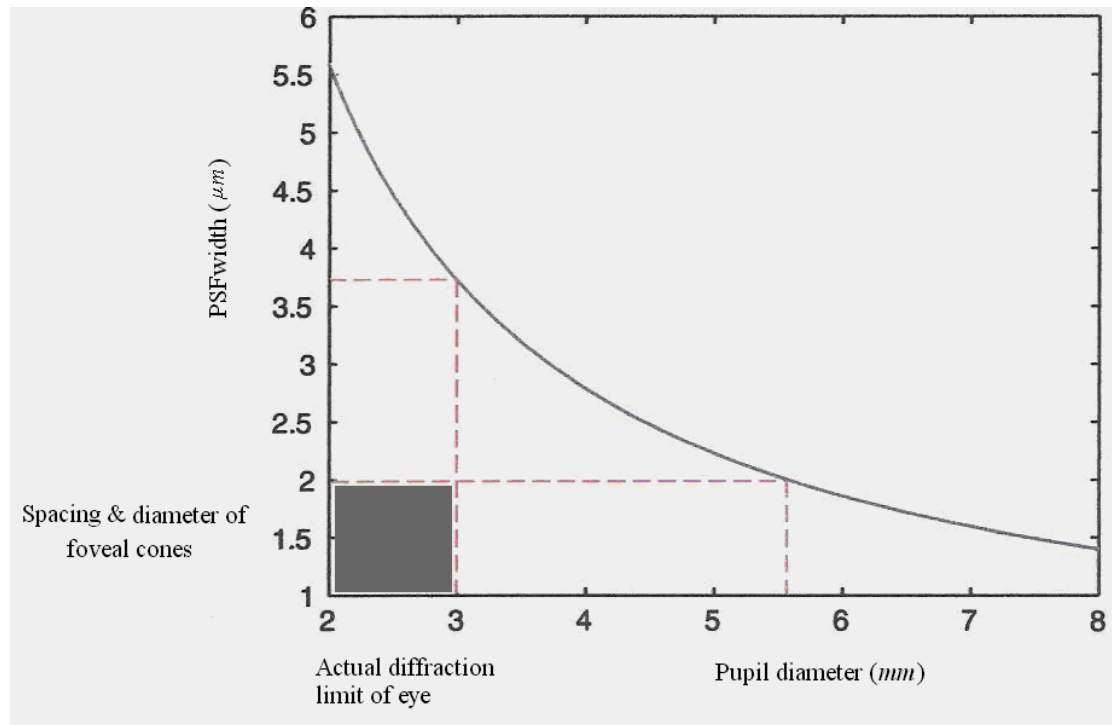


Figure (2.12): Variation in the width of the PSF with pupil diameter  
[Ham 08].

### 2.5.2 Physiological Characteristics

The *rods* and *cones* are photoreceptor cells located in the retina used to transduce light into electrical signals. Black-and-white transduction occurs in the rod shaped receptors, and color transduction occurs largely in the cone shaped receptors. The inverted retina vision system requires light to first pass through the cornea, then through the anterior chamber filled with aqueous fluid, and last, the lens, and the vitreous humor. Before reaching the retina, the light passes through the inner retina's cell layers (which contain a dense array of neural processing cells) and on past the rods and cones until it reaches the posterior (distal) end of these cells, wherein lie the so-called outer cell segments. The outer cell segments contain the photoreceptors, light-sensitive structures including the *photopigment*, where the transduction of light into receptor potentials occurs. The photopigment family of proteins

undergoes physical changes when they absorb light energy. The principal photopigment, opsin glycoprotein, is a derivative of *retinal* (a modified vitamin A molecule). Rods contain a single photopigment type called rhodopsin (rhodo meaning *rose* and opsis meaning *vision*). The cones contain one of three different kinds of photopigments called iodopsins, namely *erythrolabe* (most sensitive to red), *chlorolabe* (most sensitive to green) and *cyanolabe* (most sensitive to blue). Vision functions by changes in the retina photopigments molecule caused by light [Ber 09]. The molecule has a bent shape (*cis-retinal*) in darkness, and when it absorbs light, isomerization occurs, causing the molecule to form the “straight” form (*trans-retinal*). This causes several unstable intermediate chemicals to form, and, after about a minute, the *trans-retinal* form completely separates from opsin, causing the photopigment to appear colorless (for this reason the process is called bleaching). In order for the rods and cones to again function for vision, retinal must be converted from the *trans* back to the *cis* form. This resynthesis process, called regeneration, requires that the retina pigment epithelium (RPE) cells be located next to the rod and cone outer segments [Ber 09].

### 2.5.3 Field of View

Field of view refers to the maximum angle between the directions of two sources that can still be seen at the same time. For example, consider the ubiquitous tiger and tree combination. The images of these two items would fall on your retina as shown in figure (2.13):

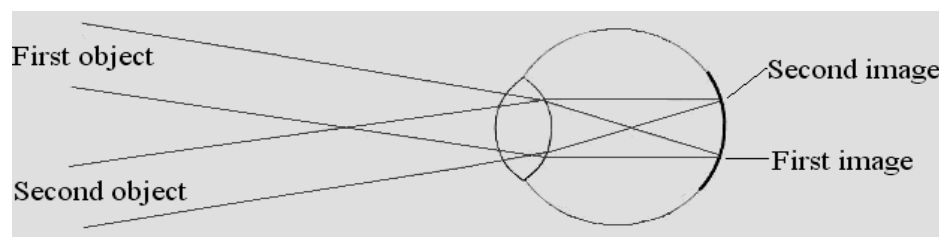


Figure (2.13): The image of the two objects [Ker 04].

Drawing the central rays for the light from these two sources gives the following diagram.

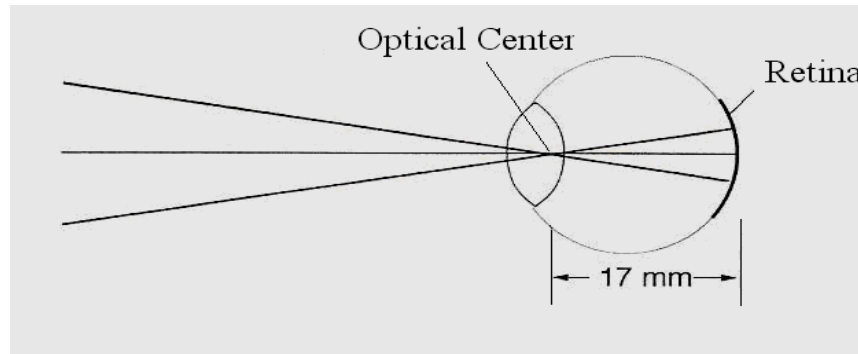


Figure (2.14): The optical center [Ker 04].

The rays are drawn through the "optic center" of the eye, (which is the point through which all the central rays pass in progressing through to the retina as shown in figure (2.14)). Because of the refractive properties of the protuberance and of the inner parts of the eye, optical center is not exactly at the entrance of the eye but inside at 17 *mm* from the retina. In fact, a relatively small angle for the eye to cover. The retina on each eye can cover an angle of about 120 degrees; 60 *degrees* on either side of central vision. If it weren't for the nose, which limits the FOV of each eye to about 45 *degrees* on the nose side, as shown in the figure (2.15), each eye would therefore have a FOV of 120 *degrees*. However, this full field of 120 *degrees* is only achievable with two eyes [Ker 04].

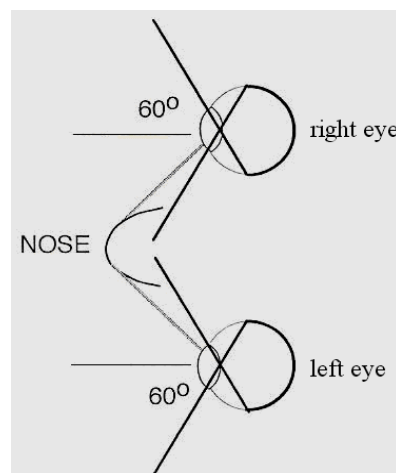


Figure (2.15): The effect of the nose on the field of view [Ker 04].

While the eye has a large FOV, it would make an extremely poor camera. This is because in its whole FOV there is only one very small region at its exact center where the view is clear. This region is called the "fovea" and it is only about  $0.2 \text{ mm}$  in diameter. In a slice through the retina it is seen to be a slight depression. Because of conical shape, vision from the side becomes more magnified. Each of these cones sends its pulses directly into the neural network within the retina. It seems that this is the reason for the depression of the fovea relative to the surrounding retina. The sensing surfaces have to be close to the far retina wall, each cone is only about  $2\mu\text{m}$  in diameter at their receptor end. Although they are very small, their size puts a limit on the detail that can be seen in any object in front of the eye. If that object is at a comfortable viewing distance of  $250 \text{ mm}$ , then the smallest dot that can be seen as a separate entity in that object would be one that subtends an angle  $\theta$  at the eye that is the same as that subtended by one cone of the fovea. (Its image would just cover the receptor surface of one of the cones) [**Ker 04**].

Since the fovea (the point on the retina have only cones without rods) is  $17 \text{ mm}$  from the optic center of the eye, one cone will subtend an angle of

$$\theta = \frac{2 \times 10^{-6}}{17 \times 10^{-3}} = 6.8 \times 10^{-5} \text{ degree}$$

A dot which subtends this angle at a distance of  $250 \text{ mm}$  has a diameter  $d$  given by

$$\frac{d}{0.25} = 1.2 \times 10^{-4}$$

$$d = 3 \times 10^{-5} \text{ m} = 0.03 \text{ mm}$$

The fovea only has a diameter of about  $0.2 \text{ mm}$ , or  $200 \mu\text{m}$ . Thus the angle of clear vision is only about 100 times that of the resolution, or

about 12 *mrad*. At a reading distance of 250 *mm* this is a spot diameter of 3 *mm* [Ker 04].

#### 2.5.4 Eye Movement

Movements of the eyes are of significance in relation to visual optics from two major points of view. First, since both optical and neural performances are optimal on the visual axis, the eye movement system must be capable of rapidly directing the eyes so that the images of the detail of interest fall on the central foveas of both eyes where visual acuity is highest ( *gaze shifting* leading to *fixation* ). A scene is explored through a series of such fixational movements for different points within the field. Second, the system must be capable of maintaining the images on the two foveas both when the object is fixed in space (*gaze holding*) and, ideally, when it is moving. Any lateral movement of the images with respect to the retina is likely to result in degraded visual performance, due to the limited temporal resolution of the visual system and the fall-off in acuity with distance from the central fovea [Bas 95].

These challenges to the eye movement control system are further complicated by the fact that the eyes are mounted in what is, in general, a moving rather than a stationary head. Movements of the eyes therefore need to be linked to information derived from the vestibular system or labyrinth of the inner ear, which signals rotational and translation accelerations of the head. The compensatory *vestibulo-ocular responses* take place automatically (i.e., they are reflex movements) whereas the fixational changes required to foveate a new object point are voluntary responses. Details of the subtle physiological mechanism which have evolved to meet these requirements will be found elsewhere [Bas 95].

## 2.6 Image Quality Measurements

The image quality are measured by many optical functions, the most interest ones are discussed in the following :

### 2.6.1 Resolution versus Point Spread Function (PSF)

An optical system is said to be able to resolve two point sources if the corresponding diffraction patterns are sufficiently small or sufficiently separated to be distinguished.

Lord Rayleigh concluded that two equally bright point sources could just be resolved by an optical system if the central maximum of the diffraction pattern of one source coincided with the first minimum of the other. This is equivalent to the condition that the distance between the centers of the patterns shall equal the radius of the central disc. The Rayleigh limit of resolution is illustrated in figure (2.16) [Sae 64]:

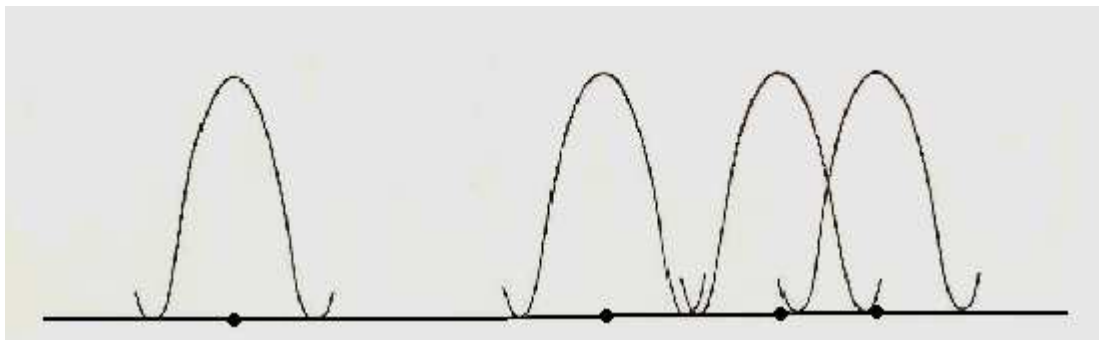


Figure (2.16): Intensity distribution in the diffraction patterns [Sae 64].

The diffraction patterns at the left are separated by a distance much greater than the radius of the central disc, and are clearly resolvable. The distance between the centers of the patterns at the right is very nearly equal to the radius of the central disc and evidently, if this distance were any less, the patterns would overlap to such an extent that they could not be distinguished as two. Although the diameter of the pupil of the eye varies with the level of illumination, it is customary in calculation of its

limit of resolution to assume a pupillary diameter of 2 mm, or a radius  $D/2$  of 1 mm. Let us assume a wavelength  $\lambda_0$  of 550 nm, to which the eye is most sensitive. Objects viewed with the unaided eye are in air, so  $n = 1.00$ . At the minimum reading distance of 25 cm (or 250 mm), the sine of the half-angle  $u$  of light admitted by the eye is very nearly

$$n \sin u = NA \quad (2.23)$$

Where  $NA = \frac{1}{D/2}$ , is the numerical aperture.

$$n \sin u = \frac{1}{250} = 0.004$$

since  $n = 1$ , the maximum numerical aperture of the eye is

$$NA = 0.004$$

Hence according to the Rayleigh criterion, the linear separation of two just resolvable point objects at a distance of (25 cm) is [Sae 64]:

$$\begin{aligned} z &= \frac{0.61\lambda_0}{NA} & (2.24) \\ &= \frac{0.61 \times 550 \times 10^{-7}}{0.004} \\ &= 6.6 \times 10^{-3} \text{ cm} \\ &\approx \frac{1}{10} \text{ mm.} \end{aligned}$$

Where  $z$  is the linear distance, This separation is good agreement with the actual limit of resolution of a normal eye [Sae 64].

Geometrical optics predicts that the image of a point produced by an image forming optical system is a point; such system is ideal and the point separation represented by delta function as shown in figure (2.17-a). Thus, PSF for a normalized illumination given as follows

$$\begin{aligned} PSF &= 1 && \text{at the center} \\ PSF &= 0 && \text{otherwise} \end{aligned}$$

In the perfect optical system, the PSF is the *Airy disc*, which is the Fraunhofer diffraction pattern for a circular pupil (i.e. there are diffraction

rings centered at the image plane) as shown in figure (2.17-b) this description is identifying the emmetropic eye [Wil 72].

The image looks clear and well resolved since the distance between each two photoreceivers (rods or cons) in retina is less than the resolution conditional distance determined by Rayleigh criterion. In the case of ametropic eye, PSF seems to be a small blurred spot with more separation width, the formed image of such PSF looks smoother and bluer due to defocusing. Thus the average  $\overline{\text{PSF}}$  is taken into account, which by the way lead to less image resolution [Wil 72].

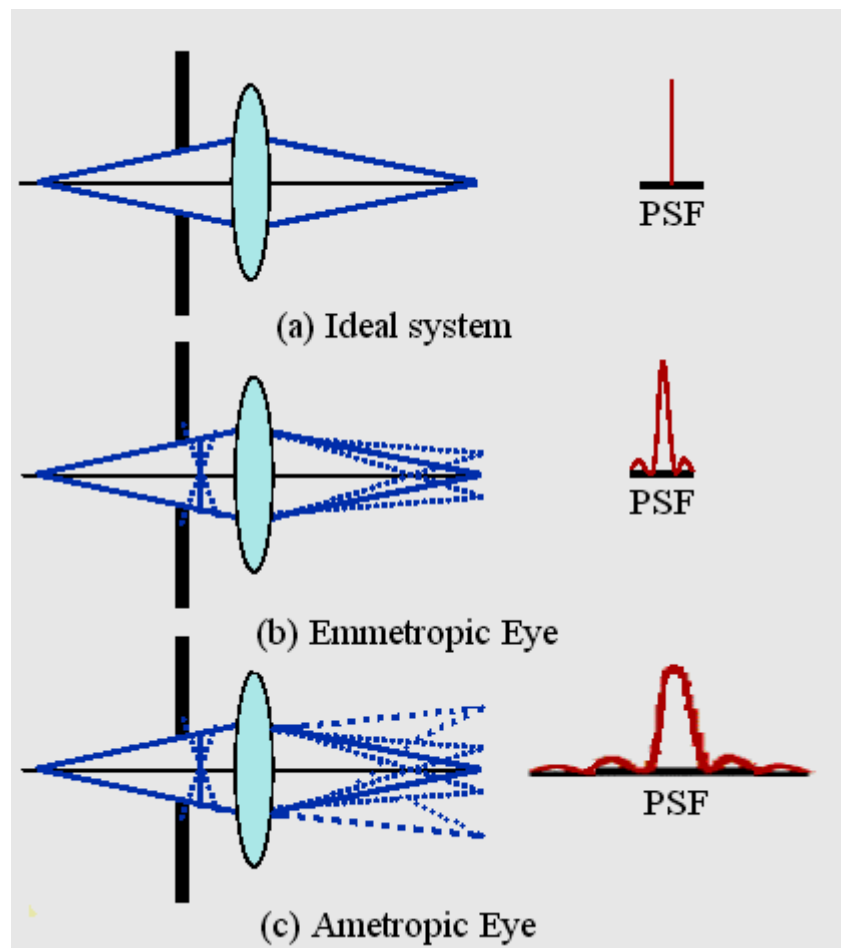


Figure (2.17): PSF of ideal system, emmetropic and ametropic eye [Wil 72].

### 2.6.2 Contrast and Modulation Transfer Function (MTF)

The term contrast is usually refers to the range of recognizable shades of gray (or colors) between the dimmest and brightest parts of an object or image. The contrast  $C$  is defined by [Wil 89]:

$$C = (W_{\max} - W_{\min}) / (W_{\max} + W_{\min}) \quad (2.25)$$

where  $W_{\max}$  and  $W_{\min}$  is the maximum and minimum flux density in the *picture* or field respectively. Because of the resemblance of this definition to that of amplitude modulation in communication theory,  $C$  is sometimes referred to as modulation contrast.

In a given optical system, the optical transfer  $T_c$  is a function of spatial frequency and is usually presented as a plot against a frequency on the abscissa; the modulus of this function is called the modulation transfer function MTF. When this magnitude function is abetted by a corresponding phase function, specifying the relative phase angle as a function of frequency, the combination is called the optical transfer function *OTF*. The phase part of the combination is the phase transfer function *PTF*. To express magnitude and phase simultaneously, the *OTF* is put in complex form [Wil 89]:

$$OTF(w) = T(w) \exp[i\phi(w)]. \quad (2.26)$$

in which  $T$  is the *MTF* and  $\phi$  is the phase difference.

The resolution and contrast of an optical system design can be characterized by the modulation transfer function, which is a measurement of the system design ability to transfer contrast from the spatial domain into the frequency domain at a specific resolution. Computation of MTF is a mechanism that is often utilized by optical manufactures to incorporate resolution and contrast data into a single specification [Wil 89]. The MTF curve has different meanings according to the corresponding frequency. Its height at frequencies of (1.5

*cycles/degree*) represents the contrast behavior of the optical system [DeA 07].

Frequencies in the gap of 3 to 12 or higher *cycles/degree* represent the sharpness-ability of a lens. MTF readings taken at 12 *cycles/degree* indicate how good a lens can transmit very fine structures. For an optimal quality based on the human eye, the lens should perform over 50% at 6 *cycles/degree*. Perceived image sharpness is more closely related to the spatial frequency where MTF is 50% (0.5), where contrast has dropped by half. Typical 50% MTF frequencies are in the vicinity of 12 to 24 *cycles/degree* for individual components and often as low as 9 *cycles/degree* for entire imaging systems [DeA 07]. Figure (2.18) shows the MTFs of the emmetropic and ametropic eyes.

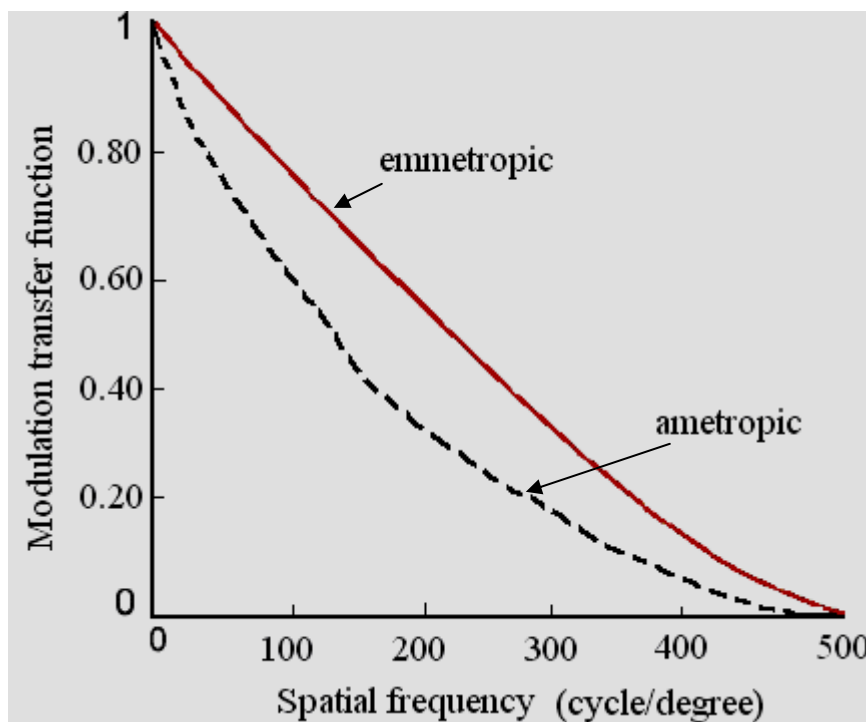


Figure (2.18): MTFs of emmetropic, and ametropic eyes [DeA 07] .

### 2.6.3 Spot Size and Spot Diagram

When a system of rays originally at a single object point is constructed, so that the rays are uniformly distributed over the entrance pupil, the plot of their consequent intersections with the image plane is called a *spot diagram*. The size of spot diagram shows to extent of the energy distribution and the shape is due to the type of aberration. When the spot diagram has been reduced to a size comparable to that of the central fringes in a diffraction pattern, ray theory causes to be as useful as wave theory [Wil 89].

Practically, the accumulation of the rays at the image plane follow *Gaussian distribution* taking into account the image point shift due to the diffraction. Thus, the image spot consists of rings surrounded the bright central spot as shown in figure (2.19a) for emmetropic eye. Whereas, the spot diagram for the ametropic eye is same in shape but larger in size, as shown in figure (2.19b) [Fun 04].

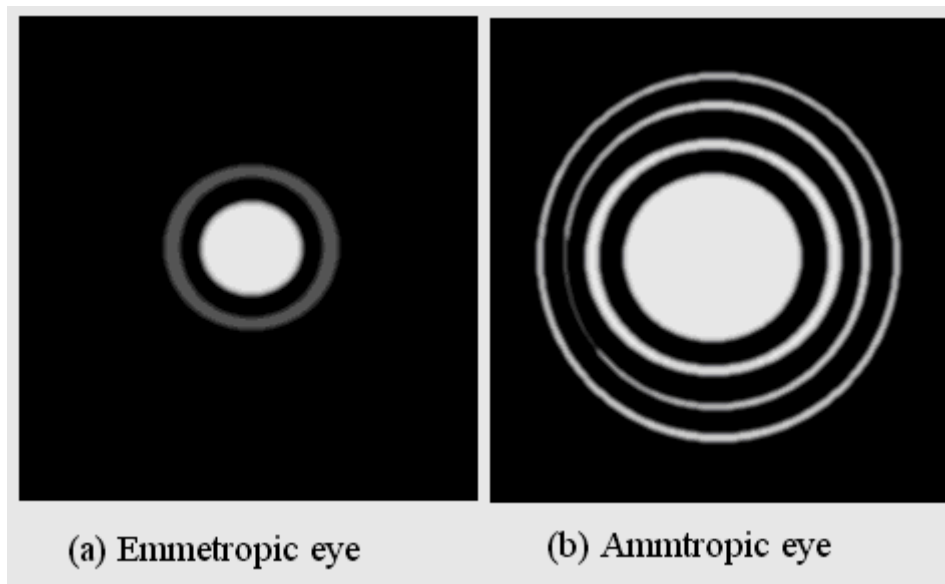


Figure (2.19): Spot distribution [Fun 04].

The spot size ( $Z$ ) is an important parameter since it determines the optical system efficiency. Theoretically the following relationship gives the size of the spot formed by a single lens under diffraction limited

condition. The diameter of the first dark ring of the Airy rings is given by:

$$Z = 2.44\lambda(f / no) \quad (2.27)$$

$$f / no = \frac{f}{D_o} \quad (2.28)$$

where  $f$  is the effective focal length, and  $D_o$  is the diameter of the aperture. The effective diameter of the blur is one half of equation (2.22) in micrometer.

Practically, some modifications should be imposed on equation (2.22) to compute spot size formed by the eye. The modification includes adding the spherical aberration term. Hence, the size of the spot formed by the eye can be calculated from the following equation [Sco 59].

$$Z_T = 2.44\lambda(f / no) + \frac{Af}{(f / no)^3} \quad (2.29)$$

where  $A$  is a constant given by the following expression [Sco 59]:

$$A = \frac{n+2}{n(n-1)^2}R^2 - \frac{4(n+1)}{n(n-1)}R + \frac{3n+2}{n} + \frac{n^2}{(n-1)^2} \quad (2.30)$$

and  $R = \frac{R_2 + R_1}{R_2 - R_1} \quad (2.31)$

where  $R_1, R_2$  are the radii of the lens, and  $n$  being the refractive index of the last lens in the optical system [Smi 66].

## 2.7 Material Properties of Human Eye

The optics of the eye are not completely transparent across the range of visible wavelengths. Even though almost all red light incident on the cornea reaches the retina, a significant fraction of light toward the blue end of the spectrum does not, and the amount of light that is absorbed changes dramatically as the eye ages. All of the optical components, including the aqueous and vitreous, act as band-pass filters

in the human eye. But the cornea and the vitreous have bandwidths that essentially exceed the visible spectrum. The lens, on the other hand, has significant absorption at the blue end of the visible spectrum, cutting off most of the light below 400 nm [Roo 09].

### 2.7.1 Refractive Index and Dispersion Coefficient

The velocity of propagation of light wave in vacuum is approximately  $3 \times 10^8$  m/s. In other media the velocity is less than in vacuum. The ratio of the velocity in vacuum to the velocity in medium is called the index of refraction of that medium ( $n$ ).

$$n = \frac{c}{v} \quad (2.32)$$

where  $c$  is the velocity of light in vacuum and  $v$  is the velocity of light in medium [Smi 08]. The index of refraction of an optical material varies with wavelength as indicated in figure (2.20) [Smi 66]:

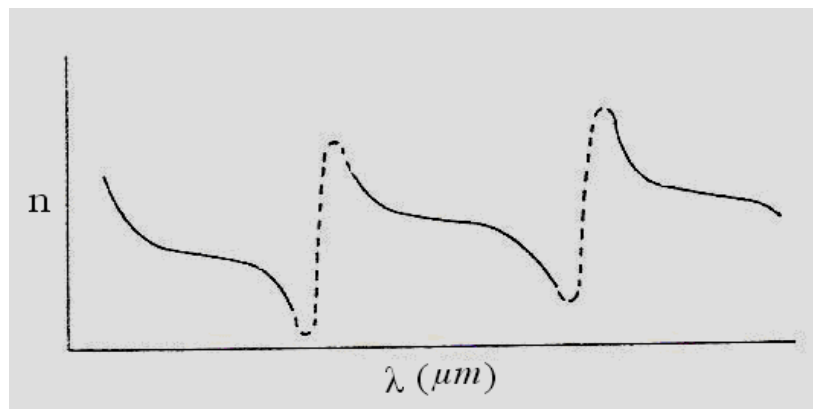


Figure (2.20): The variation of index of refraction with wavelength [Smi 66].

Because the index of refraction of the lens is 1.406 (at 0.5876  $\mu\text{m}$ ) in the central portion and reduces to 1.386 at the edge of the lens, a radial gradient formula was used for this, listed as eyelens in the above lens prescription. A photopic wavelength and weightings were used. The equation to account for dispersion in Eyelens is [Lai 06]

$$N_{oo} = 1.406 - 0.034 \times 10^{-8} \lambda^2 \quad (2.33)$$

where  $\lambda$  is in nanometers.

Since the refractive index for the vitreous material (between the lens and the retina) is nearly the same as that between the cornea and the lens, aqueous data was used for both materials. The refractive index for the cornea and the aqueous was fitted using a Conrady formula [Lai 06] (the Conrady equation is empirical and designed for optical glass in visible region) [Smi 08]:

$$N = N_o + \frac{A}{\lambda} + \frac{B}{\lambda^{3.5}} \quad (2.34)$$

Where  $N_o$ ,  $A$ , and  $B$  are the dispersion coefficients.

The variation in index with wavelength is called dispersion; when used as a differential it is written  $dn$ , otherwise dispersion is given by  $\Delta n = n_{\lambda_1} - n_{\lambda_2}$ , where  $\lambda_1$  and  $\lambda_2$  are the wavelength of the two colors of light for which the dispersion is given. *Relative* dispersion is given by  $\Delta n / (n - 1)$  and, in effect, expresses the "spread" of the colors of light as a fraction of the amount that light of a medium wavelength is bent. Figure (2.21) shows the dispersion of the white light between two surfaces [Smi 08]. For the human eye the magnitude of the dispersion coefficient is given in table (2-1):

Table (2-1): The magnitude of the dispersion coefficient of the eye [Lai 06].

Material	$N_o$	$A$	$B$
Aqueous	1.32420	0.0048714	0.00054201
Cornea	1.26536	0.0883011	-0.00616611

This yields a value of 1.336 at  $0.5876 \mu m$  for the aqueous and 1.376 for the cornea [Lai 06].

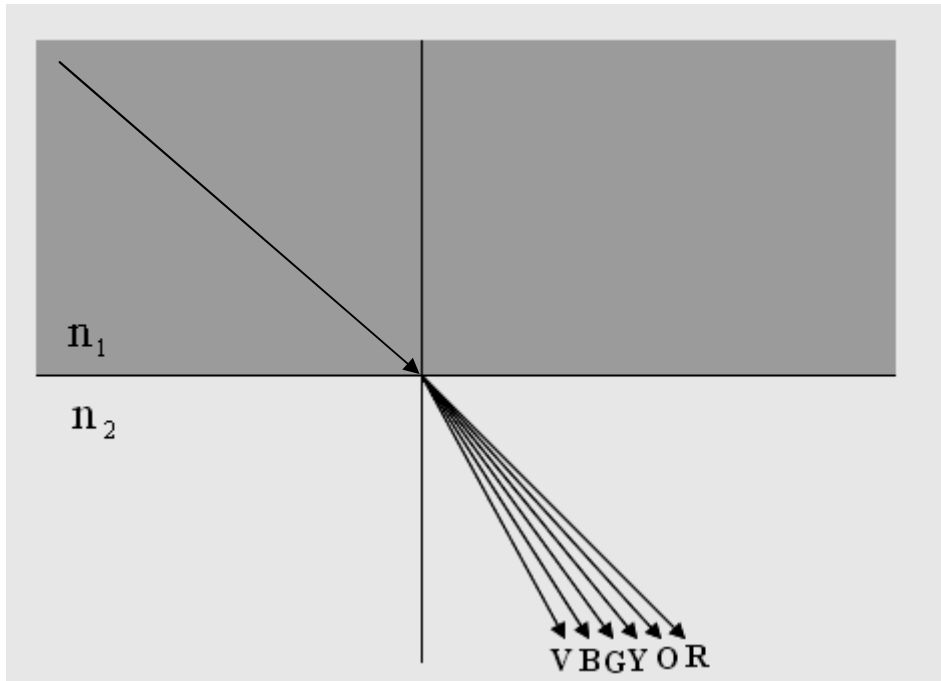


Figure (2.21): The dispersion of the white light between two surfaces (Violet, Blue, Green, Yellow, Orange, Red) [Smi 08].

### 2.7.2 Transmittance and Density

Boettner and Wolters published a comprehensive study of the contributions of light components by directly measuring spectral transmission of freshly enucleated donor eyes. Their results may suffer from postmortem artifacts, but the graph is reproduced as shown in Figure (2.22) because the data are presented in an informative way that illustrates the lens contribution relative to the other components and the cumulative effect of the absorbing tissue. The absorbance of blue light in the crystalline lens is commonly referred to as “yellowing” of the human lens. This yellowing of the lens increases dramatically as it ages [Roo 09].

The lens optical density toward the blue wavelengths increases by about 0.1 to 0.15 *log units per decade*, provided that we assume that components other than the lens change little as they age. Accelerations in this rate have been found for eyes over age 60, and it is proposed that this

increase is due to the prevalence of cataract in that age group. When eyes that had cataract were excluded from the study, it was found that a linear increase in optical density versus age was maintained. The optical density of the lens is highly variable. The optical density for any given age group might span 0.8 *log units* or more [Roo 09].

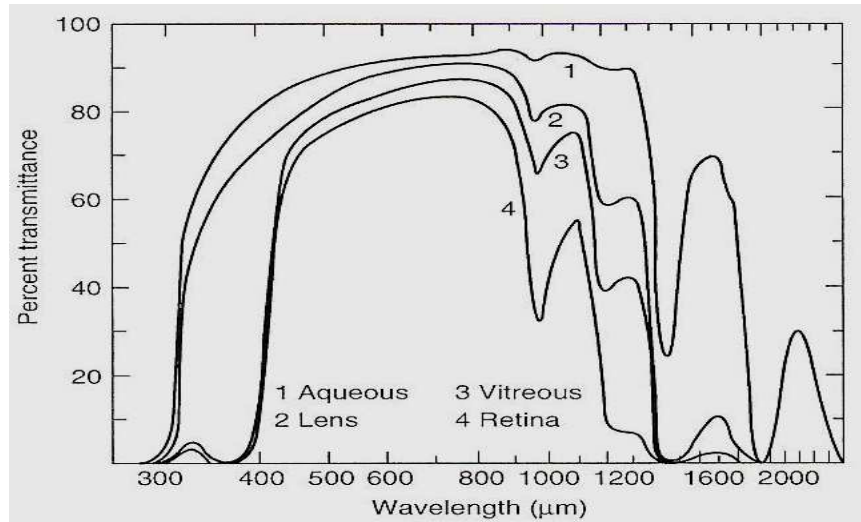


Figure (2.22): Total transmittance at the various anterior surfaces [Roo 09].

The reflection ( $R$ ) of the two medium is given by

$$R = \frac{(n' - n)^2}{(n' + n)^2} \quad (2.35)$$

Where,  $n$  and  $n'$  are the refractive indices of the two media.

The transmission of the first surface (attached to air;  $n' = 1$ ) is given (from equation 2-30) as [Roo 09]:

$$T = 1 - R = 1 - \frac{(n - 1)^2}{(n + 1)^2} = \frac{4n}{(n + 1)^2} \quad (2.36)$$

Now the light transmitted through the first surface (cornea) is partially transmitted by the medium and goes on to the second surface, where it is partly reflected and partly transmitted. The reflected portion passes (back) through the medium and is partly reflected and partly transmitted by the

first surface, and so on. The resulting transmission can be expressed as the infinite series [Smi 66]:

$$T_{1,2} = T_1 T_2 (K + K^3 R_1 R_2 + K^5 (R_1 R_2)^2 + K^7 (R_1 R_2)^3 + \dots) = \frac{T_1 T_2 K}{1 - K^2 R_1 R_2} \quad (2.37)$$

where  $T_1$  and  $T_2$  are the transmissions of the two surfaces,  $R_2$  and  $R_1$  are the reflectances of the surfaces, and  $K$  is the transmittance of the medium between them. (This equation can also be used to determine the transmission of two or more elements, e.g. flat plates, by finding first  $T_{1,2}$ , then using  $T_{1,2}$  and  $T_3$  together and so on.)

If we set  $T_1 = T_2 = 4n / (n+1)^2$  from equation (2.31) into equation (2-32), and assume that  $K = 1$ , we find that the transmission, including all internal reflections, of a completely non-absorbing plate is given by [Smi 66]:

$$T = \frac{2n}{(n^2 + 1)} \quad (2.38)$$

Similarly, the reflection is given by [Smi 66]:

$$R = 1 - T = \frac{(n-1)^2}{(n^2 + 1)} \quad (2.39)$$

It should be emphasized that the transmission of a material, being wavelength dependent, may not be treated as a simple number over any appreciable wavelength interval. For example, suppose that the filter is found to transmit 45% of the incident energy between 1 and 2 microns. It cannot be assumed that the transmission of two such filters in series will be  $0.45 \times 0.45 = 20\%$  unless they have a uniform spectral transmission (neutral density). To take an extreme example, if the filter transmits nothing from 1 to 1.5 microns and 90% from 1.5 to 2 microns, its "average" transmission will be 45%. However, two such filters, when combined, will transmit zero from 1 to 1.5 microns, and about 81% from

1.5 to 2 microns, for an "average" transmission of about 40%, rather than the 20% which two neutral density filters would transmit [**Smi 66**].

The density of a filter is the log of its opacity (the reciprocal of transmittance), thus [**Smi 66**]:

$$D = \log \frac{1}{T} \quad (2.40)$$

where  $D$  is the density and  $T$  is the transmittance of the material. Note that transmittance does not include surface reflection losses; thus, density is directly proportional to thickness. To a fair approximation, the density of a "stack" of filters is the sum of the individual densities [**Smi 66**].

*Chapter Three*

**MODELING  
AND  
ALGORITHMS**

## **Chapter Three**

### **Modeling and Algorithms**

#### **3.1 Introduction**

The human eye is a fantastic configuration of optical elements that adapted optical features to fit different situations of the imaging process. The eye makes auto-focusing according to the distance of the visual object, and it decreases or increases the pupil size (aperture) according to the illumination of the visual object, and so on other wonderful operations. These operations cannot be found in a man-made optical system, since they depend on special material characteristics (for example; the variation of the refractive index with the radius of the eye lens). Therefore, the eye gains a special importance that necessitates studying the behavior of such optical system and then putting forward a mathematical model to describe the different behavior of the eye corresponding to different situations of imaging, which prepares for the designing stage. The defects of the eye are also taken into mind through modeling and designing. In this chapter the optimal design for the human eye is established based on the genetic algorithm. The eye is assumed to consist of two optical elements: cornea and eye lens, whereas the remaining contents are just supplements for these optical elements. The optimal eye design is obtained by genetic algorithm with some restrictions related to the determination of the generic structure of the eye.

#### **3.2 Genetic Algorithm (GA)**

Genetic algorithm is an efficient search algorithm that simulates the adaptive evaluation process of a natural system. It has been successfully applied to many complex problems such as time scheduling optimization

and traveling salesman problems. The GAs have the following elements and operators [Daw 08]:

### **1- Random generation**

This process involve generate many of the chromosomes for the next step [Daw 08].

### **2- Objective computation**

The key element in GAs is the selection of a fitness function that accurately quantifies the quality of candidate solutions; a good fitness function enables the chromosomes to effectively solve a specific problem [Daw 08].

### **3- Selection**

Another key element of GAs is the selection operator which is used to select chromosomes (called parents) for mating in order to generate new chromosomes (called offspring). In addition, he selection operator can be used to select elitist individuals. The selection process is usually biased toward fitter chromosomes [Daw 08].

### **4- Crossover (Regeneration)**

Crossover is "the main explorative in GAs". Crossover occurs with a user-specified probability; called the crossover probability  $P_c$ .  $P_c$  is problem dependent with typical values in the range 0.4 and 0.8 [Daw 08].

### **5- Mutation**

Mutation is performed after crossover by randomly choosing a chromosome in the new generation to mutate. We then randomly choose a point to mutate and switch that point [Daw 08].

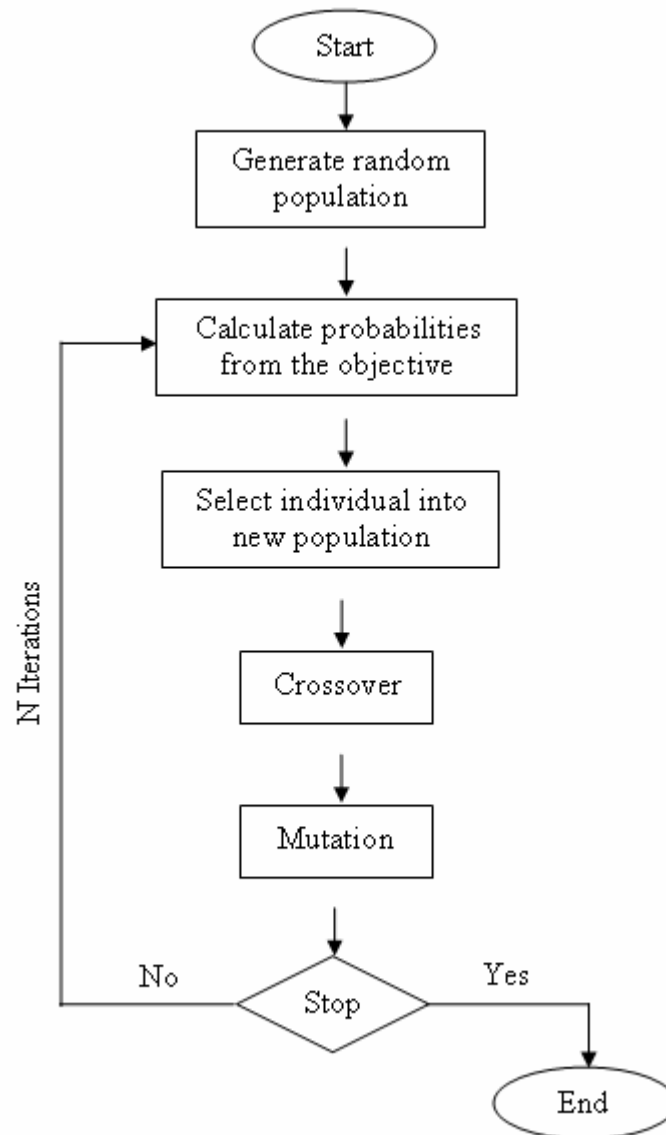


Figure (3.1): Block diagram shows the general genetic algorithm [Daw 08].

### 3.3 Genetic Algorithm based Eye Design

Genetic algorithm (GA) is employed to find out (designing) optical system of human eye, with determining its optical features for each element. The proposed approach assumes that the eye is consisting of just two optical elements; cornea and eyelens. The remaining parts are: pupil which is just a stop link between them, aqueous and vitreous are the

media in which the ray translated, and retina is a screen that presents the image. Literatures refer to that the index of refraction is approximately taking same value in different human eye; such that it is assumed to be fixed at its given average values, whereas other parameters (such as radius of curvature  $R$ , thickness  $t$ , distance between them  $d$ , and diameter  $D$ ) are assumed to be variable and their values can be optimized to achieve the fit focusing situation. Table (3-1) presents all the components of the human eye; fixed (f) and variable (v), according to the proposed approach.

Table (3-1) shows the fixed (f) and variable (v) parameters of optical element.

Optical element	Optical features							
	$R_1$	$R_2$	$t$	$D$	$d$	$n_o$	$n_1$	$n_2$
Cornea	v	v	v	v	v	f	f	f
Eye lens	v	v	v	v	v	f	f	f

The process of applying the GA on the assumed eye needed first to govern the path of the algorithm to be in the correct direction. This requires assuming two important processes: **First**, determining the variable optical parameters in the eye and then setting the minimum and maximum limits for such parameters. **Second**, finding out a proper fitness functions to measure the competence of the resulted eye design.

In GA implementation, each optical design is assumed to be an individual chromosome consists of a set of genes representing the optical parameters;  $R_1$ ,  $R_2$ ,  $D$ ,  $d$ ,  $t$ ,  $n_o$ ,  $n_1$ , and  $n_2$ . The collection of individuals is the population size ( $P_s$ ) of each generation. The genes of each individual in the first generation are chosen randomly from the range of varying each parameter (between the minimum and maximum values). The second generation is given birth by crossover the best individual

chromosomes found in the first generation, best individual is chosen according to assumed objective function. Thus, the second generation is mostly better than the first one, also the third generation is better than the second, and so on even achieving the last generation. The last generation consists of  $P_s$  individual chromosomes (eye design). The way of applying the GA approach till achieving the optimum design is clearly explained in the following sub sections:

### **3.3.1 Gene Restrictions**

In order to make the cornea is always positive (meniscus) with actual size, some restrictions it must be put for the random generation routine. Not the cornea only, but all the optical elements in the eye should be restricted. Therefore, it is necessary to determine the minimum and maximum limits for each gene to be a predefined information input the random generation routine. Thereby, genes in the first generation will be chosen randomly from their range between the minimum to maximum limits. Gene values are taken with single precision (real number). The following table shows the predefined information of the considered restriction parameters.

Table (3-2) Information table: suggested restriction parameters.

Optical element	Gene	Min limit (mm)	Max limit (mm)
Cornea (aspheric)	$R_1$	6.2	7.7
	$R_2$	6.5	7.8
	$T$	0.5	0.8
	$D$	8	8.4
	$d$	3.2	3.6
	$n_o$	1	1
	$N_1$	1.376	1.376
	$N_2$	1.333	1.333
Eyelens	$R_1$	7.1	7.8
	$R_2$	-5	-6
	$T$	2.5	2.6
	$D$	7	7.8
	$d$	16.425	16.645
	$n_o$	1.333	1.333
	$n_1$	1.38	1.402
	$n_2$	1.336	1.336

### 3.3.2 Eye Design Optimization

The variety of the refractive index of the eyelens should be fitted by a behavioral description model. Since there are just two available values from literatures (1.406 at the center of the eye lens, and 1.38 at its rim), this necessitate the fitting to be linear as follows:

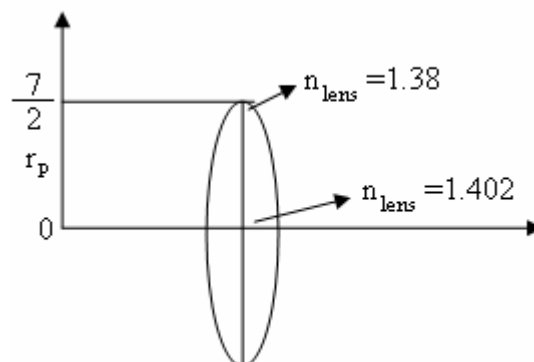


Figure (3.2): Eyelens.

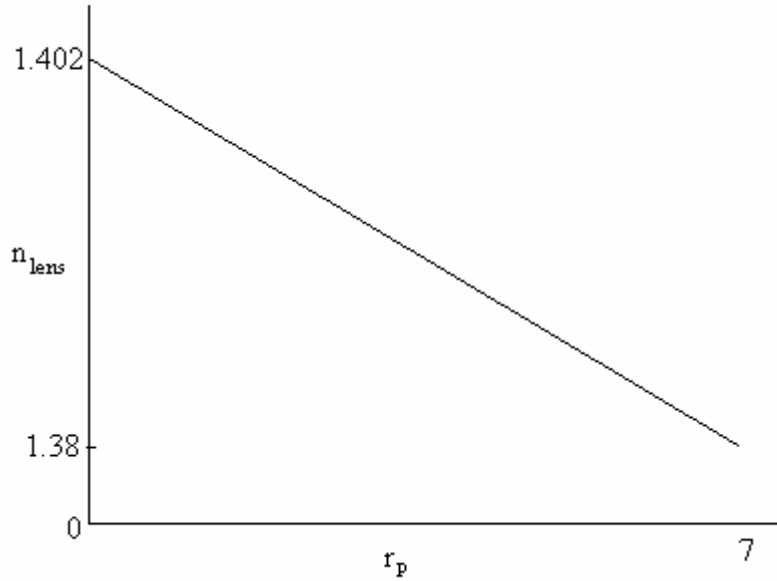


Figure (3.3): Fitting of refractive index of eyelens.

$$n_{lens} = ar_p + b \quad (3.1)$$

By substitute the given values of  $r_p$  and its corresponding  $n_{lens}$ , we get the following two equations:

$$1.402 = a(0) + b \quad (3.2)$$

$$1.38 = a\left(\frac{7}{2}\right) + b \quad (3.3)$$

Using Grammer method, one can solve the above two equations as follows:

$$a = \frac{\begin{vmatrix} 1.406 & 1 \\ 1.380 & 1 \end{vmatrix}}{\begin{vmatrix} 0 & 1 \\ 3.5 & 1 \end{vmatrix}} = \frac{1.406 - 1.380}{0 - 3.5} = \frac{0.22}{-3.5} = -0.00628$$

$$b = \frac{\begin{vmatrix} 0 & 1.402 \\ 3.5 & 1.380 \end{vmatrix}}{\begin{vmatrix} 0 & 1 \\ 3.5 & 1 \end{vmatrix}} = \frac{-4.907}{-3.5} = 1.402$$

Substitute the values of the coefficients a and b in equation (B.1).

$$n_{lens} = -0.00628r_p + 1.402 \quad (3.4)$$

$$n_{lens} = -0.00628 r_p + 1.4062 \quad (3.5)$$

Equation (3.5) describes the positional dependency of the refractive index ( $n_{lens}$ ) of the eye lens as a function of the distance ( $r_p$ ) from its center.

Later, it is very important in this stage to choose a proper optical objective function. The correct choice will lead to fast getting accurate results. In the present work, two optical fitness (or objective together) functions are chosen: The first is the *EFL*, which measures the performance efficiency for the optical system (for an emmtropic eye;  $EFL_e=16.63mm$ ). The second fitness function is the spot size (*Z*), which describe the image quality consisting by each individual design (for emmtropic eye;  $Z_e=5\mu m$ ). Therefore, the use of these two fitness function will govern the path of improving the eye design in terms of the performance and imaging. Algorithm (3.1) shows a detailed explanation about the steps of implementing the GA for agiven human eye design:

**Algorithm (3.1): GA implementation to find the optimal eye design.**

1. Determine; the population size ( $P_s$ ), number of generations ( $G_n$ ), and probability of mutation ( $P_m$ ).
2. For each gene specify; the minimum ( $Min_G$ ) and maximum ( $Max_G$ ) limits of each gene.
3. Input the spot size ( $Z_e$ ) and the effective focal length ( $EFL_e$ ) of emmetropic eye.
4. Initialization: generate ( $P_s$ ) random individual chromosomes (eye design).
5. For each individual; compute the spot size ( $Z$ ) and effective focal length ( $EFL$ ), and then compute the objective function ( $F_n$ ),  

$$F_n = |Z_e - Z| + |EFL_e - EFL|.$$
6. Scan all individuals to find the best one (minimum  $F_n$ ).
7. Select two individuals randomly, and chose the best (the best have  $F_n$  is less than that of others) for the next step "mating".
8. Crossover any two randomly chosen individuals. The crossover process is just swapping half the genes (randomly chosen) between chosen individuals for mating.
9. Get  $P$  to be randomly selected between (0-1) is the probability of mutate current generation. If  $P < P_m$  then do mutation else no mutation to do. The mutation is changing only one gene in same individual to take a random value from the range of its variety.
10. If the optimal chromosome is achieved then stop, else back to step 5.

**3.4 Skew Ray Tracing**

The skew ray tracing is a behavioral geometrical description based on the mathematical analysis for the ray paths from the object even at the

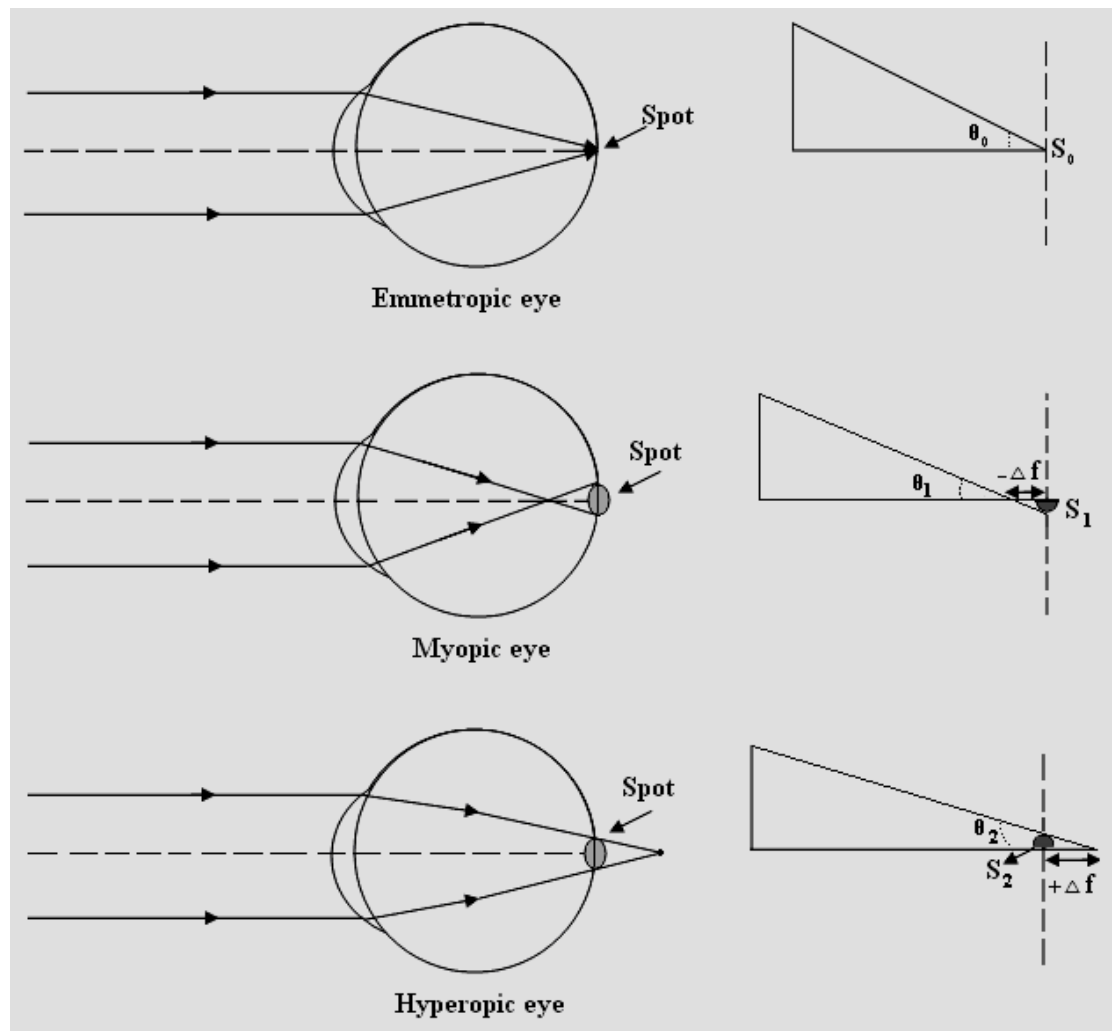
image passing through all the optical elements in the eye. Such that, ray tracing requires a 3-D computations related to the ray behavior through a sequence of material as mathematically described in the previous chapter. Actually, such computations are needed to be graphically explained in order to visually note the tracing of the rays and their behaviors. The 3-D computer aided graphics of the rays needs to determine a view point to be inclined with a specific angle from the plane  $y-z$ ,  $x-z$ , and  $x-y$ . Best position of the view point gives the chance for the observer to see all the behavioral details of the skew rays. The adopted angles of the view point are  $+30^\circ$ ,  $-30^\circ$ , and  $0^\circ$ , respectively, whereas the adopted position of the view point is same as that of the cornea with some shifting to the (-y) direction. Algorithm (3.2) explains the computations of the skew ray tracing in the eye.

**Algorithm (3.2): The implantation of skew ray tracing.**

1. Determine the position of the object, and its distance from the eye.
2. Compute the incident angles  $\alpha, \beta$ , and  $\gamma$  using trigonometry.
3. for all the rays distributed across the object occupation, do the following steps.
4. for each surface belong to the optical eye elements, do the following steps.
5. Compute the position of the incident ray on the tangent plane using equations (2.3).
6. Compute the position of the same ray on the first surface of the  $i$ th optical element using equation (2.4).
7. Compute the new values for the direction cosine's using equations (2.9).
8. If the surface is the last then stop.

### 3.5 Defects in Eye

The considered defects appear due to increasing or decreasing the EFL over or down the ideal value. This occurs when the optical features of the eye elements are not compatible with each other, this affects the spot size as shown in figure (3.4-a) and make some distortion the image resolution. If the increasing or decreasing distance added to the EFL is assumed equal to a specific distance ( $\pm\Delta f$ ) as shown in figure (3.4-b), then the spot radius (size)  $S_1$  of the myopic eye is equal to the spot radius (size)  $S_2$  of hyperopic eye, since the shaded triangle in figure (3.4-b) are equal, while the incident angles are different ( $\theta_2 < \theta_0 < \theta_1$ ).



(a) Eye Design

(b) Ray Trigonometry

Figure (3.4): The defects of the eye.

Such that, one can employ the genetic generation system to create an optical design describing the myopic or hyperopic eye, this is achieved by varying only the distination EFL to be greater or less than the ideal value by an amount of  $(\Delta f)$ . This way equivalent to create a defect in the eye determined by the defect degree  $(\Delta f)$ . In order to correct the defected eye, a thin convex lens it may be added when the defect of eye is myopia or concave when the defect of eye is hyperopia. It is capable to determine the relationship between the defect degree with the curvature of the correction lens. The attended EFL of defected eye is determined first and substituted (assumed as  $f_2$ ) in equation (2.16) to estimate  $f_1$  of the corrected lens at assumption that  $f$  is equal to the ideal value of EFL belong to emmetropic eye. The distance ( $d$ ) between the correction lens and the eye is set as the distance between the center of the eye ( $12mm$ ) and the center of the correction lens ( $30mm$ ) [Daw 89] i.e.  $42mm$ . The resulted  $f_1$  is then substituted in equation (2.15) to compute the curvature of the corrected lens ( $t=0$  for the thin lens). Algorithm (3.3) shows how implement such correction:

**Algorithm (3.3): Estimating the radii of curvature of the correction lens.**

1. Compute the  $EFL_a$  of the given emmetropic eye, let  $f_2 = EFL_a$ .
2. Consider the  $EFL = EFL_e$  (i.e.  $16.63$  for emmetropic eye).
3. Substitute both  $EFL$  and  $f_2$  in equation (2.16) to get  $f_1$ , when  $d=42mm$ .
4. Substitute  $f_1$  in equation (2.15) for a thin lens (axial thickness  $t=0$ ).
5. Compute  $R_1$  and  $R_2$  of the correction lens using equation (2.18).

### 3.6 Spot Size and Diagram Estimation

The spot image that constituted in the retina is due to collecting of received rays from the pupil. Since there is no aberration exist in the eye but only a diffraction, the spot diagram contains a central bright spot surrounded by a diffraction fringes that take a circular shape (due to circular shape of pupil) with different radii and illumination about the central spot. The smallest ring closer to the spot has a recognizable illumination, other rings are not visible due to less illumination distributed along them. The illumination decreases as going far away from the center of spot.

The distribution of such spot diagram (image) is Gaussian according to the equation (see appendix A).

$$f(x, y) = \frac{1}{2\pi\sigma_x\sigma_y} \exp\left[-\frac{1}{2}\left[\left(\frac{x-\mu_x}{\sigma_x}\right)^2 + \left(\frac{y-\mu_y}{\sigma_y}\right)^2\right]\right] \quad (3.6)$$

Where,  $\mu_x$  is the mean (expectation) value in the x-axis,  $\mu_y$  is the mean (expectation) value in the y-axis,  $\sigma_x$  is the variance of the values in the x-axis, and  $\sigma_y$  is the variance of the values in the y-axis.

The spot shape is similar about the axis  $x$  and  $y$  at view angle  $0^\circ$ , but it became extended along  $x$ ,  $y$  or both axis with varying  $\alpha$ ,  $\beta$ , or both respectively as presented in table (3-3). The amount of extension is presented by  $\sigma_x, \sigma_y$ , or both, which is proportional to the deviation of the angles  $\alpha, \beta$  from the zero. Such that, the relation between the spot size ( $Z$ ) and the angles should be modeled as follows:

Table (3.3): Spot size values as a function of  $\alpha$  and  $\beta$  [Smi 00].

$\alpha$ (degree)	$\beta$ (degree)	$Z_y$ ( $\mu\text{m}$ )
0	0	5
0	60	200
60	0	200

By rearranging the terms of equation (3.6), one gets:

$$G = G_x G_y \quad (3.7)$$

Where

$$G_x = \frac{1}{2\pi\sigma_x} \exp\left[-\frac{1}{2}\left(\frac{x-\mu_x}{\sigma_x}\right)^2\right] \quad (3.8)$$

and

$$G_y = \frac{1}{2\pi\sigma_y} \exp\left[-\frac{1}{2}\left(\frac{y-\mu_y}{\sigma_y}\right)^2\right] \quad (3.9)$$

The spot size (radius) of the 2-D image is shown in equation below [Moo 74]:

$$Z = \sqrt{(3\sigma_x)^2 + (3\sigma_y)^2} \quad (3.10)$$

According to table (3-1), one can model the linear relationship between the standard deviation and its corresponding angle to be given as (see appendix B):

$$\sigma_x = 0.767\alpha + 1.18 \quad (3.11)$$

$$\sigma_y = 0.767\beta + 1.18 \quad (3.12)$$

Algorithm (3.4) shows the steps of drawing the spot diagram and estimating the spot size.

**Algorithm (3.4): Spot size and spot diagram estimations.**

1. *Using the skew ray tracing, estimate the average value of  $\alpha$  and  $\beta$  for all the ray pass through the eyelens.*
2. *Compute the standard deviations  $\sigma_x$  and  $\sigma_y$  using equations (3.11 and 3.12).*
3. *Estimate the spot size (Z) using equation (3.10).*
4. *To show the spot diagram, follow the following steps:*
  - a- *Count the number of rays ( $N_r$ ) incident on the center of spot and the total rays ( $N_T$ ).*
  - b- *Divide the spot image into  $100 \times 100$  sub regions.*
  - c- *From  $x=1$  to  $100$  and  $y=1$  to  $100$ , illuminate each sub region with its corresponding color determined by the normalized values obtained from equation (3.7) multiplied by the normalized number of rays incident on the center of spot  $\frac{N_r}{N_T}$ .*

**3.7 Illumination of Spot Image**

The variation of pupil determines only the quantity of received illumination, it doesn't related to the amount of illumination (brightness) that enter the eye. Thus, the high illumination ( $I_o$ ) out the human body make the surrounding object to be bright and leads to create a bright spot on the retina with illumination is less than ( $I_o$ ) due to some factors related to the absorption, dispersion,...etc. the illumination can be represented the spot ( $I_s$ ) by a linear fitting model as a function of out body illumination ( $I_o$ ) as follows:

$$I_s = aI_o + b \quad (3.13)$$

Where  $a$  and  $b$  are the coefficients of the linear model, both related to the amount of the transmitted illumination toward the retina. In general, one can note figure (2.22) that describing the transmittance of only the effective optical element in the eye, to conclude that the overall transmittance in the eye is about 88% through the region of visible radiation (400-700nm wavelength). Such that, the coefficients ( $a$  and  $b$ ) of the assumed linear model that relate the image illumination with the object illumination are estimated to be;  $a = 0.88$  and  $b = 0$ , so equation (3.13) becomes:

$$I_s = 0.88I_o \quad (3.14)$$

It should be mentioned that the consideration of image illumination prepare to estimate the contrast of the image according to equation (2.25) which in turn refers to the behavior of the MTF and the resolution of the spot image.

### 3.8 The Effect of FOV on the Spot Radius

The FOV is the solid angle that describe the angular range of the eye vision. According to the literature [Hud 69], the angular range of the eye vision extended along the horizontal plane from (-60°) to (+60°), i.e. 120° in total. The horizontal extension of such range is more important than the vertical or diagonal, since most of the objects in nature are positioning in horizontal distribution.

All the object exist in the FOV are visible to the eye, the differences between them are related to the image quality. The objects lying in the position of vision target (in front of eye) are described as on-axis, such objects are imaging with high resolution. Whereas the image resolution decreases with increasing the distance from the object to the optical axis, which causes to enlarge the spot size due to the asphericity

of the eye that make the focus behind the retina at very small amount. For this reason, the eye movement (with head movement) is very necessary to make enough resolved vision and proper spot (object) size. The mathematical model that determine the variation of the spot size with the FOV depends basically on the amount of the asphericity ( $e$ ) of the eye, which is (0.011) according to some literatures [Hud 69].

The analytical study on the spot size behavior as a function of the deflection angle of the incident rays shows there is a comatic aberration is found due to asphericity characteristic of eye. Figure (3.5) shows the shape of the eye ball; the dashed is aspheric, which is the approximated shape, while the solid is elliptic, in which the eccentricity coefficient ( $e=0.012$ [Ein 09]) which is the closest shape can describe the eye. According to these shapes, the spot size ( $Z=5.136\mu m$ ) at  $0^\circ$ , and it increases with increasing the angle ( $\theta$ ) of deflecting the rays constituting the spot image. Thus, one can model the mathematical relationship between the spot size and the angle ( $\theta$ ) as follows:

$$Z = z_0 + z_\theta \quad (3.15)$$

where,  $z_0$  is the spot size at  $0^\circ$  which is  $5.136\mu m$ , and  $z_\theta$  is the spot size at any angle  $\theta$  ( $0 \leq \theta \leq 60^\circ$ ) that is given as:

$$Z_\theta = \Delta f \tan \theta \quad (3.16)$$

$$\Delta f = f_{sphere} - f_{Ellips} \quad (3.17)$$

Where  $\Delta f$  is the difference between the effective focal length of the spherical shaped eye ( $f_{sphere}$ ) and the effective focal length of the elliptical shaped eye ( $f_{Ellips}$ ) that given as:

$$f_{Ellips} = \sqrt{(X_L - X_E)^2 + (Y_L - Y_E)^2} \quad (3.18)$$

where  $X_L$  and  $Y_L$  are the coordinates of the eyelens center,  $X_E$  and  $Y_E$  are the coordinates of the position that the ray incident on, which lies at the elliptical circumference of the eye.

Figure (3.6) shows the elliptical shape of the eye at which  $a$  and  $b$  are the radii of such ellipse. It is shown the coefficient ( $a$ ) equal to the half horizontal dimension of the eye ball (i.e.  $a=11.5mm$ ). the eccentricity of such ellipse is given as:

$$e = \frac{\sqrt{a^2 - b^2}}{a} \quad (3.19)$$

Then

$$b = \sqrt{a^2 - e^2 a^2} = 11.499304mm$$

Equations (3.15 and 3.19) represent the mathematical basis needed to estimate the spot size when the angle of deflecting the ray inside the eye is given. Appendix C explains an example about how using this model and shows the spot size computations versus  $\theta$ .

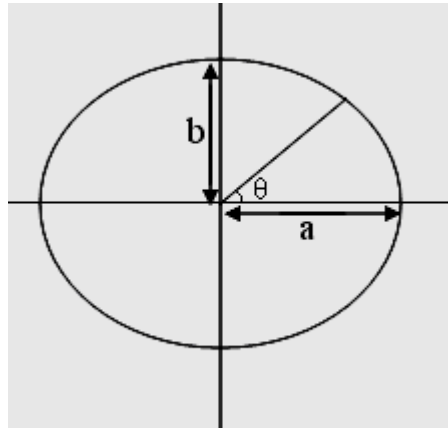


Figure (3.5): The elliptical shape of the eye.

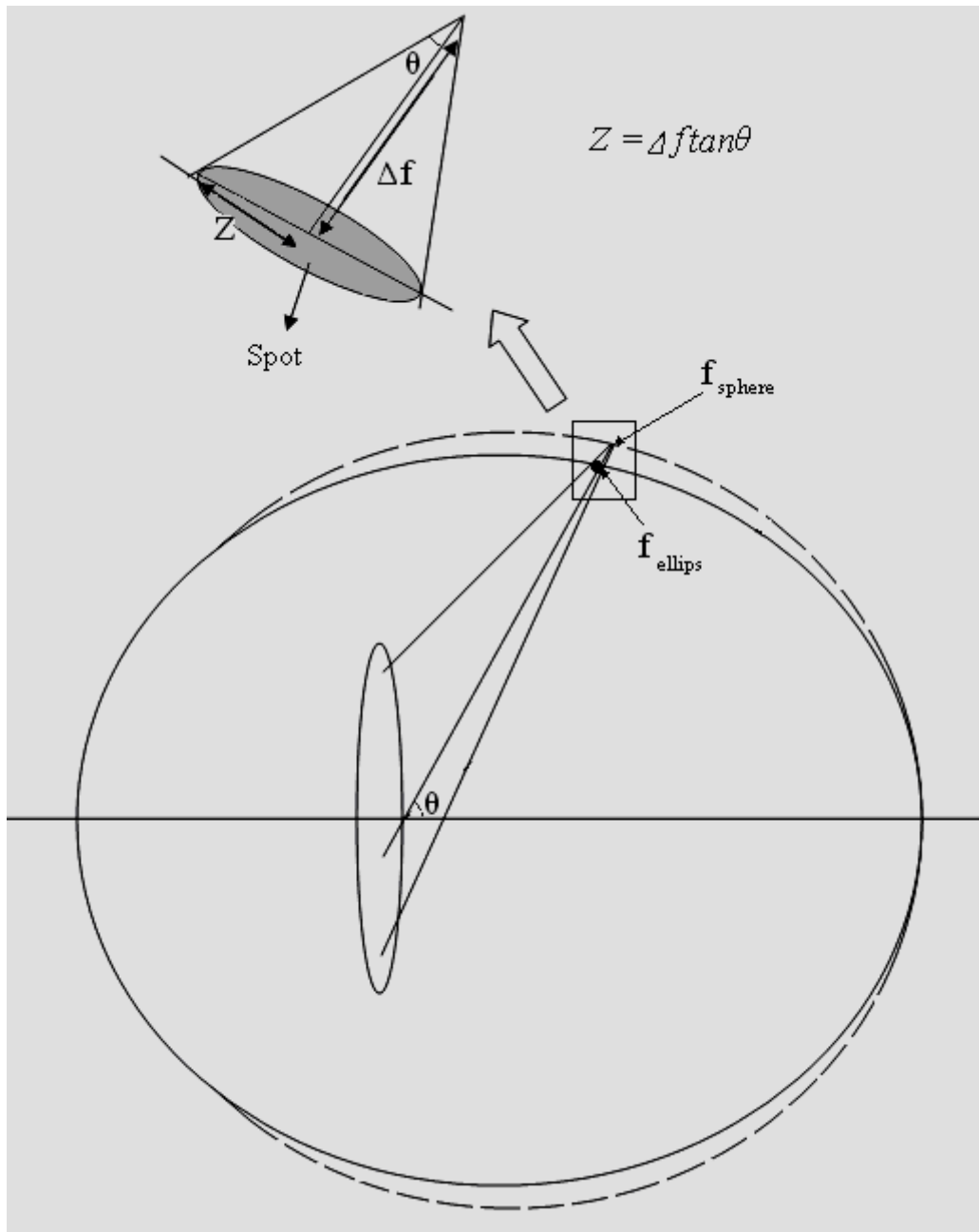


Figure (3.6): Geometrical analysis for the spot size ( $Z$ ) versus deflection angle ( $\theta$ ).

### 3.9 Object Distance Variation

The variation of the distance between the eye and the visual object don't affecting the imaging process. Since the curvature of the lens will be automatically varied to make auto focus which cancel the role of object distance variation. As a result, the image constituted on the retina

will be with the same resolution at different distances. This point out to an important conclusion; all the optical element of the eye are given as fixed through the designing stage except the eyelens, the given information of the eyelens are the averages of its optical features.

The mathematical model of the object distance related to eyelens curvature need first to classify the object distance according to the variation of the view angle ( $\delta$ :  $\delta$  may be  $\alpha$ ,  $\beta$ , or  $\gamma$ ). That means the object distance become infinity when the ray incidence angle ( $\delta$ ) is zero, and the object become far or near according to a specific amount of ( $\delta$ ). Figure (3.7) shows the cornea (8mm diameter) of the eye receives the rays from an object lies on a distance of 5000 mm (i.e. 5m).

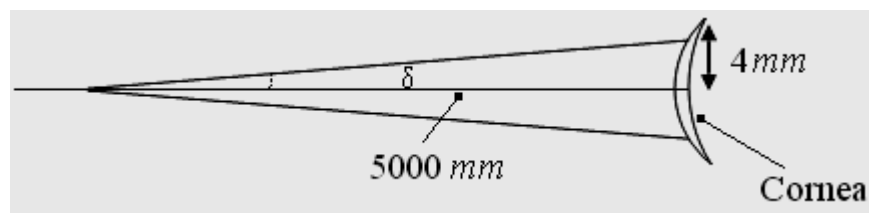


Figure (3.7): Rays incident on the cornea.

It is easy to determine the angle ( $\gamma$ ) as follows:

$$\delta = \tan^{-1}\left(\frac{4}{5000}\right) = 0.0458^\circ$$

By the same way, one can tabulate the data of  $\delta$  corresponding to the distance object ( $s$ ) as given in table (3-4) and shown in figure (3.8) below.

Table (3-4): Angle of incidence  $\delta$  correspondence to the object distance.

$s$ (m)	$\delta$ (degree)
10	0.0229
5	0.0458
3	0.0763
1	0.229
0.7	0.327
0.5	0.458
0.3	0.763
0.1	2.290

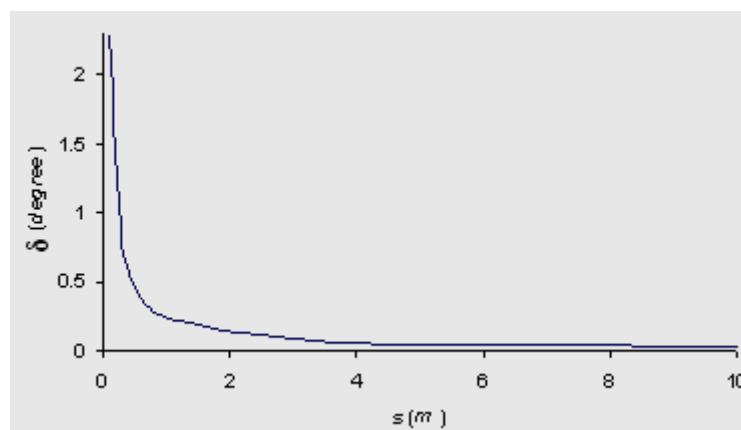


Figure (3.8): Angle of incidence versus object distance.

Therefore, one can put forward the mathematical model to govern the relationship between the  $\delta$  as a function of the object distance to be an exponential fitting as follows:

$$\delta = Ae^{-Bs} \quad (3.20)$$

where A and B are the exponential model coefficients that equal to 5.2666 and -0.4377 respectively as determined in appendix (D). the determined  $\delta$  is equal at least one of the incidence angle  $\alpha$ ,  $\beta$ , or  $\gamma$ . This situation occurs only when the object is on-axis and the angle  $\delta$  does not equal to zero (near object). This affects the computations of the

refraction angles of any skewed ray, which lead to defocus the rays on the retina and deflect the EFL from its intended value.

In order to correct this corrupt, a micro genetic algorithm (MGA) can be applied to redetermine the radii of curvatures of the eyelens ( $R_1$  and  $R_2$ ) that make the attended EFL equals to its intended value (i.e.  $16.63mm$ ). MGA is an optimization stage hybrid in the grand GA optimization which uses only when the object is near to the eye. MGA is same as GA steps except the stage of generating the random population. In the random generation of the MGA, all the optical features are fixed except the radii of curvatures of the eyelens are variable in the range of their restrictions. As a result, the output of MGA is an optimal design of eye in which both radii of the curvature of the eyelens are varying to fit the focusing process and make the attended EFL as required.

### 3.10 Human Eye Simulation

Computer simulation is often used as an adjunct to modeling systems for which simple closed form analytic solution are not possible, or it is used to test the developed system before applying it practically, which save the cost of the project. The simulation technique uses the computer graphics to show the system design, and uses the physical laws to describe the behavior of the adopted system, such that, the simulation technique create a virtual environment which is similar to the actual one. Also computer graphics can be used to display the results of the simulation. The mostly used powerful graphics is the windows Application Programming Interface (API), which encompass the Graphics Device Interface (GDI) that prepare all the drawing shapes (function) available to programmer. Polygon function is employed to draw any regular/irregular shape, it consists of points connected by lines. Polygon can be colored, moved, resized, or even deleted [Daw 08]. The

proposed optical design of human eye is regarded as a graphical system composed of multi-graphical elements; cornea, iris, pupil, eyelens, and retina. each one element is represented by an independent Polygon with a specific color, the shape of each Polygon is determined according to the optical features ( $R_1$ ,  $R_2$ ,  $D$ ,  $d$  and  $t$ ) of the specified optical element.

To show the performance of the simulated eye, the skew ray tracing is considered, and also simulated by drawing straight lines representing the ray behavior outside and inside the eye. The behavior of the simulated rays is determined by the incident angle (direction of the line) and the position of its start and end points. In addition, the object is simulated too, it is represented by a small ball that can be move in the three dimensions. Through considering the ray tracing, one should see band of rays emerging from the object toward the simulated eye at each time the object change its position.

Finally, it should be mentioned that the background color of the developed interface and the optical elements must be faint, whereas the fore color of the rays or spot diagram are shining. The reason behind that is to provide a comfortable watch for the user that uses such interface for a long time.

## *Chapter Four*

# RESULT ANALYSIS AND SIMULATION

## **Chapter Four**

### **Result Analysis and Simulation**

#### **4.1 Introduction**

This chapter includes a presentation about how implement the modeling problems of the eye discussed in the previous chapter. The presentation is associated with an explanations related to the behaviors of all parameters contributed in the eye modeling, also these behaviors are analyzed and discussed in details.

In order to test the optimal eye design resulted from the GA, it was programming by Zemax [Lai 06] to achieve the considered optical functions. The resulted eye is then presented by Zemax to estimate its optical functions. The test is carried out by comparing the attended optical functions of the optimal eye design with the published design of Blacker [Lai 06] (design no. 5 mentioned in chapter one), the optical functions of interest were the effective focal length (EFL), spot size (Z), and the modulation transfer function (MTF), which are useful in evaluating the performance of the proposed design. On this basis, all the considered situations of the eye design (such as myopia, hyperopia, object distance, illumination, and FOV) were computed and discussed in details.

Later, a simulator software was established to simulate the considered situations of the real-life eye. The simulator shows the behaviors of the virtual eye using the computer graphics tools that are automatically led by the simulator all at the same time.

#### **4.2 Proposed Genetic Eye Design**

The proposed GA approach was implemented by visual basic 6.0. The address of such approach is to find out the optimal design of the human eye that can describe the performance and imaging of real-life

eye. Through out the implementation of GA, the number of individual chromosome ( $P_s$ ) is taken to be 100 at each generation. The number of generations ( $G_n$ ) was 80 and probability of mutation ( $P_m$ ) was 0.01. The implemented software continues giving birth generations unless finding the optimal design (i.e.  $F_n=0$ ). The first randomly generation includes 100 individual chromosomes, each optical feature is assumed to be one gene in the chromosome. If the gene is fixed, it takes a specific value from the predefined information table, but when the gene is variable it takes a random value in the range of its variety. Because the randomness, eye designs in the first generations were far away from the optimal design. The results were improving consequentially even achieving the terminate condition. Table (4-1) shows the numerical optical features of the optimal design shown in Figure (4.1) that resulted by the proposed GA approach. Figure (4.2) shows the behavior of improving the results of both the spot size and EFL through GA computations, the final states of them are given in table (4-1) for the optimal genetic eye.

Table (4-1): The optical features of the optimal design resulted from GA.

Optical element	$R_1$	$R_2$	t	d	D	$n_o$	$n_1$	$n_2$
Cornea	6.489	7.657	0.561	3.420	8.224	1.000	1.376	1.333
Eyelens	7.682	-5.001	2.513	16.635	7.101	1.333	v	1.336
Retina	-11.693	-11.693	0	-	-	-	-	-

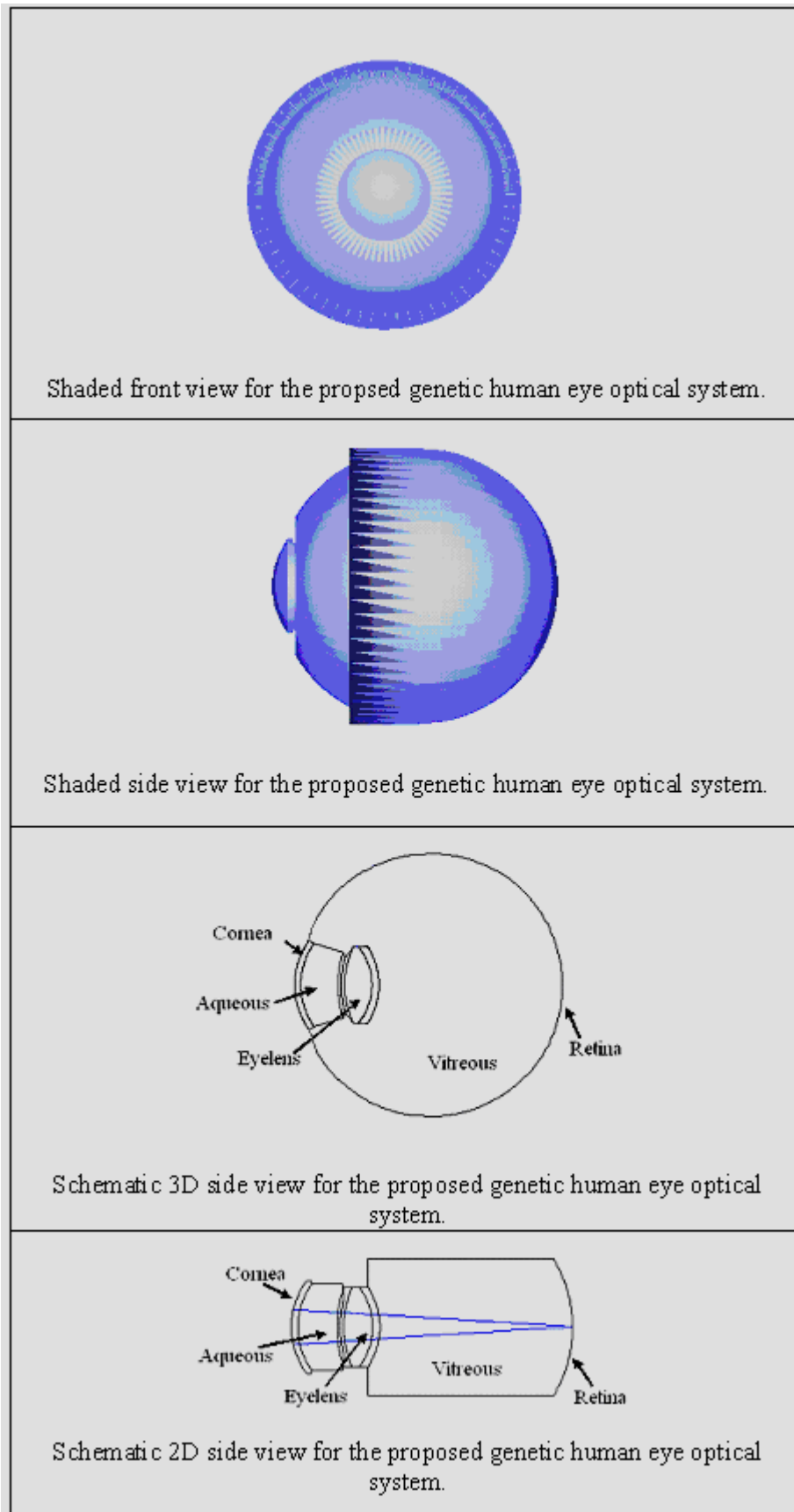
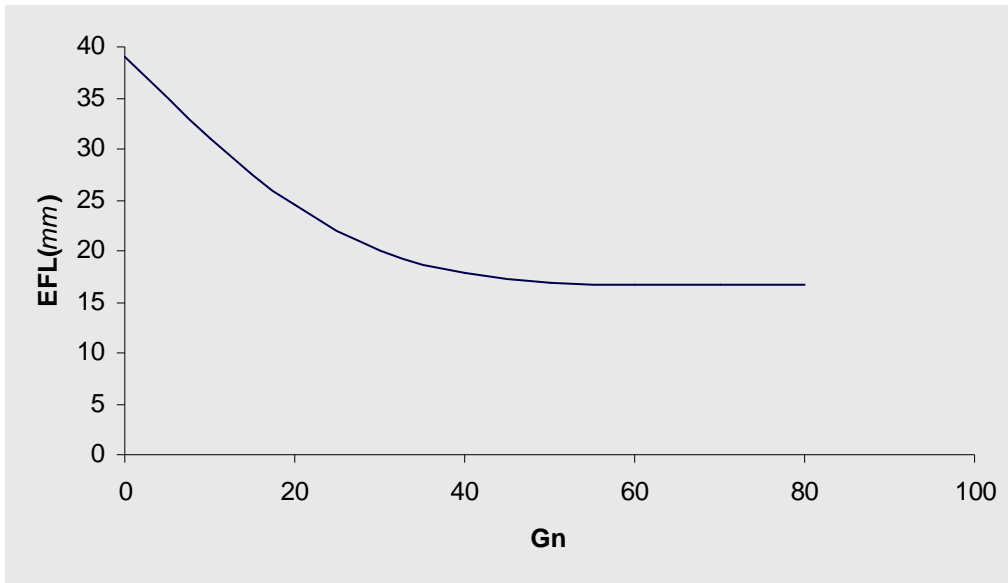
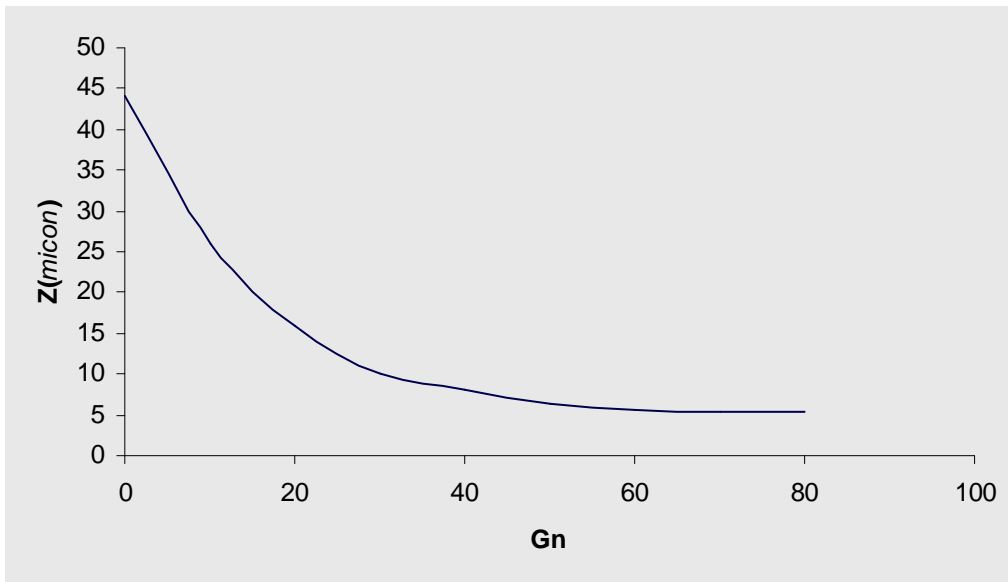


Fig (4.1): The resulted optimal eye design achieved by GA approach.



(a): EFL behavior.



(b): Spot size behavior.

Figure (4.2): The improving states for the behavior of both (a) The EFL and (b)  $Z$ .

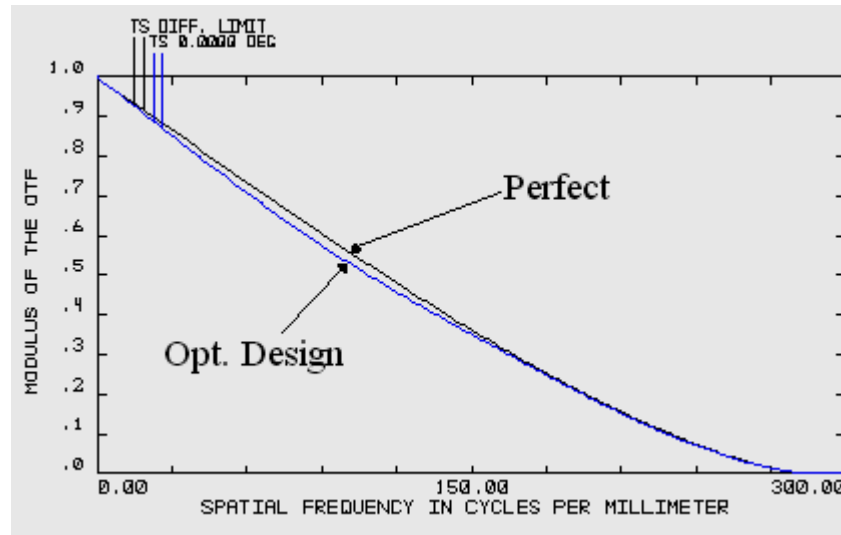
### 4.3 Genetic Eye Evaluation

Ultimately, the effectiveness of the proposed approach is determined by comparing different chosen optical performance measures between the resulted optimum eye design and its perfect state. The resulted optimal design is evaluated by testing its performance and imaging with help of Zemax software. In order to show the optimal eye design in Zemax, it is required to define some information for Zemax, related to optical and material properties of the eye elements. Equations (2.33 and 2.34) were used to define the relation of the refractive index to the wavelength through the visible region, the transmittance of the cornea was defined by equation (2.36) and the transmittance for other elements are defined by equation (2.38) whereas equation (2.40) defines the density for each optical element in the eye. The evaluation includes two tests; performance test and imaging test, both are carried out as follows:

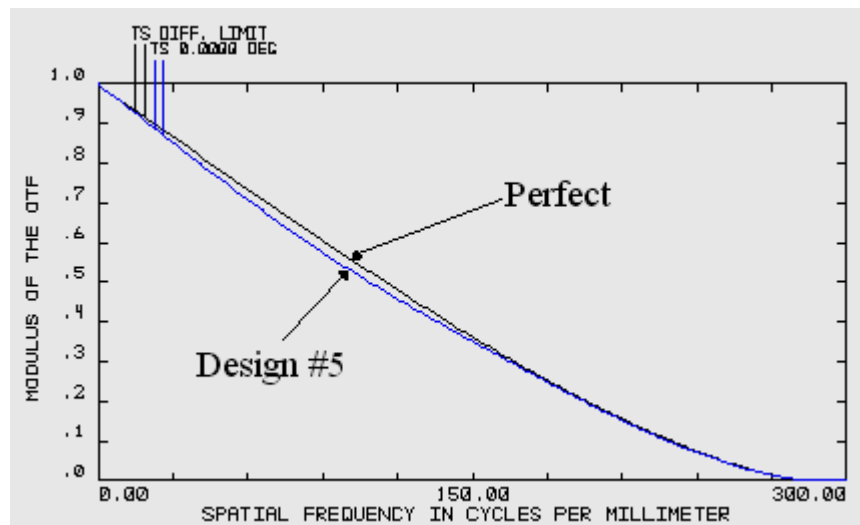
#### 4.3.1 Performance Test

The MTF can be used to test the performance of any optical system. MTF describes the amount of aberration and associated defocusing in the optical system. Figure (4.3) shows the MTF for the optimal design in comparison with the perfect case achieved by Zemax. It can be noticed that the MTF of the optimal design is very close to the perfect, also it is identifying the MTF of that estimated in (design no. 5 in chapter one). It is thought that the MTF of the optimal design does not achieve the perfect for two reasons: **First**, because the fitting function of the refractive index of the eyelens, which was linear fitting, such function is infrequently found in nature. **Second**, because the residual spherical aberration, which does not affect the quality of the vision since it is less than the spacing between any two vision sensors in the retina. Such least amount of aberration appears in the MTF with no effect on the vision quality. The

behavior of the MTF shows high image contrast of the optimal eye since the MTF approach to the perfect, thus it can be regarded the performance of genetic eye is acceptable as that of the real-life eye.



a- MTF of the optimal eye design comparing with the perfect case.



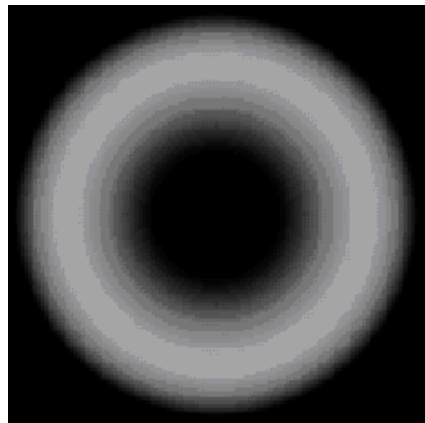
b- MTF of the design #5 comparing with the perfect case.

Figure (4.3): The MTF behavior.

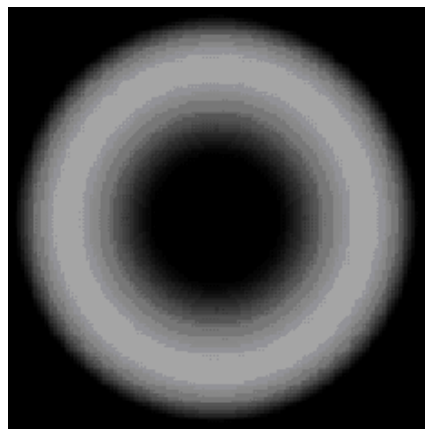
### 4.3.2 Imaging Test

The test of the optimal design imaging depends on the size and diagram of the constituted spot by the rays falling on the retina. Least spot size means less rays separation and sharper imaging, which lead to

higher resolution. Actually, the spot size of the optimal design invented by applying GA approach was  $Z_{optimal}=5.316\mu m$ , while  $EFL_{optimal}=16.630mm$ . These results ensure our interpretation related to the two reasons mentioned in the performance test. In fact, EFL is good since it optimized to be reached the target value, whereas the spot size was departing from the intended by a very small value, but it retained acceptable value due to it is originally vary through allowed computational errors. Fig (4.4) demonstrates the spot diagram of the optimal design, which is same as the perfect case (diffraction only without aberration) both achieved by Zemax. Moreover, the comparison between the resulted spot diagram with that pictured in design no. 5 (chapter one) shows no noticeable difference in between.



a- Spot image of the optimal eye design.



b- Spot image of the design #5.

Figure (4.4): Spot image achieved by Zemax at  $0^\circ$  inclination.

## 4.4 Human Eye Simulation

The simulation of human eye needs to build dedicated software to simulate the behavior and situations of human eye, such software is called *simulator*. The simulator plays the role of human eye, it sense and obey to various vision conditions. Algorithms (3.1 - 3.4) are used to implement the simulator. Other algorithms are used to create the various conditions that the simulator deals with. Figure (4.5) shows the interface of the simulator software, it is shown that the simulator contains a number of tools that are designed to change the vision situations. Also, the simulator can draw the proposed design or another generated eye design by GA. However, the simulator can stand for any eye design, it feels the received skewed rays and then forms the retinal image.

It is observable that the traces of the skew rays are naturally behaves. The change of the object position leads to change of the behavior of the ray traces, and causes mostly to change the position of the image on the retina. The density (amount) of the considered rays is related to the amount of illuminating that out eye surroundings.

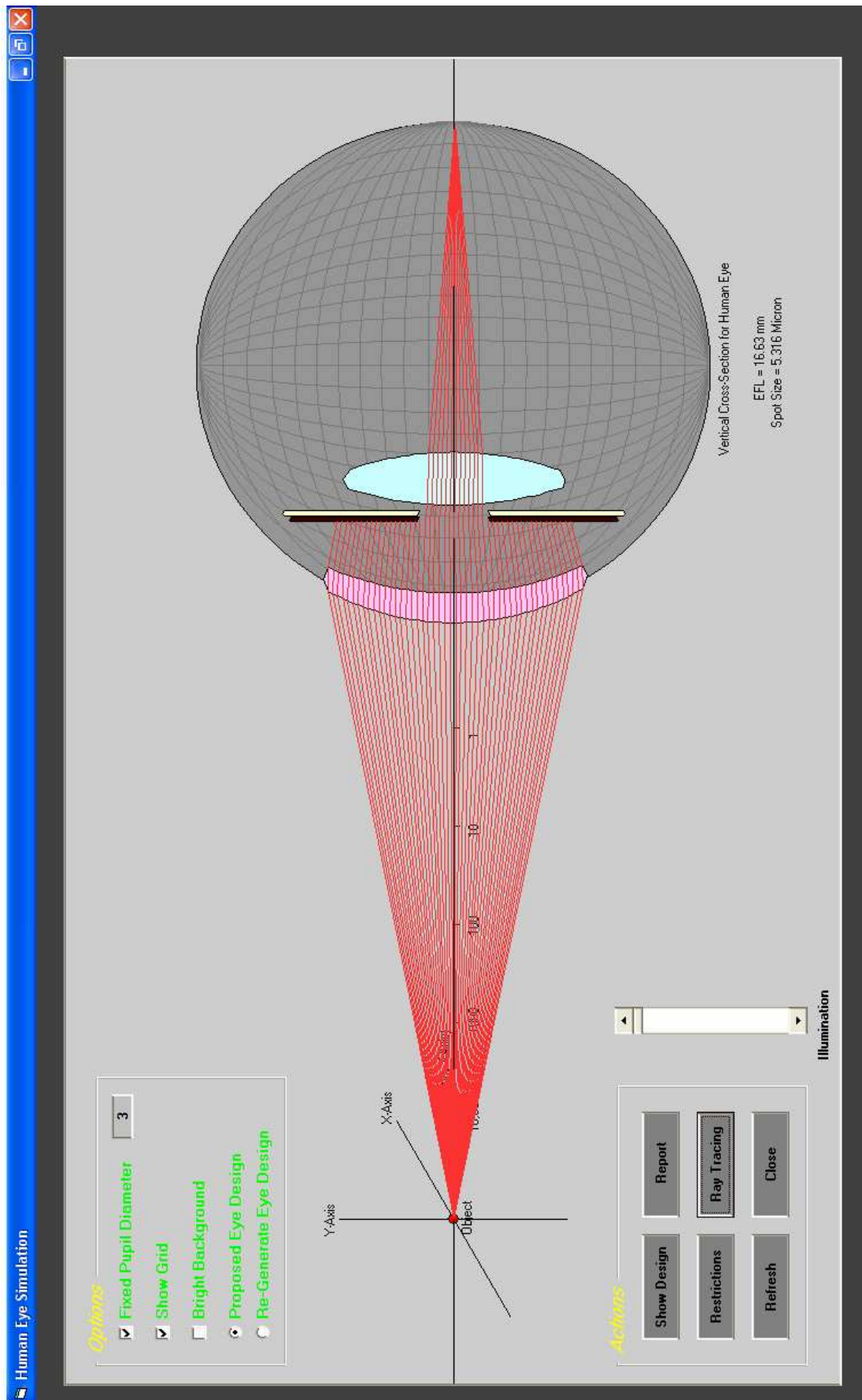


Figure (4.5): The interface of human eye simulator.

## 4.5 Eye Defects Simulation

In order to create a myopic or hyperopic eye designs defected by  $\pm 1$  degree, one can assume the EFL of the optimal eye is decreased/increased by  $1\text{mm}$  and let the MGA operating to yield the defected designs. As a result, the myopic eye is regenerated to be as shown in figure (4.6), the numerical optical features of such design are given in table (4-2). Also, the hyperopic eye and its numerical optical features are shown in figure (4.7) and table (4-3), whereas table (4-4) shows the resulted EFL and spot size for the proposed emmetropic genetic eye, myopic eye, and hyperopic eye.

Table (4-2): The optical features of myopic eye.

Optical element	$R_1$	$R_2$	t	d	D	$n_0$	$n_1$	$n_2$
Cornea	6.617	7.628	0.637	3.230	8.109	1.000	1.376	1.333
Eyelens	7.690	-5.350	2.530	16.644	7.680	1.333	v	1.336
Retina	-11.693	-11.693	0	-	-	-	-	-

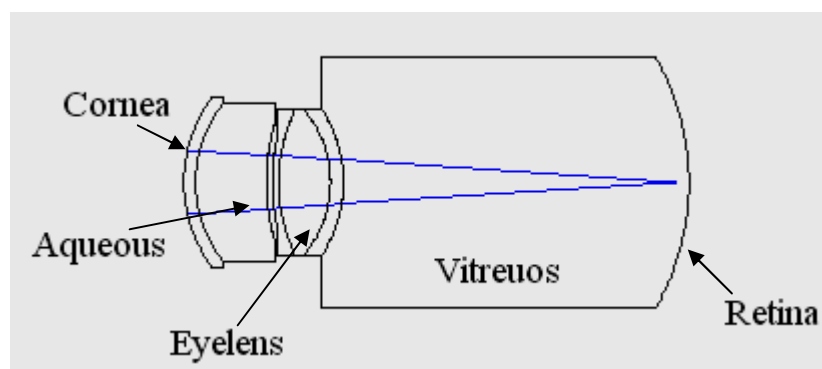


Figure (4.6): The myopic eye of optimal design.

Table (4-3): The optical features of hyperopic eye.

Optical element	$R_1$	$R_2$	t	d	D	$n_o$	$n_1$	$n_2$
Cornea	6.393	7.715	0.571	3.517	8.269	1.000	1.376	1.333
Eyelens	7.682	-5.020	2.550	16.539	7.207	1.333	v	1.336
Retina	-11.693	-11.693	0	-	-	-	-	-

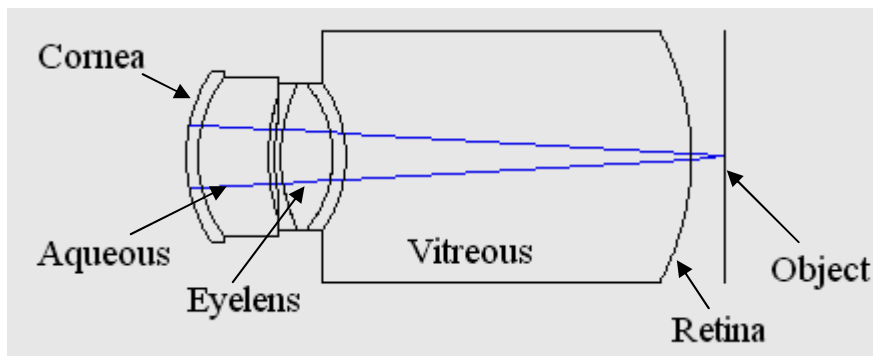


Figure (4.7): The hyperopic eye of optimal design.

Table (4-4): the spot and the effective focal length for three cases.

Eye	$Z$ ( $\mu m$ )	EFL (mm)
Emmetropic	5.316	16.63
Myopic	8.23	15.63
Hyperopic	8.23	17.63

Figures (4.8a and 4.9a) shows the simulator which is imitating the considered myopic and hyperopic eyes, which makes the focus of rays before or across the retina position by just  $1mm$ . To correct the defected eye, the computer program (corrector) associated with the simulator suggests existing a correction lens of optical features which are determined according to the adopted correction method. Figures (4.8-b and 4.9-b) present how the correction lens was added to the defected eye which make the rays focusing better than that of myopic or hyperopic eye

shown in figures (4.8b and 4.9b). The radii of curvature both surfaces of the correction lens are printed down it.

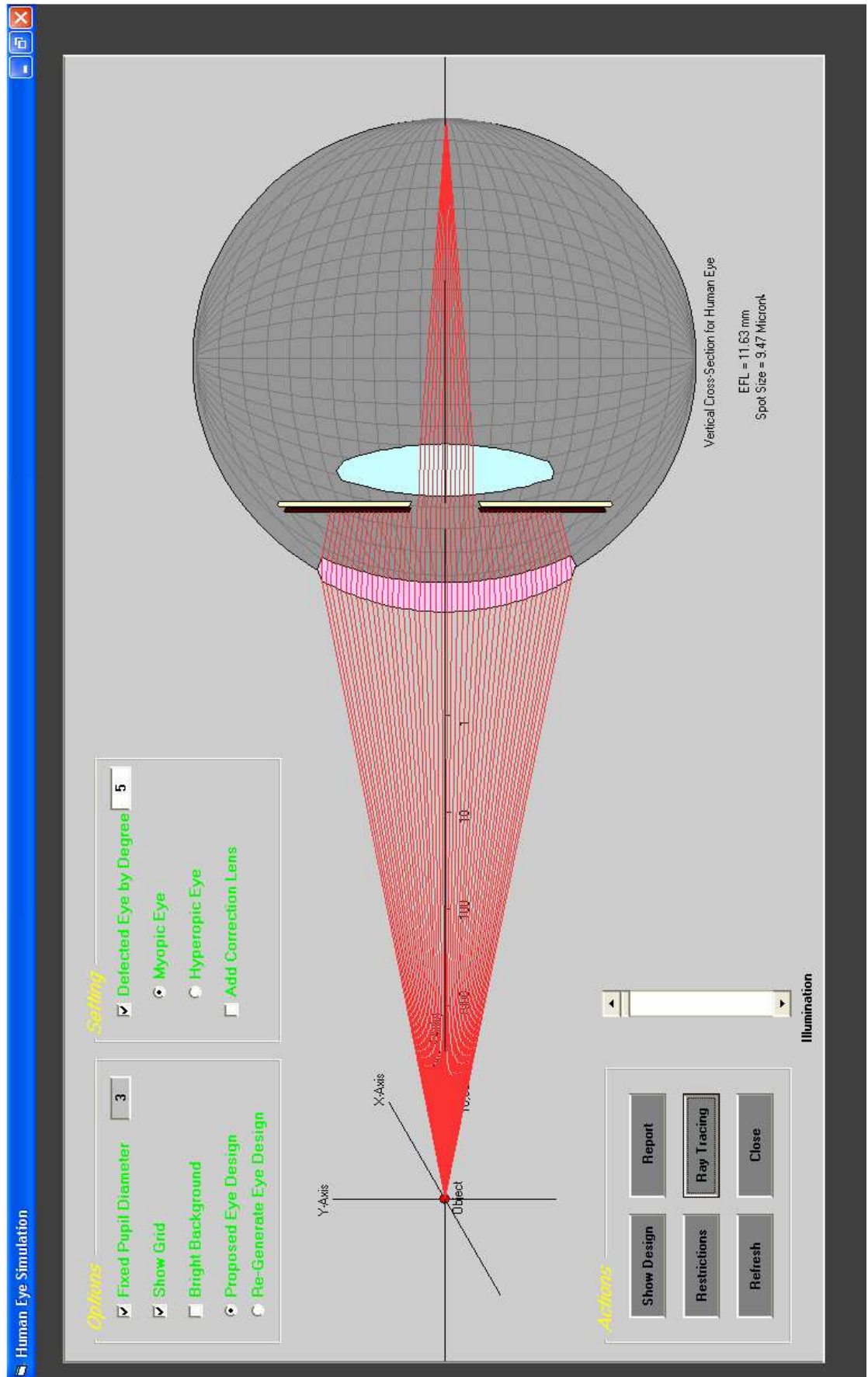


Figure (4.8-a): simulated myopic eye.

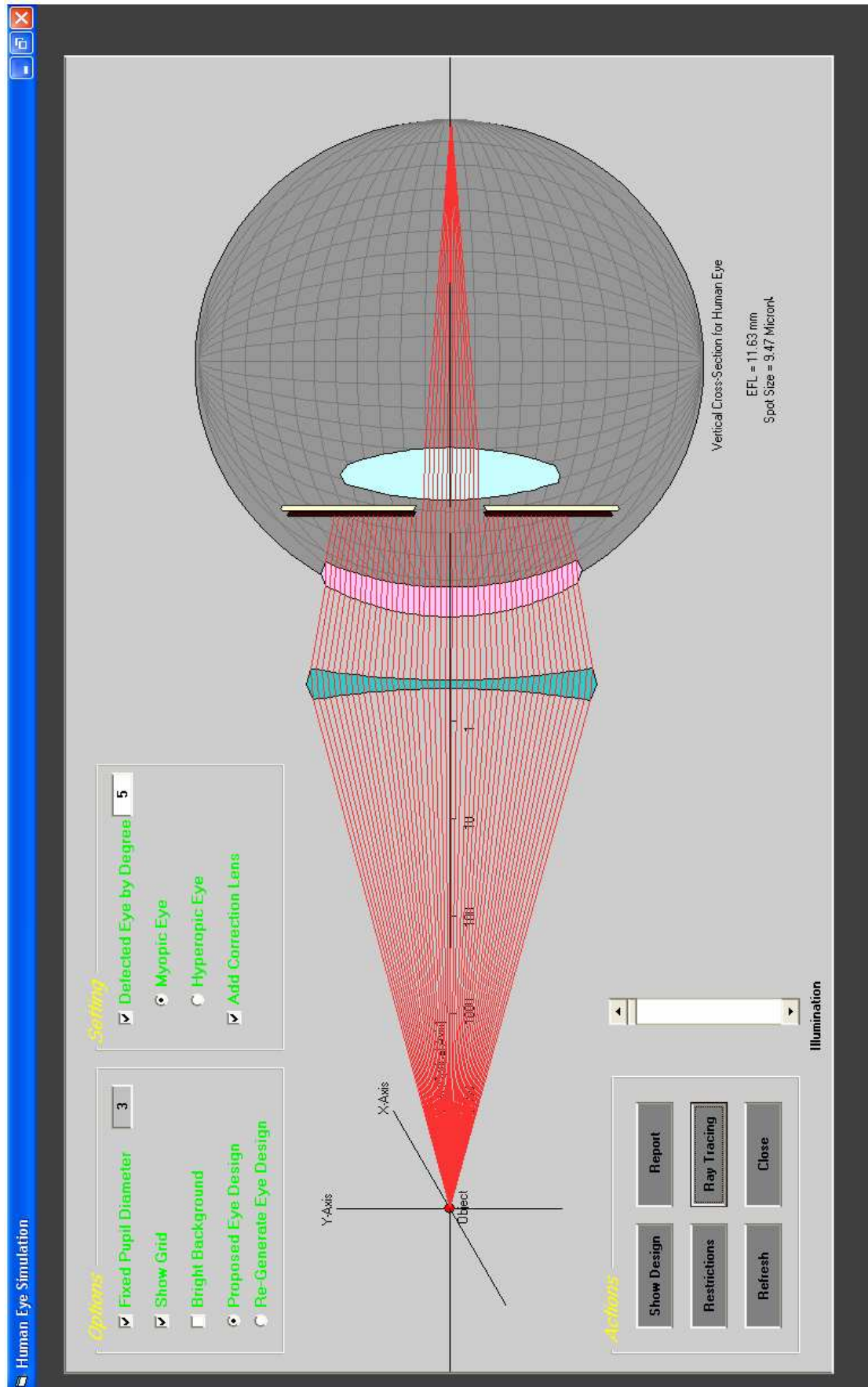


Figure (4.8-b): Correction of myopic eye.

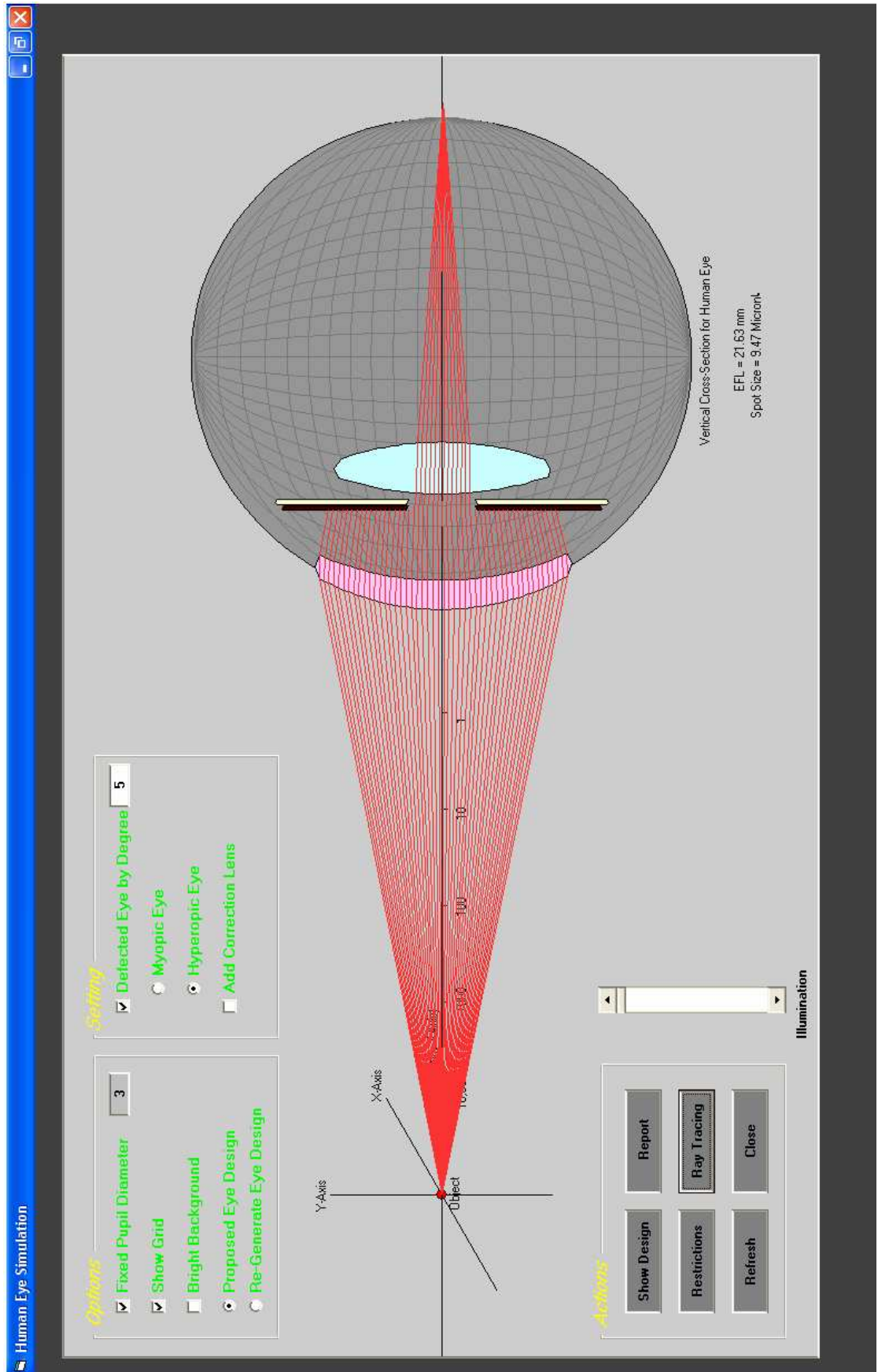


Figure (4.9-a): Simulated hyperopic eye.

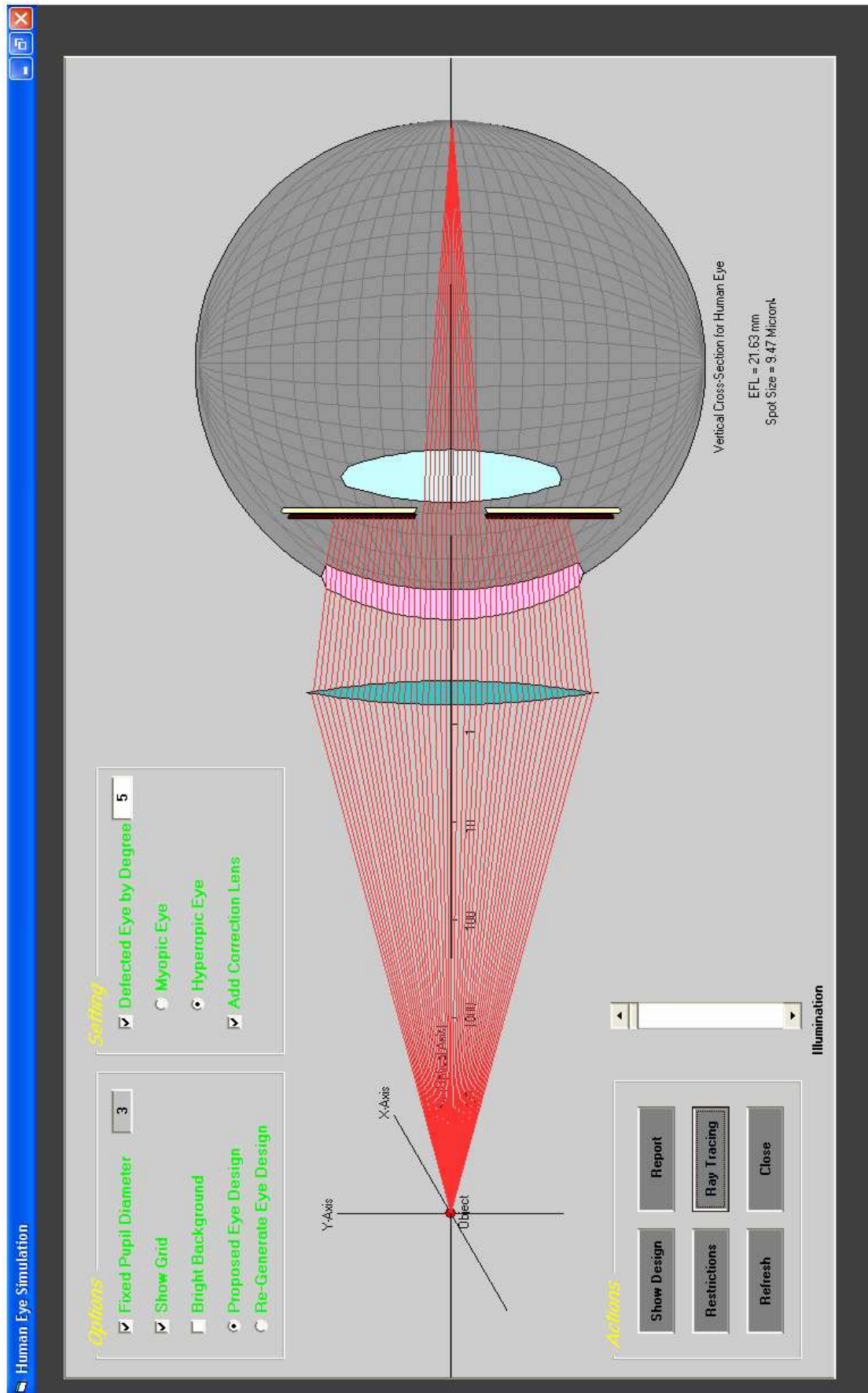


Figure (4.9-b): Correction of hyperopic eye.

## **4.6 Spot Simulation**

The problem of simulating the spot formation and spot size estimation are adopted in the simulator design. The proposed model of image formation made its size dynamic and depends on the incident angles of the rays, whereas the out eye illumination governs the auto-behavior of the pupil and the color intensity of the retinal image. Figure (4.10) shows the behavior of the simulator when it sees a distant object. The retinal image seen by the simulator is drawn in the square down left the simulated eye, such image is constituted from collecting the rays incident on a retinal area in which the optical axis path through its center.

The estimated spot size was printed under the image. The amount of illumination was set by a specific control tool called "Illumination". It is noticeable that the central spot is disappeared, this is due to a physical reason related to the amount of the phase difference ( $180^\circ$ ) between the incident and reflected rays at the center of vision screen. This leads to reverse the color of the central spot to become black rather than white.

Also, it is shown that the spot image is greatly similar to that extracted by Zemax shown in figure (4.4), this ensure the successful implementation of the skew ray tracing since it is the process that guide the rays toward the retina, and then these rays are employed to form the spot image.

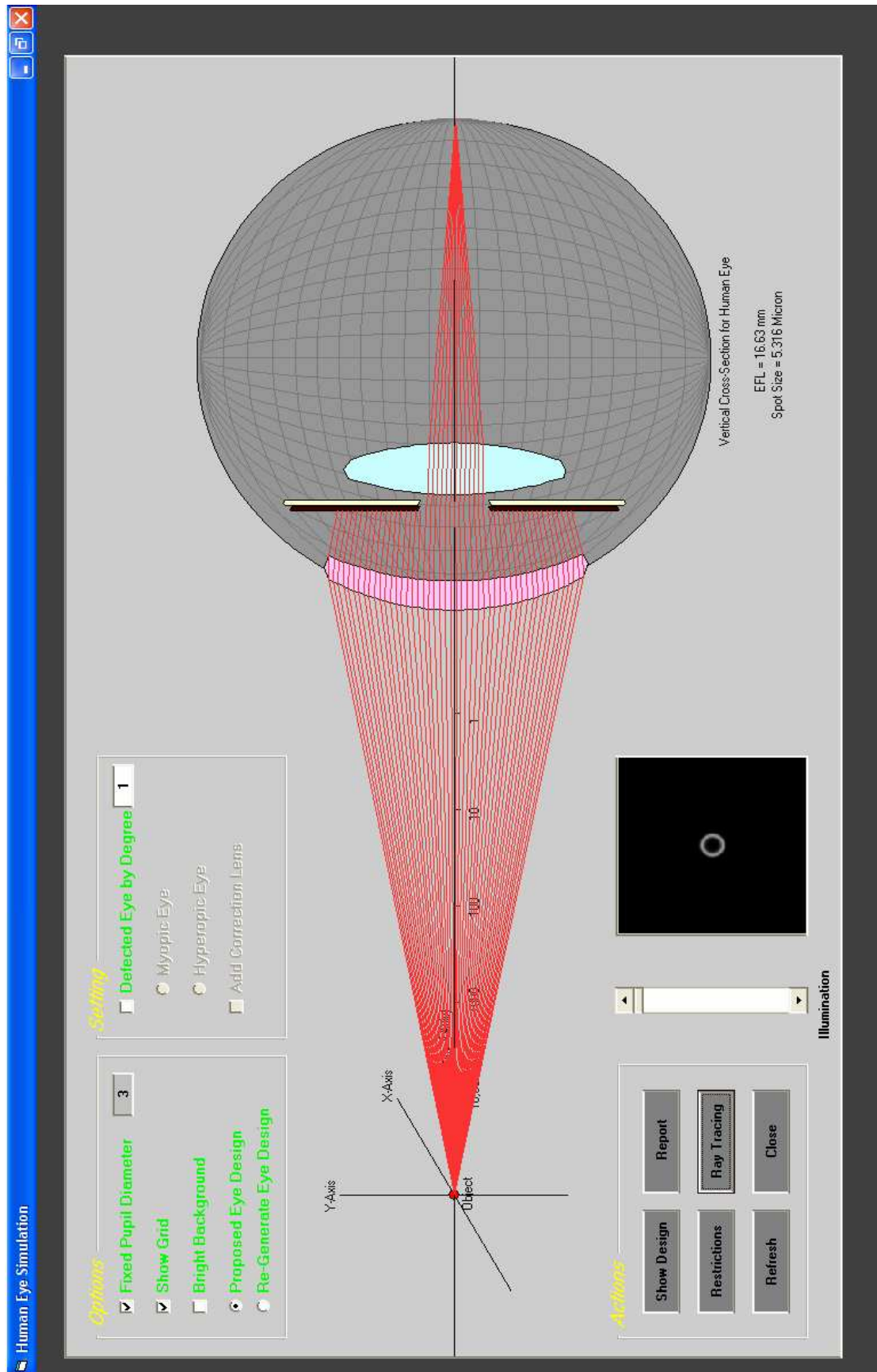


Figure (4.10): The simulator interface shows the spot diagram and spot size results.

## 4.7 Simulated Spot versus Incident Angles

It is noticeable that the variation of incident angles of skew rays is greatly affect the shape and size of the spot. Figure (4.11) shows a schematic picture given by Zemax to presents the oblique rays incident on the retina.

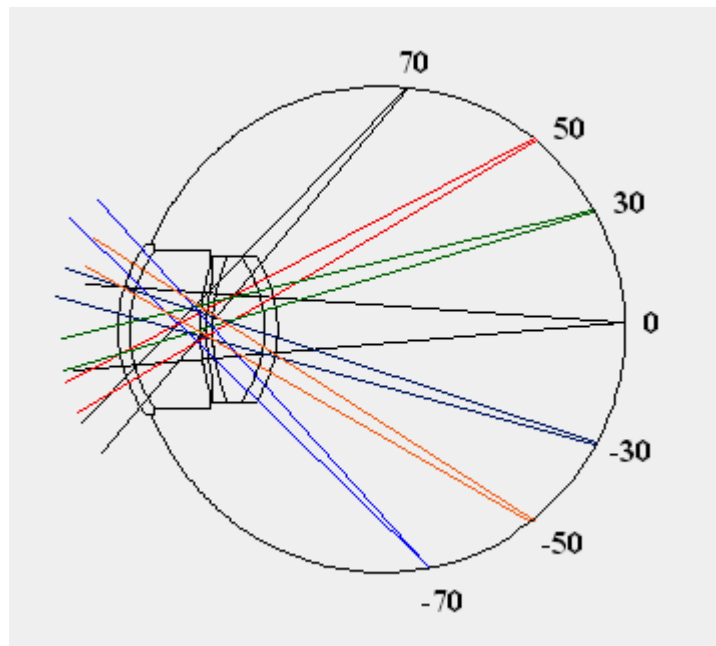


Figure (4.11): Different rays incident on the eye at different angles.

The simulator could imitate the situation of oblique rays as shown in figure (4.12). It is seen that the spot image suffers of an extension, the type of spot extension may be longitudinal or transverse according to the values of the angles  $\gamma$  and  $\beta$ . Also, the amount of the spot extension is related to the difference between the angles  $\gamma$  and  $\beta$ . Figure (4.13) presents an oblique rays incident on the eye with a specific  $\gamma$  angle ( $\alpha$  and  $\beta$  are set to be zeros), which causes to make a vertical extension in the spot diagram depending on the value of  $\gamma$ .

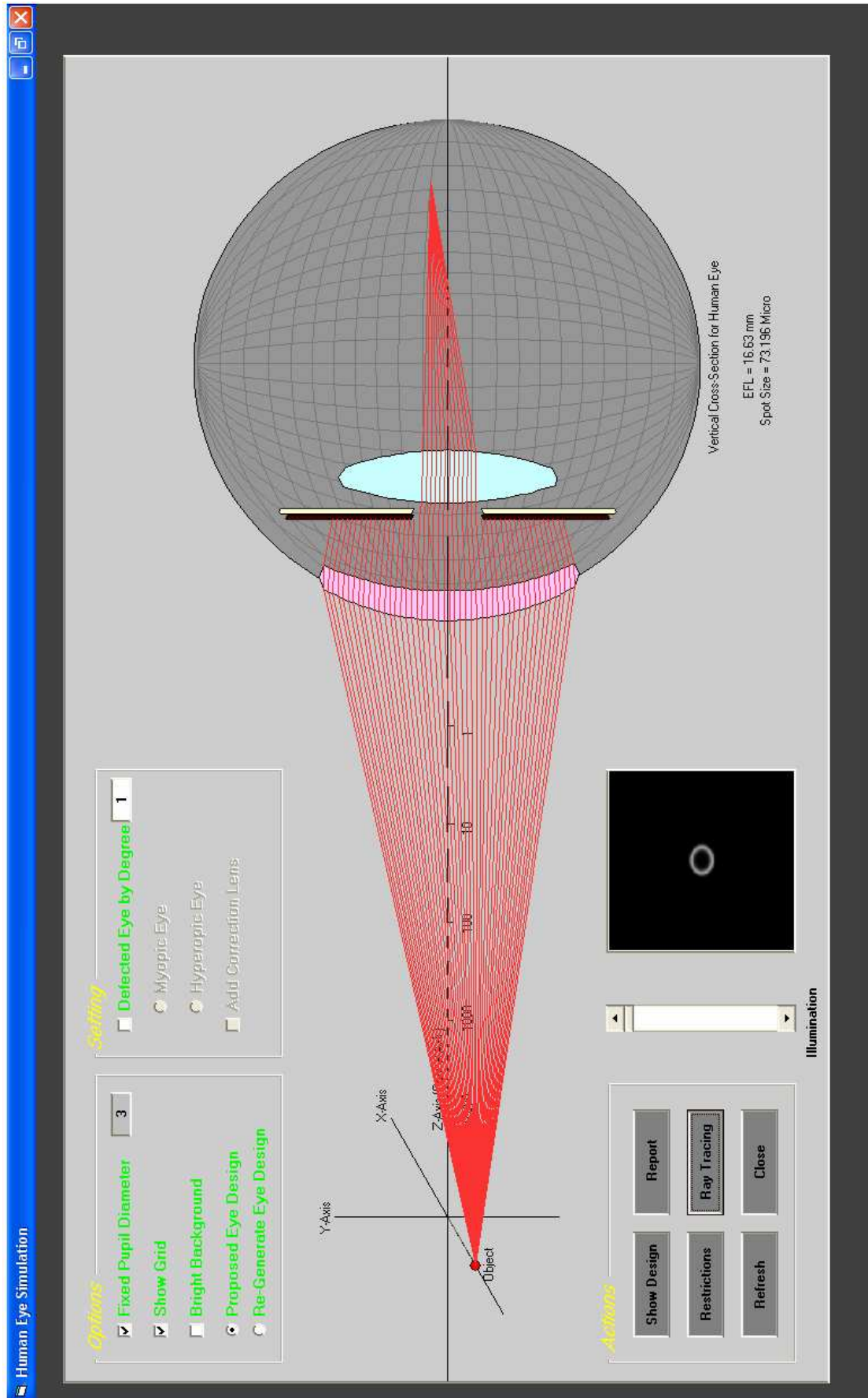


Figure (4.12): The situation of oblique rays.

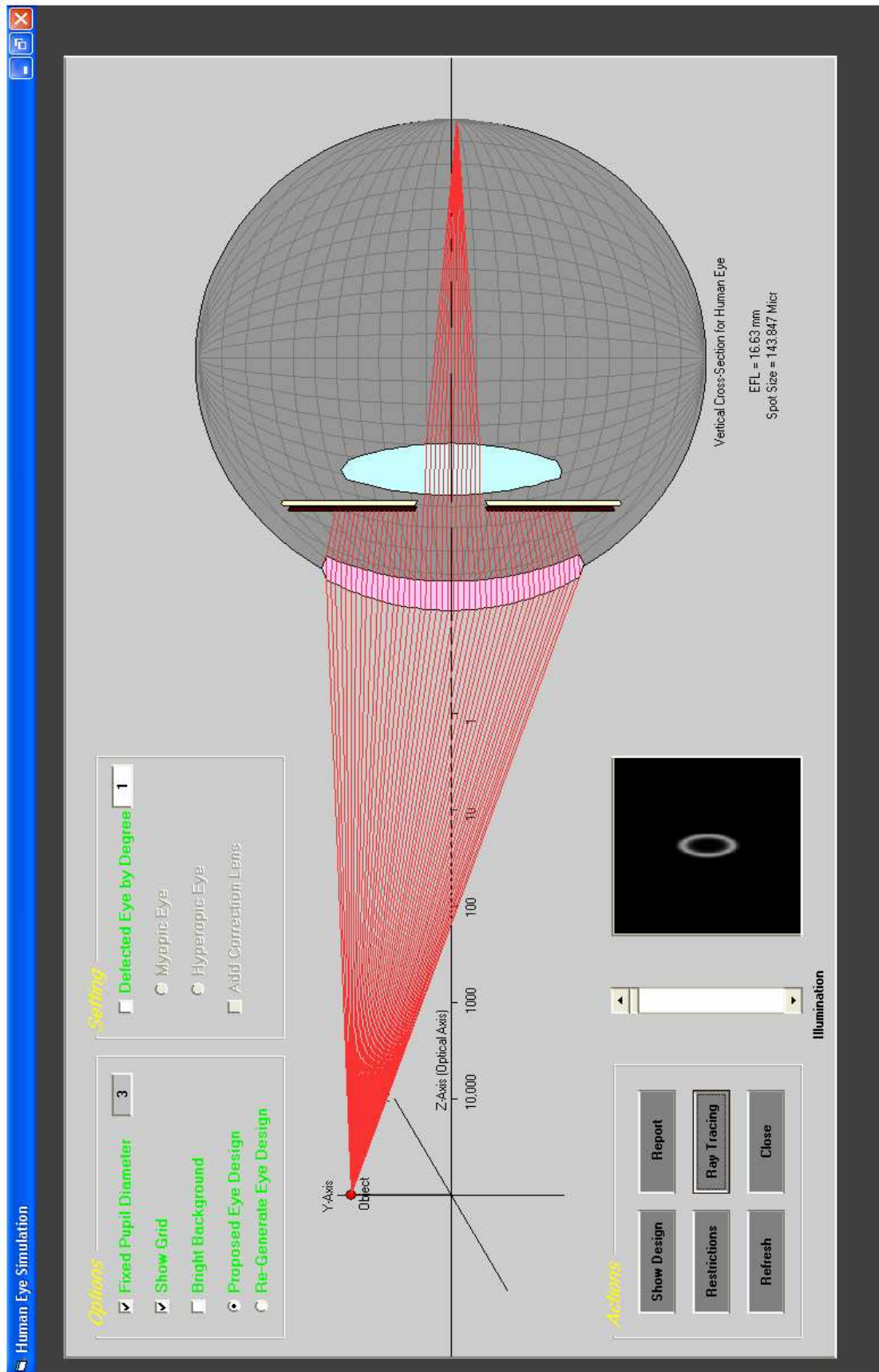


Figure (4.13): The relation between the extension in the spot diagram with angle.

In addition, the deflection of incidence angle ( $\gamma$  and  $\beta$ ) values from the zero leads to a monotonic increasing in the spot size. Table (4-5) shows the variation of the spot size as a result to the variation of  $\gamma$ , this behavior is pictured in figure (4.14), the spot image shows in figure (4.15 and 4.16). In spite of the spot size increases exponentially with  $\gamma$ , the magnification that occurs in the spot size is still small and neglectable since it come from abnormal state at which a comatic aberration is generated. The 2-D magnification due to coma aberration affects the image resolution, such that the spot separated along more expanded region, which lead to make the image seems to be blurred.

Table (4-5): show the spot radius as a function of angle using Zemax.

Angle ( <i>degree</i> )	Spot Radius ( $\mu m$ )
<b>0</b>	<b>5.341</b>
<b>±5</b>	<b>12.69</b>
<b>±10</b>	<b>17.10</b>
<b>±15</b>	<b>24.15</b>
<b>±20</b>	<b>36.4</b>
<b>±25</b>	<b>50.6</b>
<b>±30</b>	<b>67.44</b>
<b>±35</b>	<b>86.69</b>
<b>±40</b>	<b>108.08</b>
<b>±45</b>	<b>131.78</b>
<b>±50</b>	<b>156.57</b>
<b>±55</b>	<b>183.055</b>
<b>±60</b>	<b>210.22</b>

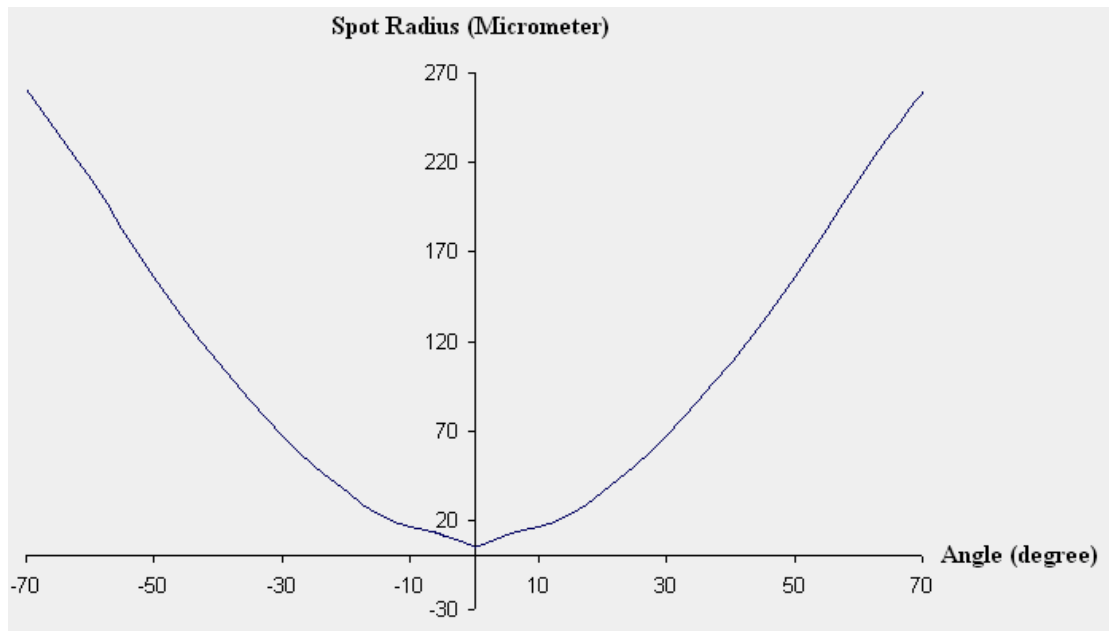


Figure (4.14): Spot radius versus incident angle.

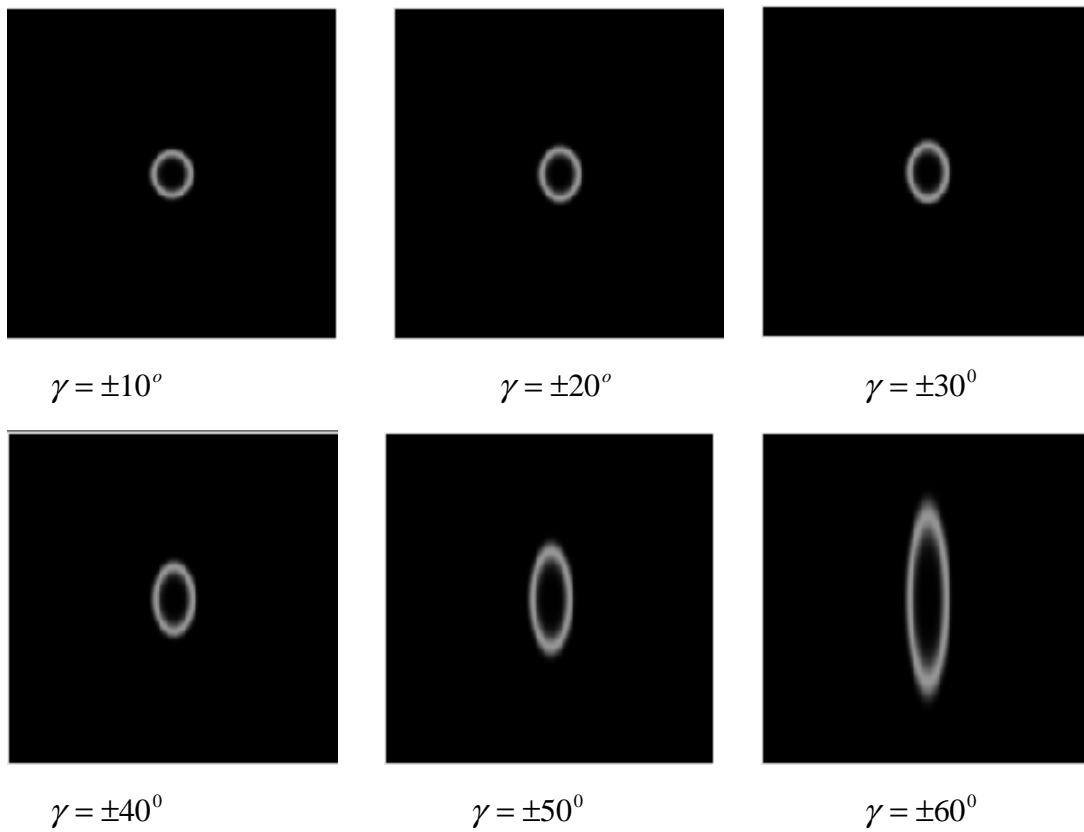


Figure (4.15): The simulated spot image versus incident angle by simulation.

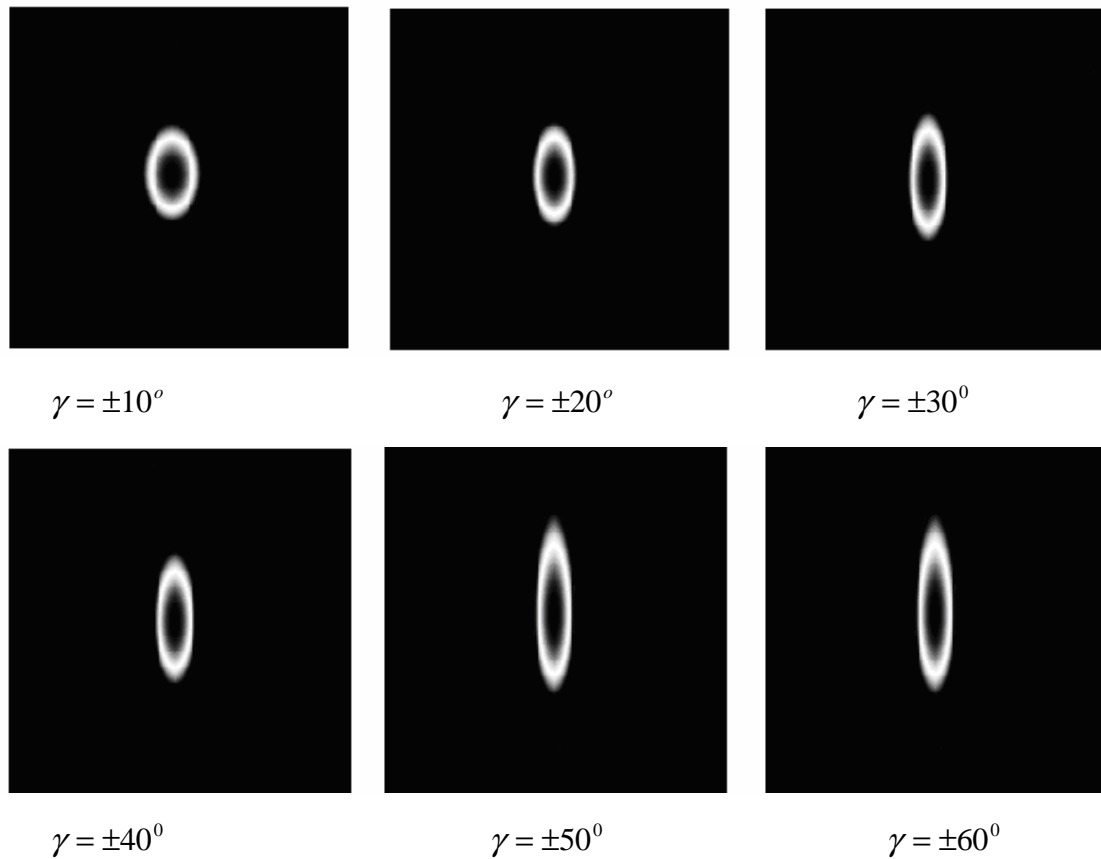


Figure (4.16): The spot diagram versus incident angle given by Zemax

#### 4.8 Simulated Spot versus Object Distance

To simulate the imaging process of near or far object, the distance between the simulated eye and the object in the simulation interface is set to be  $10m$  divided in terms of logarithmic scale as shown in figure (4.17). By considering several images for different objects distances ( $S$ ), it is found that the spot diagram and spot size remained at they were in all the considered cases. In correspondence, the radii of curvature of the eyelens were varying at each case to fit the eye design that makes the spot diagram and spot size as intended. Figure (4.18) shows the simulated spot diagram and size for six cases at which the object distance was varied. Whereas figure (4.19 and 4.20) referred to the amount of  $R_1$  and  $R_2$  variation of the eyelens for the same consider cases.

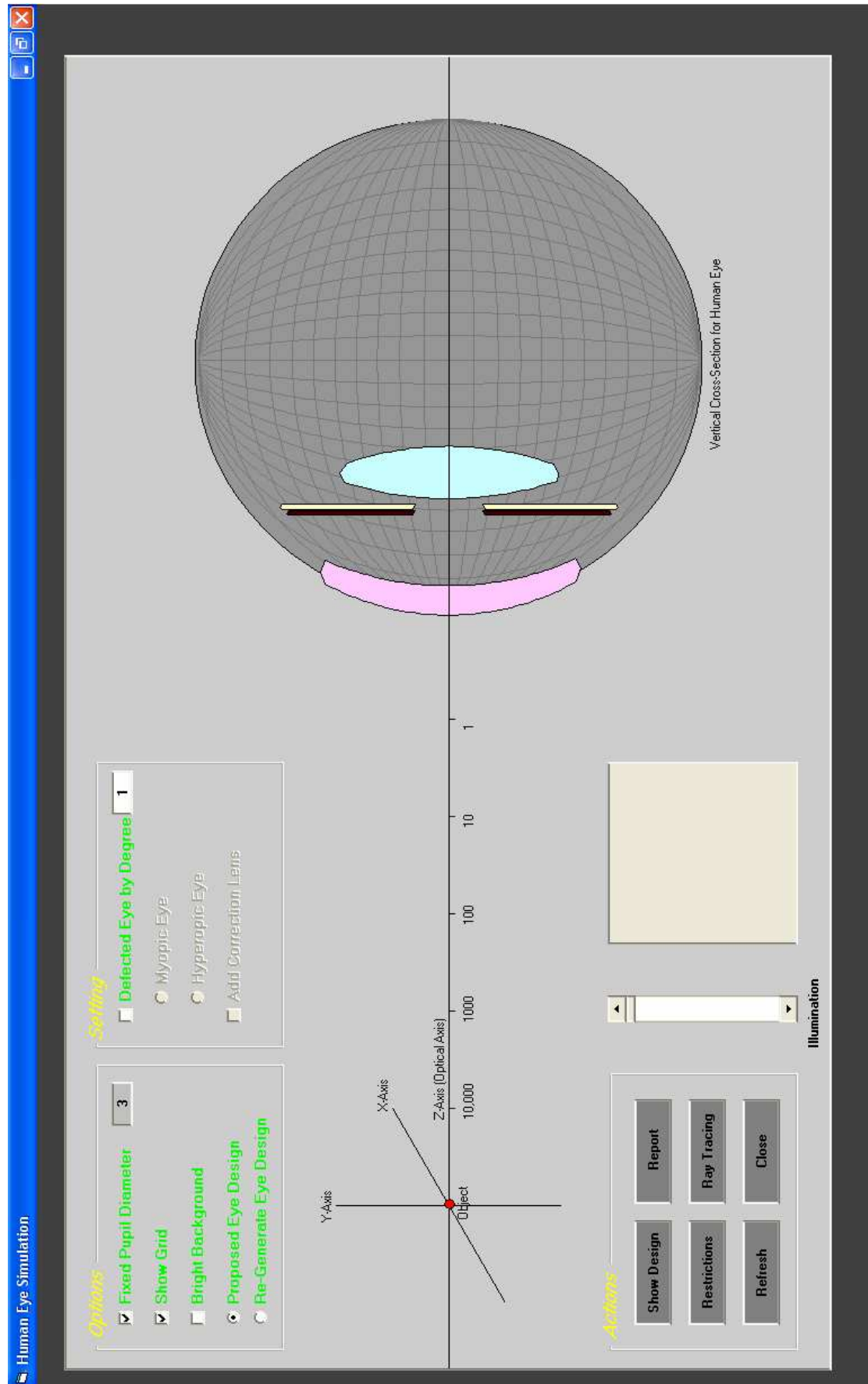


Figure (4.17): The object distance is logarithmically scaled.

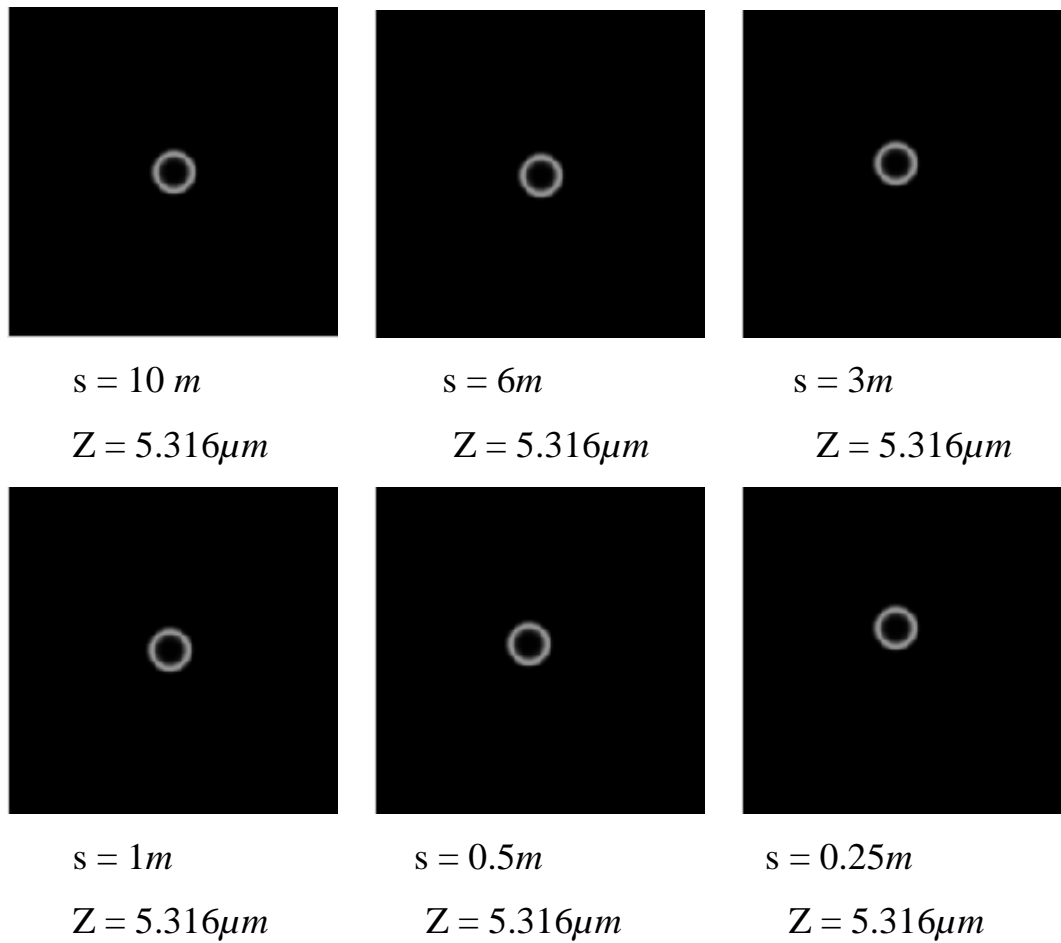


Figure (4.18): The spot diagram and size for different object distance.

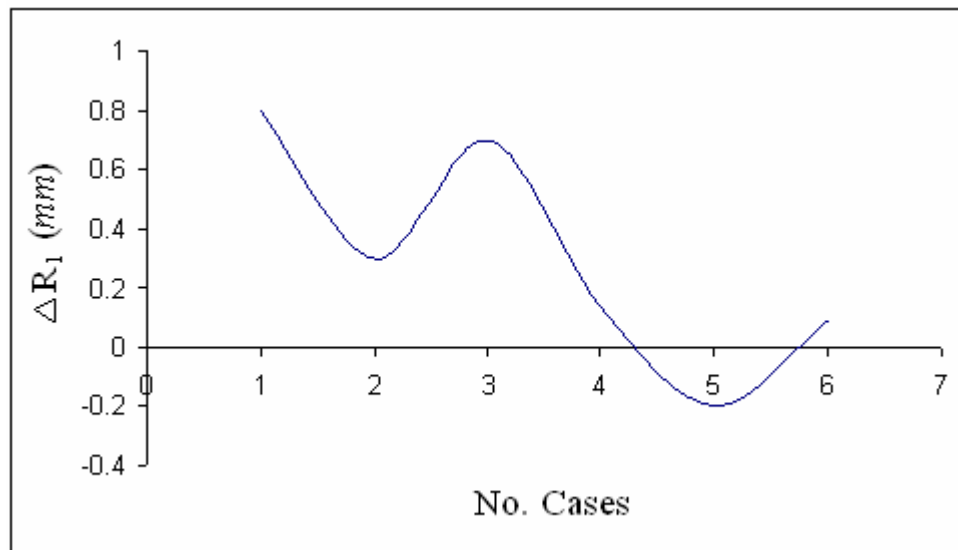


Figure (4.19): The variation in  $R_1$  of the eyelens with respect to its value at reading distance ( $0.25 \text{ m}$ ) due to the object distance variation in the six considered cases.

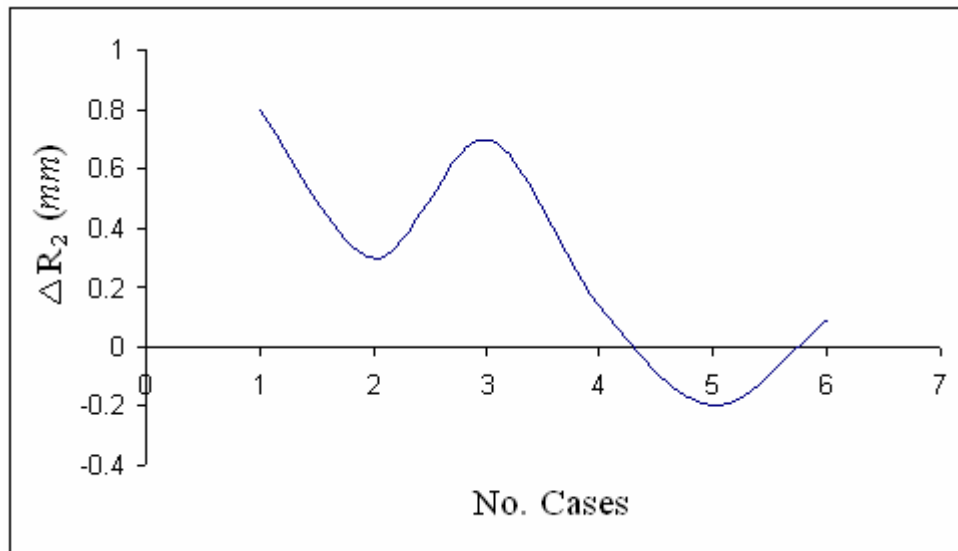


Figure (4.20): The variation in  $R_2$  of the eyelens with respect to its value at reading distance ( $0.25m$ ) due to the object distance variation in the six considered cases.

Moreover, the EFL was found equal to its intended value at each considered case, which point out to an acceptable imaging process carried out at each with a satisfied image resolution. That means the image resolution doesn't vary with the object distance variation, which refers to successful simulator behaviors in such cases.

## *Chapter Five*

# CONCLUSION AND FUTURE WORK

## **Chapter Five**

### **Conclusion and Future Work**

#### **5.1 Conclusion**

From the investigations one may draw the following conclusions:

1. The GA was a successful tool that can be achieve an optimal design for the human eye.
2. The choice of the EFL and spot size as two fitness functions constituting the objective function were satisfied since the GA based designing always gave an acceptable solution through short time.
3. The optimal eye design can approachly reach the intended values of the objective functions through few times of iteration.
4. The proposed optimal eye design has the ability to describe the performance and imaging of the real-life human eye.
5. The human eye simulator succeeded in imitating the eye activities such as; skew ray tracing, spot imaging, and the interaction with the effects of vision simulations.
6. The process of creating a myopic or hyperopic eye is closer to the real situation, but the correction method that based on predefined optical features for the eye is unapplicable and far away from the reality.
7. The estimation of spot diagram and spot size gave a results that are similar to that extracted by Zemax, and identical to that expected from the theoretical basis.
8. The relation between the spot and the angles of incidence makes the spot diagram vary to be vertically or horizontally extended by an amount proportional to the difference between the considered angles.

9. The variation of the object distance affects only the resolution of the image because it also vary the incidence angles that lead to an effective defocusing. The use of MGA to optimize the eyelens made better focusing and higher resolution.
10. In general, the simulator could imitate the behaviors of the human eye in different vision situations related to the illumination, incidence angles, and object distance. This ensure the correct path of the modeling and computations.

## **5.2 Future Work**

The following topics may be suggested for future work in the field of the present investigation.

1. One can use another more accurate optimization method such as Ant Colony Optimization (ACO) instead of GA to achieve the optimal human eye design.
2. One can consider the general state of eye situations and defects, and then build a dedicated software to simulate the eye activities and appear the events in 3-D graphical show.

## **References**

- Alpern M. (1978) [Alp 78]  
"The eyes and vision"  
*Handbook of Optics*.
- Artal P., Benito A. and Taberero J. (2006) [Art 06]  
"The human eye is an example of robust optical design"  
*Journal of Vision*, **31**: 224-226.
- Bass M. (1995) [Bas 95]  
"Handbook of Optics"  
McGraw-Hill, Inc, **1**, p360.
- Bergman J. and Calkins J. (2009) [Ber 09]  
"Why the Inverted Human Retina is a Superior Design"  
*Creation Research Society Quarterly*, **45**: 85-87.
- Boutry G. A. (1961) [Bou 61]  
"Instrumental Optics"  
Bell and Bain, LTD, **1**, p175.
- Breault Research Organization (2008) [Bre 08]  
"Using the Advanced Human Eye Model (AHEM)"  
*ASAP Technical Publication*, **2**: 1-5.

Carvalho L. A. (2003) [Car 03]

"A Simple mathematical model for simulation of the human optical system based on in vivo corneal data"

*SBEB - Sociedade Brasileira de Engenharia Biomédica, ISSN, 35*: 115.

Carvalho L. A., Castro J. C., Schor P. and Chamon W. (2007) [Car 07]

"A software simulation of human-schack patterns for real corneas"

*Institute de Fisica de São Carlos (IFSC – USP), Brazil, 20*: 93-95.

Dawson E. and Clark A. (2008) [Daw 08]

"Discrete Optimization: A Powerful Tool For Cryptanalysis"

*Information Security Research Center, Queensland University of Technology, 2*: 36-50.

de Almeida M. S. and Carvalho L. A. (2007) [DeA 07]

"Different schematic eyes and their accuracy to the in vivo eye: A quantitative comparison study"

*Brazilian Journal of Physics, 37*(2): 213-216.

Donnelly W. J. and Roorda A. (2003) [Don 03]

"Optical pupil size in the human eye for axial resolution"

*Optical Society of America, 20*(11): 227-233.

Donnelly W. J. (2008) [Don 08]

"The advanced human eye model (AHM): A personal binocular eye modeling system inclusive of refraction, diffraction, and scatter"

*Journal of Refractive Surgery, 19*: 217-218.

Dubin A., Cherezova T., Belyakov A., & Kudryashov A. (2008) [Dub 08]

"Human retina imaging: widening of high resolution area"

*Journal of Modern Optics*, **55**(4): 671-681.

Einighammer J., Oltrup T., Bende T., and Jean B. (2009) [Ein 09]

"The individual virtual eye: a computer model for advanced intraocular lens calculation"

*Journal Optima*, **2**(2): 30-35.

Fundamental Optics (2004) [Fun 04]

<http://www.mellesgriot.com>

Hampson K.M. (2008) [Ham 08]

"Adaptive Optics and Vision"

*Journal of Modern Optics*, **55**(21): 25-31.

Hudson, R. D. (1969) [Hud 69]

"Infrared system engineering"

*John Wiley & Sons, United States of America*, **51**: 137-140.

Jenkins F.A and White H.E. (1981) [Jen 81]

"*Fundamentals of Optics*"

McGraw-Hill Book Company, USA, **4**, p81.

Kerr D. A. (2004) [Ker 04]

"The Eye and its Limitations"

*Physics for the life science*, **20**: 54-62.

- Kimball J. W. (2009) [Kim 09]  
"The human eye"  
<http://users.rcn.com/jkimball.ma.ultranet/BiologyPages/V/Vision.html>
- Laikin M. (2006) [Lai 06]  
"LENS DESIGN 4<sup>th</sup> edition"  
Taylor & Francis Group, LLC, 1, p442.
- Mood A. M., Graybill F. A. and Boess D. C. (1974) [Moo 74]  
"Introduction to the theory of statistical"  
McGraw-Hill, London, p205.
- Navarro R. (2009) [Nav 09]  
"The optical design of the human eye: a critical review"  
*Journal Optom*, 2(1): 17-23.
- Pedrotti L. S. and Pedrotti F. L. (1998) [Ped 98]  
"Optics and Vision"  
*Optical society of America*.
- Pedrotti F.A. and Pedrotti L.S. (1988) [Per 88]  
"Introduction to Optics"  
Practice-Hall International, Inc, USA, 3, p554.
- Roorda A. (2009) [Roo 09]  
"Human visual system- image formation"  
*University of Houston College of Optometry Houston, TX*, 15: 56-60.

- Saers F.W. (1964) [Sae 64]  
*"Optics"*  
Addison – Wesley Publishing Company, Inc., UK, 1, p132.
- Sakamoto J. A., Harrison H. B. and Alexander V. G. (2008) [Sak 08]  
"Inverse optical Design of the human eye using likelihood method & wave front sensing"  
*Optics Express*, 16(1): 304-306.
- Sanders D. R. and Koch D. D. (1993) [San 93]  
"An atlas of corneal topography"  
*Journal of Modern Optics*.
- Schanzlin D. J. and Robin J. R. (1992) [Sch 92]  
"Corneal topography: measuring and modifying the cornea"  
*Journal of Refractive Surgery*.
- Scott R. M. (1959) [Sco 59]  
*"Optics for infrared system "*  
IRE, 1, p(1956-1960).
- Shannon R. R. (1997) [Sha 97]  
*"The art and science of optical design"*  
Cambridge University Press, United States of America 1, pp58.

- Smith W. J. (1966) [Smi 66]  
*"Modern Optical Engineering"*  
McGraw-Hill Book Company, USA, **1**: 247.
- Smith W. J. (2008) [Smi 08]  
*"Modern Optical Engineering"*  
McGraw-Hill, United States of America, **2**: 338.
- Stellpflug C. (2009) [Ste 09]  
"Basic Eye Development and Associated Problems"
- Tocci M. D. (2007) [Toc 07]  
"How to Model the Human Eye in ZEMAX"  
*Contrast optical design & Engineering, INC*, **11**: 49-54.
- Tunnacliffe A. H. (1989) [Tun 89]  
"Introduction to Visual Optics"  
*Optics Express*.
- Von Helmholtz H. (2000) [Von 00]  
"Helmholtz's treatise on physiological optics"  
*Optical society of America*.
- Welford W. T. (1974) [Wel 74]  
"Aberrations of the Symmetrical Optical System"  
*Academic Press*, **31**(2): 51-52.

Williams C. S. and Becklund, O. A. (1972) [Wil 72]

*"Optics"*

John Wiley & Sons, United States of America **1**, p(150-151).

Williams C. S. and Becklund, O. A. (1989) [Wil 89]

*"Introduction to optical transfer function"*

John Wiley & Sons, Canada, **2**, p162.

Zajac H. (1974) [Zaj 74]

*"Optics"*

Addison-Wesley, INC, **1**, p459.

## Appendix A

The Gaussian distribution of any natural phenomena takes a bell shape distributed along x-y plane, such shape be suitable to describe most of the natural behaviors that is done by changing the mean ( $\mu$ ) or the variance ( $\sigma^2$ ) to fit the intended behavior. The general formula of the Gaussian distribution in 2-D space is given as [Moo 74]:

$$f(x, y) = \frac{1}{2\pi\sigma_x\sigma_y\sqrt{1-\rho^2}} \exp\left[\frac{-1}{2(1-\rho^2)}\left[\left(\frac{x-\mu_x}{\sigma_x}\right)^2 - 2\rho\left(\frac{x-\mu_x}{\sigma_x}\right)\left(\frac{y-\mu_y}{\sigma_y}\right) + \left(\frac{y-\mu_y}{\sigma_y}\right)^2\right]\right] \quad (A.1)$$

where,  $\mu_x$  is the mean (expectation) value in the x-axis.

$\mu_y$  is the mean (expectation) value in the y-axis.

$$\mu = E(t) = \int_{-\infty}^{\infty} tf(t)dt \quad (A.2)$$

$\sigma_x^2$  is the mean variance of the values in the x-axis

$\sigma_y^2$  is the mean variance of the values in the y-axis

$$\sigma^2 = E(t^2) - \mu^2$$

$\rho$  is the correlation coefficient between the attended values in the x and y axis ( $|\rho| \leq 1$ ).

In the natural case, where the distribution is smooth without irregularities, the correlation coefficient becomes zero ( $\rho = 0$ ), and equation (A.1) becomes:

$$f(x, y) = \frac{1}{2\pi\sigma_x\sigma_y} \exp\left[-\frac{1}{2}\left[\left(\frac{x-\mu_x}{\sigma_x}\right)^2 + \left(\frac{y-\mu_y}{\sigma_y}\right)^2\right]\right] \quad (A.3)$$

Which is the popular formula of the Gaussian distribution that almost used to fit the behavior of the natural phenomena.

## **Appendix B**

Let  $\psi$  is  $\alpha$  or  $\beta$ , and  $\sigma$  is  $\sigma_x$  or  $\sigma_y$ , then:

$$\sigma = a\psi + b$$

Using table (3-1), one can set the following two equations

$$1.18 = a(0) + b \quad (B.1)$$

$$46.2 = a(60) + b \quad (B.2)$$

Where the values of  $\sigma$  are driven from equation (3.10), by solving equations (1 and 2) for a and b, one gets

$$a = 0.767$$

$$b = 1.18$$

thus,

$$\sigma = 0.767\psi + 1.18$$

## **Appendix C**

at  $\theta = 60^\circ$

$a = 11.5\text{mm}$  (half the horizontal dimension of eye ball)

$e = 0.011$  (eccentricity of eye ball)

$$b = \sqrt{a^2 - e^2 a^2} = \sqrt{(11.5)^2 - (0.011)^2 (11.5)^2} = 11.499304\text{mm}$$

$$X_E = a \cos 60 = 11.5 \cos 60 = 5.75$$

$$Y_E = b \sin 60 = 11.499304 \sin 60 = 9.958397$$

$$X_L = 7.279$$

$$Y_L = 0$$

$$\begin{aligned} f_{\text{Ellipse}} &= \sqrt{(X_L - X_E)^2 + (Y_L - Y_E)^2} \\ &= \sqrt{(-7.279 - 5.75)^2 + (0 - 9.958397)^2} = \sqrt{268.92916} = 16.39906\text{mm} \end{aligned}$$

$$\Delta f = f_{\text{sphere}} - f_{\text{Ellipse}} = 16.63 - 16.39906 = 0.23094\text{mm} = 230.94\mu\text{m}$$

$$Z_\theta = \Delta f \sin 60 = 230.94 \sin 60 = 200\mu\text{m}$$

$$Z_o = 5.1\mu\text{m}$$

$$Z = Z_o + Z_\theta = 5.1 + 200 = 205.1\mu\text{m}$$

## **Appendix D**

$$\delta = A \exp(-Bs) \quad (D.1)$$

To find the values of the coefficients A and B, one can use the  $x^2$  fitting method for the data of table (3.3) as follows:

$$\delta = A \exp(-Bs) \quad (D.1)$$

$$\ln \delta = \ln(A \exp(-Bs))$$

$$\ln \delta = \ln A - Bs$$

$$\ln \delta = c - Bs \quad (D.2)$$

Where

$$c = \ln A \quad (D.3)$$

$$x = \sum_{i=1}^n (\delta_i - \delta'_i)^2 \quad (D.4)$$

Where  $\delta_i$  is the theoretical values of  $\delta$  and  $\delta'_i$  are the experimental ones, and n is the number of data samples. Substitute equation (D.2) in equation (D.4), one gets:

$$x^2 = \sum_{i=1}^n (\ln \delta_i - c + Bs_i)^2$$

To achieve the value of the coefficients c and B, make  $\frac{\partial x^2}{\partial c} = 0$  and

$$\frac{\partial x}{\partial B} = 0$$

$$\frac{\partial x^2}{\partial c} = \sum_{i=1}^n 2(\ln \delta_i - c + Bs_i)(-1) = 0$$

$$-2 \sum_{i=1}^n (\ln \delta_i - c + Bs_i) = 0$$

$$c \sum_{i=1}^n 1 + B \sum_{i=1}^n s_i = \sum_{i=1}^n \ln \delta_i$$

$$nc + B \sum_{i=1}^n s_i = \sum_{i=1}^n \ln \delta_i \quad (D.5)$$

$$\frac{\partial x^2}{\partial B} = \sum_{i=1}^n 2(\ln \delta_i - c + Bs_i)(-s_i) = 0$$

$$c \sum_{i=1}^n S_i + B \sum_{i=1}^n S_i^2 = \sum_{i=1}^n S_i \ln \delta_i \quad (D.6)$$

One can solve the two equations (D.5 and D.6) to get the coefficients  $c$  and  $B$ .

$$c = \frac{\sum_{i=1}^n \ln \delta_i \sum_{i=1}^n s_i - \sum_{i=1}^n s_i \ln \delta_i \sum_{i=1}^n s_i}{n \sum_{i=1}^n s_i^2 - (\sum_{i=1}^n s_i)^2} \quad (D.7)$$

$$B = \frac{n \sum_{i=1}^n s_i \ln \delta_i - \sum_{i=1}^n s_i \sum_{i=1}^n \ln \delta_i}{n \sum_{i=1}^n s_i^2 - (\sum_{i=1}^n s_i)^2} \quad (D.8)$$

By substituting the data of both  $\delta$  and  $s$  found in table (3.3) in equations (D.7 and D.8), one can obtain:

$$c = 1.5808$$

$$B = 1.1427$$

$$A = e^c = 4.8588$$

## المستخلص

يهدف هذا البحث الى محاكاة المنظومة البصرية للعين البشرية بأستخدام الخوارزميه الجينية. ان الخصائص المفترضة لمحاكاة المنظومة البصرية تتضمن سعة البقعة، المخطط البقي، و البعد البؤري الفعال. تم تحديد هذه الخصائص بواسطة بعض العلاقات الرياضية التي تعطي كفاءة و دقة عمل المنظومة المتبناة، وقد تم العمل في مرحلتين:

ثم استخدم تعديل الخوارزمية الجينية (GA) في المرحلة الاولى للحصول على افضل تصميم و ذلك بتعديل الصفات للعناصر البصرية للعين. ثم اختبار التصميم المعدل للعين بأستعمال برنامج زيماكس (Zemax). الاختبار تضمن هدفين هما: تقدير نوعية الصورة و تحديد الاداء الامثل لمنظومة العين البصريه المقترحه.

المرحلة الثانية تتمثل في تنفيذ برنامج خاص لمحاكاة تصرف المنظومه البصريه للعين البشرية. البرنامج استخدم برنامج (Visual Basic 6) الذي يعمل ضمن بيئة نظام تشغيل النوافذ (Windows) وهو قادر على رسم تصميم العين و حساب الدوال البصرية المفترضة لتحديد كفاءة محاكي العين.

اظهر المحاكى نتائج جيده لكل من حجم البقعة و شكلها و كذلك البعد البصري المؤثر. وان العمل الحالي اكتسب الضمانة العلمية عندما وجد ان الدوال البصرية المفترضة و المحسوبة بواسطة المحاكى تطابق تصرفات مثيلاتها المستحصلة بواسطة برنامج زيماكس (Zemax). و هذا يؤكد صحة مسار تصميم العين بناءً على الخوارزمية الجينية و نجاح التصميم المقترح للعين.



جمهورية العراق  
وزارة التعليم العالي والبحث العلمي  
جامعة النهرين  
كلية العلوم

# محاكاة العين البشريه بأستخدام الخوارزميه الجينيه

رساله

مقدمه الى كلية العلوم في جامعة النهرين  
كجزء من متطلبات نيل درجة الماجستير  
في  
الفيزياء

من قبل

لؤي عبد الصاحب رسول الطائي

المشرف

د. سهى موسى الأوسي  
د. محمد صاحب الطائي

1432 هـ  
2010 م

محرم  
كانون الأول